INLAND NORWAY UNIVERSITY OF APPLIED SCIENCES

Faculty of Applied Ecology, Agricultural Sciences and Biotechnology

Valentina Krivenjeva

Master's Thesis

Bioinformatic Analysis of RNA-seq Data from Cultivated Strawberry (*Fragaria x ananassa*) and Experimental Validation of New Transcripts Related to Cold Tolerance

Master Degree in Applied and Commercial Biotechnology

2018

Consent to lending by University College Library YES ☐ NO ☐

Consent to accessibility in digital archive Brage YES ☐ NO ☐

Acknowledgement

My passion to work with bioinformatics and molecular biology had been fulfilled by getting involved in this master thesis project. It was a great opportunity for me to practice bioinformatics techniques and the wet-lab work which enabled me to gain an immense knowledge that is useful for my future research.

I would like to express my gratitude to my supervisors Rafi Ahmad and Robert Wilson. I am profoundly grateful to them that helped me with their excellent supervision, continuous guidance and valuable advice throughout the project.

A special thank goes to my friend of life, my fiancé Ardian Sinani, for his support and endless love that he gave me through these years that we studied together. Also, heartfelt thanks go to my family for their love, support, and encouragement.

The master degree at the Inland Norway University of Applied Sciences would have been impossible without the scholarship from the QUOTA program.

Abbreviations

ADH	Alcohol Dehydrogenase
B2G	Blast2GO
BLAST	Basic Local Alignment Search Tool
bp	base pair
CA	Cold acclimation
CBF	C-repeat Binding Factor
cDNA	Complementary DNA
CDPK1	Calcium-dependent protein kinase 1
CHS	Chalcone Synthase
COR	Cold Regulated
CPM	Counts Per Million
DE	Differential Expression/ Differentially Expressed
DNA	Deoxyribonucleic acid
DRE	Dehydration-Responsive Element
DREB	Dehydration-Responsive Element Binding factors
EdgeR	Empirical analysis of Differential Gene Expression in R
FC	Fold Change
FDR	False Discovery Rate
FPKM	Fragments Per Kilobase Million
F3H	Flavonoid 3'- Hydroxylase
GBL	Graminor Breeding Limited
GO	Gene Ontology
HOS1	High expression of osmotically responsive genes 1
h	Hour
HSP	Heat Shock Proteins

ICE1	Inducer of CBF Expression 1
LEA	Late Embryogenesis Abundant
MFLP	Microsatellite-anchored Fragment Length Polymorphism
mRNA	messenger RNA
MPSS	Massive parallel signature sequencing
MYB	Myeloblastosis
NA	Not Available
NGS	Next Generation Sequencing
PCR	Polymerase Chain Reaction
RFOs	Raffinose family oligosaccharides
RNA	Ribonucleic Acid
RNA-seq	Ribonucleic Acid Sequencing
ROS	Reactive Oxygen Species
RPKM	Reads Per Kilo –base per million Mapped reads
RSEM	RNA-seq by Expectation Maximization
RT-qPCR	Real Time-PCR
SAGE	Serial Analysis of Gene Expression
SAM	Sequence Alignment/Map
SUMO	Small Ubiquitin related Modifier
TF	Transcription Factor
TMM	Trimmed Mean of M-values
ZAT	Zinc finger of *Arabidopsis Thaliana*

Table of Contents

Abstract

The cultivated strawberry (*Fragaria* × *ananassa*) is an important plant consumed around the world for its flavour and nutritional value. The strawberry floral organs are very sensitive to cold stress, which often leads to economic loss. To gain insight into the transcriptome contributing to cold tolerance, a comprehensive transcriptome analysis comparing octoploid strawberry (Fragaria × ananassa) cultivars was performed. RNA-seq method was used to identify transcripts associated with freezing tolerance. By performing pairwise differential expression analysis was determined the number of differentially expressed transcripts of two cultivars 'Jonsok' and 'Elsanta' that differ in the response to low-temperature stress. Moreover, the most up- and down-regulated transcripts were selected from samples treated at 2 °C through different time points 0, 1, 5, 48, 240 h. In addition, the expression profiles of 21 transcripts associated with cold tolerance were identified. Several transcripts including dehydrin COR47-like, transcription factor ICE1, chalcone synthase, cytosolic aldolase, alcohol dehydrogenase, dehydrin Xero2, E3 ubiquitin- ligase HOS1 and cleavage stimulating factor 64-like, were validated using RT-qPCR. A high compliance was obtained between bioinformatics analysis and experimental results obtained from RT-qPCR. We assume that these transcriptome data will provide a valuable foundation for further characterization of the molecular mechanisms and potentially for analysis at the proteomic level.

1. Introduction

1.1 Background

Strawberry is a commercially important crop with high demand in Norway. However, the strawberry industry goes through many challenges because of the harsh climatic conditions. Therefore, it is a challenge to fulfill demand and maintain a significant profit. There is a need to bring a diverse variety of strawberry cultivars that could adapt to the Norwegian growth conditions. Graminor Breeding Limited (GBL) is a plant breeding company that develops plant varieties suitable for the Norwegian climate. This company is associated with the national Norwegian strawberry breeding program since 2002. Graminor brings different cultivars to the market, which are winter hardened and frost tolerant allowing farmers to gain profitability by producing high-quality strawberries (Nes, Gullord, Alsheikh, & Sween, 2008). Differences among cultivars in winter survival potential have been known to the industry and also experimentally confirmed for both, octoploid *Fragaria* × *ananassa* (Nestby & Bjørgum, 1999) and diploid *Fragaria vesca* (Sønsteby & Heide, 2011) genotypes. In the current project are included two different cultivars of strawberry. The first is 'Jonsok', which is an older Norwegian cultivar and it is mostly grown in Finland, as it is highly resistant to cold climatic conditions. 'Elsanta' is another cultivar of strawberry, but it is not so popular in Nordic countries. 'Elsanta' cannot show tolerance to the low temperatures and plant damage is more common (Davik, Daugaard, & Svensson, 2000). Strawberry plant is susceptible to the cold stress injury, which is one of the largest factors affecting quality and productivity of crop in temperate regions. In order to withstand freezing conditions several characteristics are required, such as gene repression, metabolism changes, transcriptional activation, alteration of membrane composition, activation of scavengers for reactive oxygen species, and accumulation of cryoprotective molecules (sugar, proteins, and compatible solutes). These characteristics have an important role in resisting damage from freezing cold climatic conditions in many organisms and plant species (John, Anjum, Sopory, Akram, & Ashraf, 2016).

A major breakthrough for analyzing the strawberry genome in more detailed manner is the development of new technologies such as Next Generation Sequencing (NGS). NGS includes whole genome sequencing, genome resequencing, transcriptome profiling or RNA-seq, characterization of epigenome and ChIP-sequencing. NGS based, RNA sequencing

(RNA-seq) is a powerful alternative than whole genome expression profiling techniques, such as the microarray. This technique provides a wholesome view of the transcripts expression levels and transcriptional structure. RNA-seq is considered a powerful tool for transcriptome analysis and can determine gene expression profile up to single cell level (Ching, Huang, & Garmire, 2014). The data set produced from the RNA-seq is used for further computational analysis, like quality control, transcriptome assembly, estimation of the transcript abundance, normalization, and differential gene expression analysis (Yang & Kim, 2015).

1.2 Strawberry (*Fragaria*) & Cultivated Strawberry (*Fragaria x ananassa*)

The strawberry (genus *Fragaria*) is a plant which belongs to family *Rosaceae*. As low-growing herbaceous plants, strawberries have a fibrous root system and a crown from which arise basal leaves (Figure 1). Typically they have three leaflets, but the leaflets number may vary from one or five. The flowers, usually are white, borne in small clusters on slender stalks arising from the leaf axils. The root system with aging becomes woody and the crown (of mother plant) sends out runners (stolons) that touch ground and root, thus enlarging the plant vegetatively (Hummer, Bassil, & Njuguna, 2011; Poling, 2012; Trejo-Téllez & Gómez-Merino, 2014).

Worldwide, there are more than 20 *Fragaria* species (Gaafar & Saker, 2006). All of them have seven basic types of chromosomes that are common. However, the key to the classification of strawberry species is that they exhibit different polyploidy. The woodland strawberry (*Fragaria vesca*) is a diploid species and has two sets of the seven chromosomes (14 chromosomes total), and others strawberry are tetraploid (four sets, 28 chromosomes total), hexaploid (six sets, 42 chromosomes total), octoploid (eight sets, 56 chromosomes total), or decaploid (ten sets, 70 chromosomes total) variety (Gaafar & Saker, 2006; Husaini & Neri, 2016; Staudt, 1999).

The cultivated strawberry *(Fragaria* × *ananassa)* is an important fruit, which originated from natural hybridization between *Fragaria virginiana* and *Fragaria chiloensis*. Due to good flavor, fragrance and nutritional value it is a very popular crop (Hossain et al., 2018; Qiao et al., 2016). The genome of *F.* × *ananassa* is among the most complex of crop plants, containing eight sets of chromosomes derived from as many as four different diploid ancestors (Shulaev et al., 2011). As an octoploid species, the genome size of one chromosome

is estimated to be from 708 to 720 Mb (Akiyama, Yamamoto, Ohmido, Ohshima, & Fukui, 2001; Hirakawa et al., 2014).

Strawberry fruits come from a perennial growing system, and winter survival is a limiting factor for the industry of strawberry. However, plants vary greatly in their ability to survive at low temperatures. Also, this variation can be seen among cultivars of the same plant (J. C. Kim et al., 2001). As it is mentioned above, 'Jonsok' and 'Elsanta' are two strawberry cultivars that differ in their ability to survive winter hardiness (Davik et al., 2000; Husaini & Neri, 2016).

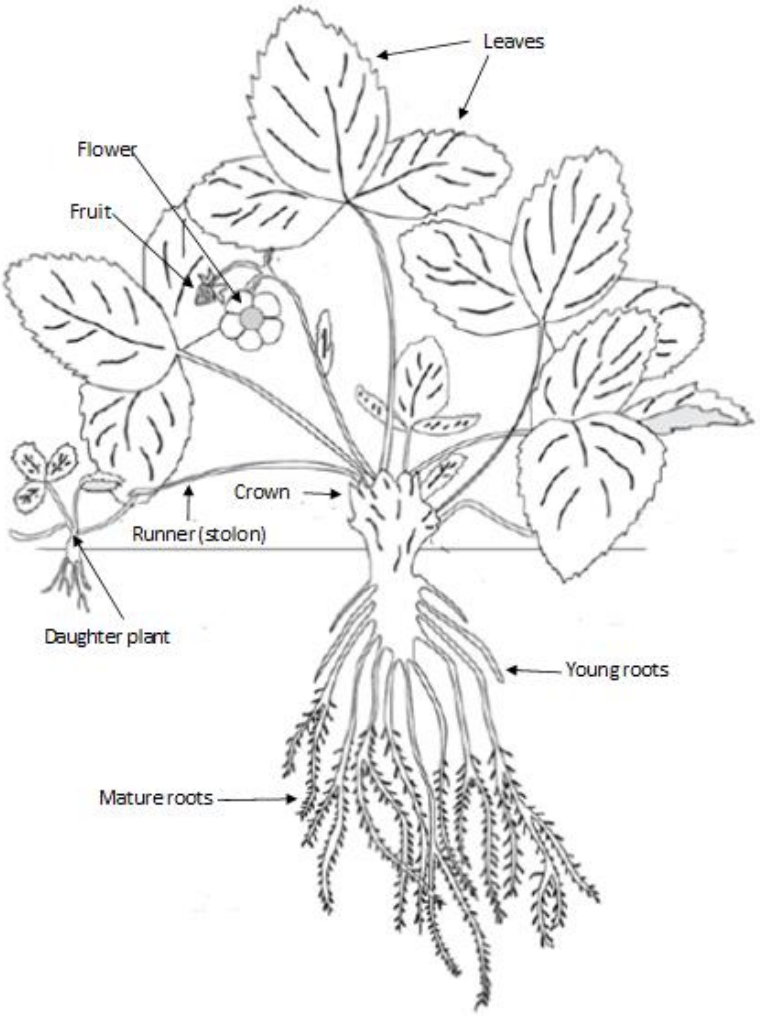

Figure 1. *Strawberry plant structure. The basic anatomical structures that make up strawberry plant are: leaf, runner, crown, root system and daughter plant. Picture modified from Trejo-Téllez & Gómez-Merino* (2014)

1.3 Abiotic stress impact on plant

As sessile organisms, plants have to cope with abiotic stress conditions like cold, drought, heat, and salt to adapt to constantly changing environments (Madhava Rao, 2006). The abiotic stress conditions usually act as major negative factors limiting crop productivity, quality, survival, and geographical distribution of plants (Beck, Fettig, Knake, Hartig, & Bhattarai, 2007; Xin & Browse, 2000). Cold stress is a major environmental factor that adversely affects the plant growth and crop productivity which causes significant crop losses (Wei et al., 2017). The intensity of these losses varies depending on the stress level, responsiveness and tolerance capacity of the plant species (Bita & Gerats, 2013; You & Chan, 2015). Low-temperature stress outside of the optimum range of plant tolerance can cause damages at the physiological, cellular, and molecular level, which is expressed by various phenotypic changes on plants (Yadav, 2010). Cold stress affects the water relations of a plant, as well as the whole plant level, causing damages and adaptation reactions (Beck et al., 2007).

1.4 Cold tolerance in plants

Plants differ in their tolerance to chilling and freezing temperatures (Cavender-Bares, 2007). Chilling tolerance is the ability of a plant to tolerate low temperatures (0–20 °C) without injury or damage (X. Wang et al., 2018). After a period of exposure to chilling temperatures plants can increase their tolerance to freezing stress (< 0 ºC), through a complex adaptive process called cold acclimation (Michael F Thomashow, 2010). Both, chilling tolerance and cold acclimation (CA) are associated with biochemical and physiological changes (S. A. Kim et al., 2013; Miura & Furumoto, 2013b; Tuteja, 2012). These changes include alterations in lipids, proteins and carbohydrate compositions, which are brought by changes in gene expression (J. C. Kim et al., 2001). Changes in the expression of some genes during cold tolerance have been suggested previously by Guy et al., (1985) and became an established fact after of various genes have been described in different plants including, Arabidopsis (Gilmour, Artus, & Thomashow, 1992; Hajela, Horvath, Gilmour, & Thomashow, 1990; Horvath, McLarney, & Thomashow, 1993), tomato (Schaffer & Fischer, 1988), alfalfa (Monroy et al., 1993), potato (Baudo, Meza-Zepeda, Palva, & Heino, 1996; van Berkel, Salamini, & Gebhardt, 1994), rice (Aguan, Sugawara, Suzuki, & Kusano, 1993), spinach (Neven, Haskell, Hofig, Li, & Guy, 1993) and rapeseed (Sáez-Vásquez, Raynal, Meza-Basso, & Delseny, 1993).

1.5 Cold regulated genes and role in freezing tolerance

When plants are exposed to low-temperature stress, several genes are expressed but not all of them are involved in freezing tolerance. This means there is a change in gene expression of the cell depending on the type of signal they receive from the environment and the cell requirement (Sanghera, Wani, Hussain, & Singh, 2011).

In general, genes induced during cold stress have two major functions: to produce important metabolic proteins that function to protect plant cells from stress, and regulation of genes involved in receiving stress signals from the environment (Fowler & Thomashow, 2002).

Previous studies show that a large number of low temperature initiated/induced genes encode key metabolic enzymes, late embryogenesis-abundant (LEA) proteins, detoxification enzymes, a large class of molecular chaperons known as heat shock proteins (HSP), protein kinases and transcription factors (TF) that have special role in the process of plant adaptation to low temperatures (Goyal, Walton, & Tunnacliffe, 2005; Joaquín Medina, Catalá, & Salinas, 2011; Singh, Foley, & Oñate-Sánchez, 2002; Michael F. Thomashow, 1998; W. Wang, Vinocur, Shoseyov, & Altman, 2004).

The low-temperature induced genes are collectively called cold-regulated genes (COR) (Chinnusamy, Zhu, & Zhu, 2006; Ganeshan, Vitamvas, Fowler, & Chibbar, 2008). These genes are induced stepwise i.e. during the earlier phase of CA are induced genes involved in C-repeat binding factors (CBFs) and those involved in signal transduction whereas, later are induced genes that function in cellular metabolism and protection against freezing damage (Buko, 2011; P. Jain, 2014).

In wild diploid and cultivated strawberry were described three key enzymes as associated with cold tolerance: (Chalcone synthase, flavonoid 3’-hydroxylase, dihydroflavonol 4-reductase) from the phenylpropanoid biochemical pathway (Koehler et al., 2012), as well as the dehydrins, alcohol dehydrogenase and galactinol (Davik et al., 2013).

1.6 Cold tolerance pathways/mechanisms in plants

Cell membranes are considered to be the primary targets of cold injury in plants (Chaves, Gil, & Delrot, 2015). Through membrane rigidification and/or other cellular changes, which might induce a calcium signature and activate protein kinases necessary for cold acclimation, plants sense low-temperature stress (Miura & Furumoto, 2013b; Örvar, Sangwan, Omann, & Dhindsa, 2000; Sangwan, Foulds, Singh, & Dhindsa, 2001).

The C-repeat-binding factor (CBF1–3) regulon, also known as dehydration-responsive element-binding factor (DREB1B, -1C, and -1A, respectively) is a system of gene expression in plants that regulates the numerous cellular components to adapt to the cold stress (Gilmour, Sebolt, Salazar, Everard, & Thomashow, 2000; Michael F Thomashow, Gilmour, Stockinger, Jaglo-Ottosen, & Zarka, 2001). Cold stress through sumoylation and phosphorylation process induces ICE1 (Inducer of CBF Expressions), which is critical for activation of transcription of CBFs. ICEs are transcription factors controlling cold signaling through the regulation of CBF/DREB1s (Miura & Furumoto, 2013a). ICE1 is expressed and localized in the nucleus, but it induces expression of CBFs only under cold stress. Approximately 40% of the cold-regulated genes (COR) and 46% of cold-regulated transcription factor genes are regulated by ICE1, suggesting that ICE1 functions as a master regulator controlling CBF3/DREB1A and many other COR genes (Lee, Henderson, & Zhu, 2005). Ubiquitylation and proteosomal degradation of ICE1 is mediated by HOS1 (high expression of osmotically responsive genes1), which is a ring finger protein having ubiquitin E3 ligase activity and is the negative regulator of CBF regulon (Beck et al., 2007; Dong, Agarwal, Zhang, Xie, & Zhu, 2006). CBFs regulate the expression of genes involved in phosphoinositide metabolism, transcription, osmolyte biosynthesis, ROS detoxification, membrane transport, hormone metabolism and signaling and many others cellular protective functions (L. Ciarmiello, Woodrow, G, & Carillo, 2011; Venkateswarlu, Shanker, Shanker, & Maheswari, 2011). The expression of c-repeat binding factors/dehydration responsive element binding1 (CBF/DREB1b) genes was found to be induced rapidly and the transcripts accumulated within 15 min of exposure to low temperature in Arabidopsis (Joaquın Medina, Bargues, Terol, Pérez-Alonso, & Salinas, 1999; Michael F Thomashow et al., 2001). Not all low temperature-induced genes are responsive to the CBF regulatory pathway. Part of the CBF regulon are only 12 % of COR genes (Fowler & Thomashow, 2002). SUMO (small ubiquitin-related modifier) conjunction or sumoylation is a SIZ1 (a SUMO E3 ligase) mediated post-translational modification that by blocking its ubiquitination regulates the ICE1, thereby enabling the CBF3/DREB1A transcription (Miura

& Furumoto, 2013b). The expression of CBFs is negatively regulated by MYB15 and ZAT12. CBFs induce the expression of ZAT10, which might down-regulate the expression level of COR genes (Chinnusamy, Zhu, & Sunkar, 2010).

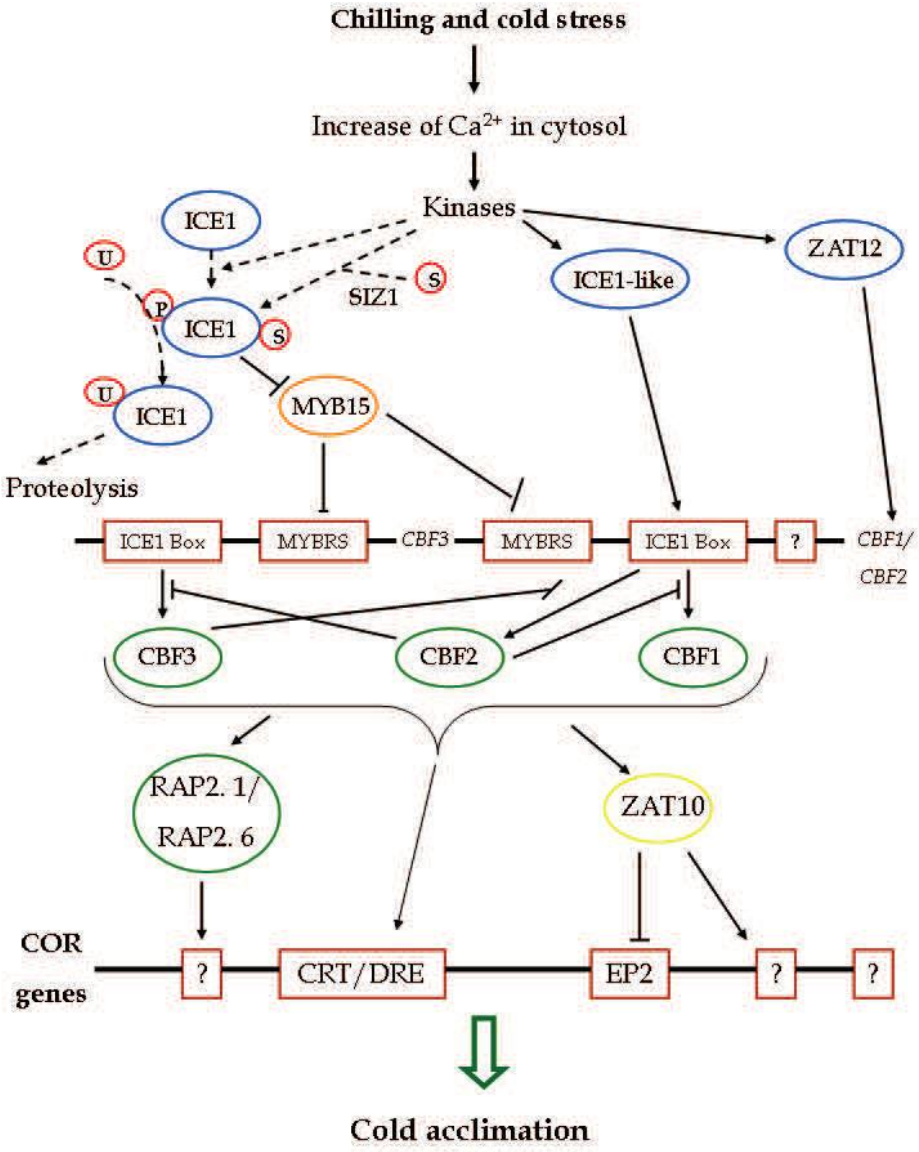

Figure 2*. Diagram of cold-responsive transcriptional network in Arabidopsis. Low temperature-stress-induced calcium signature is necessary for cold acclimation. The stress created during cold activates the ICE1 protein which induces transcription of CBFs and other transcription factors. CBFs regulate expression of COR gene by inducing the ZAT10. C2H2 zinc finger transcriptional repressors are positively regulated by CBFs and negatively regulated by the LOS2. MYB15 and ZAT12 negatively regulate the expression of CBFs. ICE1 proteolysis and ubiquitination are mediated by HOS1, which regulates CBF regulons. Abbreviations: CBF, C-repeat binding factor (an AP2-type transcription factor); HOS1, high expression of osmotically responsive genes1 (a RING finger ubiquitin E3 ligase); ICE1, inducer of CBF expression 1; LOS2, low expression of osmotically responsive genes 2; MYB, myeloblastosis; SIZ1, SAP and MiZ1 (a SUMO E3 ligase); P, phosphorylation; S, SUMO (small ubiquitin-related modifier); U, ubiquitin. Broken arrows indicate post-translational regulation; solid arrows indicate activation, whereas lines ending with a bar show negative regulation; the two stars (**) indicate unknown cis-elements. Figure taken from L. F. Ciarmiello et al.* (2011).

1.7 Next-generation sequencing technologies

Sanger sequencing was the first developed sequencing method by Sanger and Coulson (1975). This technique is still used widely today but some limitations in this technology showed the need for new and improved technologies (Keogh & Chinnery, 2013). So, to fulfill the limitations of the Sanger method, scientists developed next-generation sequencing technologies or NGS (de Magalhães, Finch, & Janssens, 2010; Shapshak et al., 2017). The term NGS is used to describe a number of different modern sequencing technologies including, Illumina (Solexa) sequencing, Roche 454 sequencing, Ion torrent: Proton / PGM sequencing, SOLiD sequencing, PacBio (Pacific Biosciences), and Nanopore sequencing, (Kalia & Kumar, 2017; Phillippy, 2017). These recent technologies allow sequencing of DNA and RNA much more quickly and cheaply than the previously used Sanger sequencing, and as such have revolutionized the study of genomics and molecular biology (Kumar, Dasgupta, & Ranjan, 2018). The major application of NGS technologies is in transcriptional studies (de Magalhães et al., 2010). High throughput sequencing technologies have recently become a popular methodology used among other applications to measure global expression with high accuracy. One of most regarded technology that uses deep-sequencing for transcriptome profiling is RNA-seq. This powerful technique is known to provide precise measurement of levels of transcripts and their isoforms (Z. Wang, Gerstein, & Snyder, 2009).

1.7.1 RNA-seq

The technology of sequencing transcribed RNA followed by mapping and quantification of transcripts is known as RNA-seq, which have provided a powerful approach for studying the entire transcriptomes (Z. Wang et al., 2009; X. S. Zhang, Pei, Zhao, Tang, & Fang, 2018). RNA-seq is used to measure gene expression, identify the mRNAs, non-coding RNAs and small RNAs (Chen et al., 2016; Y. Wang et al., 2016). The information acquired from RNA-seq greatly increases the understanding in many other areas beyond revealing gene expression pattern, such as the discovery of many novel isoforms of mRNA transcripts and mechanisms of alternative splicing (D. Kim & Salzberg, 2011; Trapnell, Pachter, & Salzberg, 2009).

RNA-seq offers several solid advantages over hybridization-based methods. Firstly, it does not require a priori knowledge of the query genome, thus it can be used to sequence the transcriptome of an organism with no available sequence genome and it can detect novel transcripts (Hurd & Nelson, 2009). Secondly, it has high reproducibility but low noise level. Furthermore, it has a broader dynamic range and been shown to be an accurate platform for

quantifying gene expression level (S. Zhao, Fung-Leung, Bittner, Ngo, & Liu, 2014). Summarizing, it is the first sequencing method that potentially allows the entire transcriptome to be surveyed in a very quantitative and high-throughput manner (Ching et al., 2014; Z. Wang et al., 2009). Therefore, it is quickly replacing microarrays as the platform for gene expression profiling (Ching et al., 2014; Hurd & Nelson, 2009).

The procedure of RNA-sequencing involves different steps: taking purified RNA samples, shearing it, converting to cDNA, and sequencing on NGS platforms such as Illumina Genome Analyzer, Roche 454 Life-sciences or Applied Biosystems Solid sequencing systems (Han, Gao, Muegge, Zhang, & Zhou, 2015). This process can generate millions of short reads (25-700 bp) taken from one or two ends (paired-end reads) of the cDNA fragments (Jeggari, 2013).

1.8 RNA-seq data preparation for gene expression analysis

The millions of short reads generated from sequencing platforms can be reconstructed or mapped on a reference genome, this process is called transcriptome assembly (Finotello & Di Camillo, 2015). In order to investigate the transcript expression or perform gene quantification a complete transcriptome annotation and assembly is needed (Trapnell et al., 2012).

Transcriptome assembly is the core step of RNA-seq data analysis among all (Tjaden, 2015). Assembly can be done by using either reference-based or *de novo* assembly (Figure 3). In reference-based assembly, reads are mapped back to the sequenced or existed reference genome. While, in *de novo* assembly reads are compared to each other to reconstruct expressed isoforms without the need of using a reference genome (Conesa et al., 2016; Lischer & Shimizu, 2017; Robertson et al., 2010; Rodriguez et al., 2013). *De novo* assembly involves assembling transcripts by combining overlapping reads, is necessary when a high-quality reference genome is not available (Martin & Wang, 2011; Tjaden, 2015). For reconstructing transcriptomes from RNA-seq data for analyzing the diverse model and non-model organisms, are developed modern and popular software including Trinity (Grabherr et al., 2011) and CLCbio Genomic Workbench (Bio, 2012). The Trinity software, which is mainly developed for *de novo* transcriptome assembly from short-read RNA-seq data, was found to be successful, efficient, and sensitive in assembling full-length transcripts (Q.-Y. Zhao et al., 2011).

After construction of *de novo* transcriptome assemblies evaluating the accuracy and completeness of that is very important and this can be done by using different tools, including DETONATE (Bo Li et al., 2014), TransRate (Smith-Unna, Boursnell, Patro, Hibberd, & Kelly, 2016) and rnaQUAST (Bushmanova, Antipov, Lapidus, Suvorov, & Prjibelski, 2016).

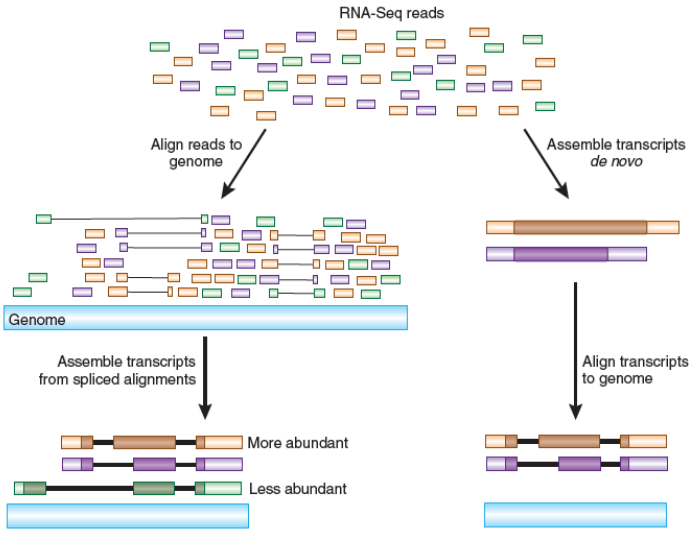

Figure 3: *Strategies for reconstructing transcripts from RNA-seq reads. Figure taken from* Haas & Zody (2010).

Functional annotation is very important in the biological interpretation of experimental results (Conesa & Götz, 2008). There are available various types of annotation tools with a more or less elaborated strategy to have a limitation with large sequencing data (Götz et al., 2008). Conesa et al., 2005, designed a bioinformatics tool called Blast2GO (B2G), that allows automatic and high throughput sequence annotation and integrate functionality for annotation-based data mining. B2G usually consists of 5 steps automated process that runs simultaneously: BLASTing, mapping, annotation, statistics analysis and visualization; with the advanced functionalities and minimal computational setup (Conesa et al., 2005).

1.9 Gene expression analysis

Gene expression analysis includes investigation of the pattern of expressed genes at the transcription level, under specific circumstances or in a specific cell (Lovén et al., 2012).
The use of molecular techniques such as serial analysis of gene expression (SAGE), massive parallel signature sequencing (MPSS), microarray expression profiling, and more recently RNA-sequence analysis of transcript abundance, has allowed an unprecedented look at the workings of the genome (Frigessi et al., 2005; M. Jain, 2012; O'Brien, Costin, & Miles, 2012; Z. Wang et al., 2009). The relative abundances of the RNAs transcribed from the genes reflect the expression level of the corresponding genes, for a specific developmental stage or physiological condition (Finotello & Di Camillo, 2015). Although RNAs are not the final products of the transcription-translation process, the study of gene expression and differential gene expression can unveil important aspects about the cell states under investigation (Finotello & Di Camillo, 2015). RNA-seq combined with appropriate bioinformatics tools provides a wonderful approach to identify and quantify the expression of transcripts and their isoforms (C. Zhang, Zhang, Lin, & Zhao, 2017). If the aim of an RNA-seq study is the detection of DE genes and if a well-annotated transcriptome assembly is available, a basic data processing pipeline consists in the following steps: read mapping, read counting, counts normalization and detection of differentially expressed genes (Finotello & Di Camillo, 2015).
Read mapping is a process where reads are mapped to the reference genome or to the transcriptome sequences reconstructed using de novo assembly strategies (see Figure 4). The task at this step is to find the genomic location where each short read best matches to the reference genome or transcript set (Lunter & Goodson, 2011). In order to produce the quantitative expression data, reads must be mapped to a reference sequence (Langmead & Salzberg, 2012). Read mapping output produce a SAM (Sequence Alignment/Map) file which includes information about the reference and read sequences, each read mapping location and the quality of alignment (H. Li et al., 2009). Bowtie is an ultrafast, memory-efficient short read aligner which has alignment speed of more than 25 million reads per hour (Langmead, Trapnell, Pop, & Salzberg, 2009). Bowtie is integrated into the RSEM (RNA-seq by Expectation Maximization) (B. Li & Dewey, 2011) a read counting package, which saves the time of a user by doing Bowtie alignment and quantifying transcripts abundances (W. Li, Richter, Jung, Zhu, & Li, 2016).

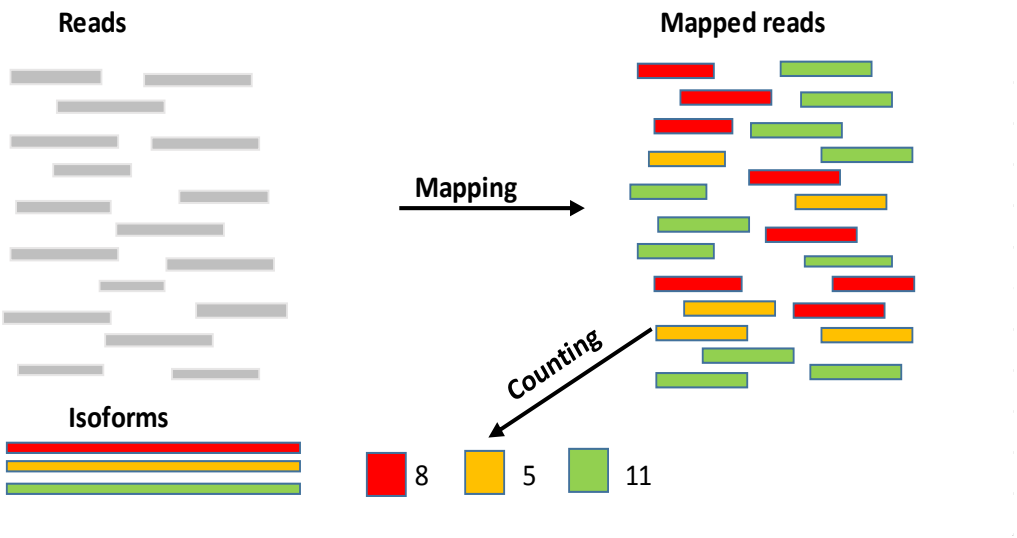

Figure 4. *Read mapping and counting process.*

Read counting is performed after read mapping step is completed (Figure 4). This process includes counting the number of reads that have mapped to the gene and isoform levels (Finotello & Di Camillo, 2015). The RNA-seq reads do not map always uniquely to a single gene or isoform, which is a great complication in counts computation process (B. Li & Dewey, 2011). More recent methods, such as RSEM, is a software tool for quantifying transcript abundances from RNA-seq data and calculate maximum likelihood estimates of isoform expression levels using the Expectation-Maximization algorithm (Finotello & Di Camillo, 2015). As it does not rely on the existence of a reference genome, it is useful for quantification with de novo transcriptome assemblies. RSEM uses Bowtie aligner to map reads to a reference sequence and for each read it records every possible alignment and their quality score, which are later used to determine the count estimates (B. Li & Dewey, 2011; Liu, 2014).

Normalization is a method which applies to remove systematic technical effects that occur during data creation to ensure that technical bias has minimal impact on the results. Normalization in RNA-seq data has two possible levels, one is based on transcript length and another level is based on expression level between libraries (Oshlack & Wakefield, 2009).

Robinson & Oshlack (2010), introduced a scaling factor called Trimmed Mean of M-values (TMM), which is an integrated method into an RNA-seq analysis package called edgeR (Empirical analysis of Differential Gene Expression in R), a package written in R language. A trimmed mean is the average after removing the upper and lower x% of the data. TMM algorithm run parallel with differential expression calculations and is considered as a well-built method (Robinson & Oshlack, 2010).

1.9.1 Differential gene expression analysis

Differential expression analysis means taking the normalized read count data and performing statistical analysis to highlight genes that have changed significantly in abundance across experimental conditions (Anders et al., 2013; Oshlack, Robinson, & Young, 2010). For the identification of differentially expressed genes between different treatments groups based on RNA-Seq data have been developed many software packages (Z. H. Zhang et al., 2014). The most commonly used software packages are: edgeR (Robinson, McCarthy, & Smyth, 2010), DESeq (Anders & Huber, 2010), Cuffdiff (Trapnell et al., 2013), PoissonSeq (J. Li, Witten, Johnstone, & Tibshirani, 2012), baySeq (Hardcastle & Kelly, 2010) and limma (Smyth, 2004). Z. H. Zhang et al. (2014) evaluated the performance of three software tools, edgeR, Cuffdiff and DESeq for differential expression analysis of RNA-Seq data while considering a number of important parameters, including the number of replicates, sequencing depth, and the unbalanced data within or between experimental groups. The authors observed that edgeR performs better than DESeq and Cuffdiff in terms of the ability to uncover true positives with the default FDR setting (FDR<0.05) and this reflects that edgeR could always detect more DEGs than the other two tools. Moreover, Z. H. Zhang et al. (2014) confirmed that the biological replicates are a key factor for differential expression analysis and that the software tools perform much better when the biological replicates available. However, in experiments designed with few numbers of replicates, the edgeR package is a recommended tool from previous studies (Schurch et al., 2016; Z. H. Zhang et al., 2014).

The edgeR package introduced by Robinson et al. (2010), is part of Bioconductor project that was initially developed for serial analysis of gene expression. This method is applicable to emerging technologies such as RNA-seq, which give expression data in digital format. The software correctly find out the changes in its expression between two or more groups, when at least one of the groups has logarithmic measurements on a specified condition. The data can be summarized into a table of counts, with rows corresponding to genes (tags, exons or transcripts) and columns to samples.

The differential expression calculation use following equation for each gene g and sample i, which can be modeled by a negative binomial distribution,

$$Y_{gi} \sim \mathrm{NB}\ (M_i\, p_{gj},\, \phi_g)$$

Where, *Mi* is the library size (total number of reads), ϕg is the dispersion parameter which is variable for sample to sample and *pgj* is the relative abundance of gene *g* in experimental group *j* to which sample *i* belongs (Robinson et al., 2010).

1.9.2 Real-time PCR

Real-time polymerase chain reaction (RT-qPCR) is commonly used to measure gene expression (Livak & Schmittgen, 2001). It is very sensitive in detecting small changes in expression and is best suited for studies of small subsets of genes (Huerta & Burke). The disadvantage of this method is that the sequence of the specific gene of interest must be known, hence real-time PCR can only be used for studying known genes (Smith & Osborn, 2009).
Real-time PCR can be used to assess gene expression, by converting a cell's mRNA into cDNA via reverse transcription, followed by several rounds of PCR to amplify and detect the genes of interest. TaqMan or SYBR-green probes can be used to detect the product in 'real-time'. (Jensen, 2012). Gene expression studies using RT-qPCR include the comparison of the expression level of one gene (the target) with the expression level of another gene (the reference or calibrator). Stable and secure unregulated transcript such as a house-keeping gene (transcript) are used as reference gene. Expression level of the genes can be compared across tissue types and in response to an experimental treatment (Livak & Schmittgen, 2001).

1.10 Aim of the study

The aim of the work presented in this master thesis was to perform bioinformatics analysis and follow-up experimental validation of the RNA-seq data from two Strawberry cultivar's 'Jonsok' and 'Elsanta' that differ in freezing tolerance, for further identification of transcripts related to cold tolerance. The above mentioned aim was achieved by the following specific aims:

- From previously de-novo assembled transcriptome, perform pairwise differential expression analysis using edgeR and identify various sets of differentially expressed transcripts with respect to control (0 h) versus different cold stress time points (1 h, 5 h, 48 h and 240 h)
- In depth, analysis of the DE results to identify the most up- and down regulated transcripts from the results of each pairwise comparison of both cultivars
- Identification of transcripts related to cold tolerance and expression profiles of these transcripts in both cultivars
- Perform RT-qPCR and sequence the PCR product for the selected genes related to cold tolerance
- Comparison of the results obtained from RT-qPCR with the results from bioinformatic analysis of RNA-seq data to confirm the bioinformatics analysis of RNA-seq data

2. Material and Methods

The research work was carried out at Inland Norway University of Applied Sciences (INN) from February 2017 – May 2018. The project is in collaboration with Graminor Breeding Limited (GBL), the authority responsible for providing the required data to this scientific research. The project is divided into two sections 1) Gene expression analysis of RNA-seq data, 2) Experimental validation of selected genes. All the analysis were performed under the INN environment and the main bioinformatics platform used in this project was the software package edge R included in Blast2GO version 5.0.13.

2.1 Ethics Statement

The necessary permits were obtained from the GBL, the authority responsible for providing the required RNA-seq data to this research work. The dataset used in this study was provided by GBL by signing the confidential disclosure agreement since the data were not publicly available.

2.2 RNA-seq data set

RNA-seq dataset used in this study were standard Illumina data set (Paired-end) from two different strawberry cultivars, 'Elsanta' and 'Jonsok' in FASTQ format. Both of these cultivars datasets included the treatment at 2° C at five different time points: 0 h (control), 1 h, 5 h, 2 days (48 h) and 10 days (240 h). For each time point were three different replicates of paired-end Illumina reads (Table 1).

In previous study that was part of this project, RNA-seq data from two Strawberry (*Fragaria x ananassa*) cultivars that differ in tolerance to low temperatures were assembled. Different variations of de novo and reference-based assemblies were performed using CLC main workbench and Trinity software. However, assemblies containing all sample replicate files from each time point were chosen as best assemblies and were named as JAD (assembly of 'Jonsok' cultivar) and EAD (assembly of 'Elsanta' cultivar). Also, the transcripts were functionally annotated for the selected assembly using Blast2GO software (Bhandari, 2016). By using the count data produced by a read counting package RSEM (RNA-seq by Expectation Maximization), it was created a matrix containing the counts of RNA-seq

fragments for each sample in a simple tab-delimited text file. These files were used to perform differential gene expression analysis.

Table 1. *Details of Illumina data sets for the strawberry cultivars Elsanta and Jonsok*

Cold Treatment time at 2° C	Cultivars			
	Elsanta		Jonsok	
	File name	Size (GB)	File name	Size (GB)
0 h (control)	Elsanta0hrR1CGATGTR1.fastq Elsanta0hrR1CGATGTR2.fastq	21.5	Jonsok0hrR1CGATGTR1.fastq Jonsok0hrR1CGATGTR2.fastq	22.1
	Elsanta0hrR2CAGATCR1.fastq Elsanta0hrR2CAGATCR2.fastq	19.0	Jonsok0hrR2CAGATCR1.fastq Jonsok0hrR2CAGATCR2.fastq	14.9
	Elsanta0hrR3GTGAAAR1.fastq Elsanta0hrR3GTGAAAR2.fastq	18.3	Jonsok0hrR3GTGAAAR1.fastq Jonsok0hrR3GTGAAAR2.fastq	20.0
1 h	Elsanta1hrR1CGATGTR1.fastq Elsanta1hrR1CGATGTR2.fastq	17.1	Jonsok1hrR1CGATGTR1.fastq Jonsok1hrR1CGATGTR2.fastq	21.2
	Elsanta1hrR2CAGATCR1.fastq Elsanta1hrR2CAGATCR2.fastq	21.5	Jonsok1hrR2CAGATCR1.fastq Jonsok1hrR2CAGATCR2.fastq	21.1
	Elsanta1hrR3GTGAAAR1.fastq Elsanta1hrR3GTGAAAR2.fastq	19.5	Jonsok1hrR3GTGAAAR1.fastq Jonsok1hrR3GTGAAAR2.fastq	17.2
5 h	Elsanta5hrR1CGATGTR1.fastq Elsanta5hrR1CGATGTR2.fastq	20.7	Jonsok5hrR1CGATGTR1.fastq Jonsok5hrR1CGATGTR2.fastq	24.0
	Elsanta5hrR2CAGATCR1.fastq Elsanta5hrR2CAGATCR2.fastq	18.2	Jonsok5hrR2CAGATCR1.fastq Jonsok5hrR2CAGATCR2.fastq	18.1
	Elsanta5hrR3GTGAAAR1.fastq Elsanta5hrR3GTGAAAR2.fastq	16.9	Jonsok5hrR3GTGAAAR1.fastq Jonsok5hrR3GTGAAAR2.fastq	10.6
48 h (2 days)	Elsanta2daysR1CGATGTR1.fastq Elsanta2daysR1CGATGTR2.fastq	19.1	Jonsok2daysR1CGATGTR1.fastq Jonsok2daysR1CGATGTR2.fastq	16.6
	Elsanta2daysR2CAGATCR1.fastq Elsanta2daysR2CAGATCR2.fastq	15.1	Jonsok2daysR2CAGATCR1.fastq Jonsok2daysR2CAGATCR2.fastq	18.4
	Elsanta2daysR3GTGAAAR1.fastq Elsanta2daysR3GTGAAAR2.fastq	19.3	Jonsok2daysR3GTGAAAR1.fastq Jonsok2daysR3GTGAAAR2.fastq	15.9
240 h (10 days)	Elsanta10daysR1CGATGTR1.fastq Elsanta10daysR1CGATGTR2.fastq	18.9	Jonsok10daysR1CGATGTR1.fastq Jonsok10daysR1CGATGTR2.fastq	19.7
	Elsanta10daysR2CAGATCR1.fastq Elsanta10daysR2CAGATCR2.fastq	16.5	Jonsok10daysR2CAGATCR1.fastq Jonsok10daysR2CAGATCR2.fastq	25.5
	Elsanta10daysR3GTGAAAR1.fastq Elsanta10daysR3GTGAAAR2.fastq	21.2	Jonsok10daysR3GTGAAAR1.fastq Jonsok10daysR3GTGAAAR2.fastq	14.5

2.3 Identification of differentially expressed transcripts

Differentially expressed (DE) transcripts across different time points for both cultivars were identified and clustered by performing pairwise analysis using 'edgeR Bioconductor' package (Robinson et al., 2010) included in Blast2GO software version 5.0.13 (Conesa et al., 2005).

The Pairwise DE Analysis allows identification of DE genes in a pairwise comparison of two different experimental conditions. This comparison in our study was between control (0 h) versus each treatment time point, for example, J00vsJ01, J00vsJ48 or E00vsE05.

To perform DE analysis it was necessary to create a matrix containing the counts of RNA-seq fragments for each sample in a simple tab-delimited text file using the expected count data produced by RSEM. Since biological replicates are present, was created a tab-delimited text file to indicate the relationship between conditions, E00 or J00 are control samples while E01, E05, E48, E240, J01, J05, J48, J240 are respective test samples for 'Elsanta' as (E) and 'Jonsok' (J) cultivars. The tab-delimited text file and the count matrix were used as input files in Blast2GO software, in order to identify DE transcripts for each pair of samples.

The expression differences compared with edgeR, leads to a ranked list of genes with associated, log fold change (log FC), log- counts per million (log-CPM), p-values, false discovery rate (FDR).

Fold change (FC) is a unit used to estimates the biological significance and is often used in gene expression analysis of microarray, RT-qPCR and RNA-seq to measure the change in gene expression level. The log2FC is the log-ratio of a gene's or a transcript's expression values in two different conditions and is used to confirm the significance of the differential expression between the different samples. In the present study, transcripts with logFC > 1 were characterized as up-regulated and transcripts with logFC < −1 as down-regulated.

Genes with very low counts across all libraries provide little evidence for differential expression analysis. They also add to the multiple testing burdens when estimating false discovery rates, reducing power to detect differentially expressed genes. These genes should be filtered out prior to further analysis. Counts Per Million (CPM) is a filter to exclude genes with low counts across libraries. Log CPM is the log counts per million, which can be understood as measuring expression level. In the dataset, we chose to retain genes if they were expressed at a counts-per-million (CPM) above 0.5.

The False Discovery Rate (FDR) controls the number of false discoveries in those tests that result in a discovery (i.e. a significant result). This approach determines adjusted p-values for

each test. In our analysis, the number of DE transcripts was detected by using the FDR <0.05, that implies 5% of significant tests will result in false positives.

In the RNA-seq experiments that have purpose identification of DE genes, the presence of biological replicates is necessary. In this experiment, each treatment time point of two cultivars consists of three biological replicates. However, the minimum number of samples reaching CPM filter was two. This was done because in one group was missing one replicate. However, in order to avoid compositional biases between libraries, a TMM (Trimmed mean of M values) normalization method was applied.

The results from pairwise comparison analysis between control and different cold treatment time points of two strawberry cultivars were used for selection of the most up- and down-regulated transcripts and identification of the transcripts associated with cold tolerance.

2.3.1 Selection of the most DE transcripts

The selection of 30 most differentially expressed transcripts of ‘Jonsok’ and ‘Elsanta’ cultivar was done based on their expression level (log2FC). The pairwise DE analysis gives a ranked list with information including log2FC, log-CPM, FDR. Then, from the lists of eight pairwise comparisons manually were selected the 15 top most up-regulated and 15 most down-regulated transcripts based on the log2FC values. In the analysis, a particular transcript is defined as most differentially expressed either up-regulated or down-regulated, if its log2FC value was in the list of highest or lowest one.

2.3.2 Selection of transcripts related to cold tolerance

To select transcripts related to cold tolerance first it was necessary to check in literature and understand the cold tolerance pathway mechanism in plants. Also, it was very helpful a list with the transcript names suggested from Stephen Randall, professor of Biology, at Indiana University-Purdue University Indianapolis. Based on that were selected 21 genes, including all isoforms. Also, were selected the data about changes in expression level (logFC) of these isoforms at all treatment time points. The selection was done manually based on the description name on the functional annotation list generated by Blast2GO. To make sure that all the isoforms were selected for a particular gene, a blast check was performed against assembly because for some isoforms there was no description name available.

2.4 Primer design

Gene-specific primer pairs were designed for six targets: dehydrin COR47-like, CDPK1 (calcium-dependent protein kinase 1), aldo keto reductase, chalcone synthase, cytosolic aldolase, and transcription factor ICE. The primers were designed using the CLC Genomic Workbench primer design tool using the following parameters: primer length 17-26 nt; melting temperature (Tm) 56-62 °C; % GC content 30-70; NaCl 50 mM; dNTPs 0.1 mM; Mg Cl_2 1,5 mM. The amplicon lengths were between 100-450 base pairs. In Table A1 in Appendix are shown the primer pairs sequences for these six targets, the reference PP2A and the four other primer pairs that are used for sequencing.

2.5 RNA-seq data validation by RT-qPCR

In order to confirm the expression obtained in the RNA-seq data, the RT-qPCR was performed. Steady-state gene expression levels of each target were analyzed by RT-qPCR using Eva Green® to monitor dsDNA synthesis. Each reaction contained 3.15 µl 5X Hot FIREpol EvaGreen qPCR Mix plus ROX (Solis BioDyne), 1.5 µl (1mM) primer mix (Forward/ Reverse) and cDNA template (1/100) up to 15 µl. The samples were loaded on the AB17500 RT-qPCR detection system (Applied Biosystems, USA) for analyzing. The thermal cycling parameters were as follow: 12 min at 95 °C, 40 cycles consisting of 15 s at 95 °C, 30 s at 58 °C and 32 s at 72 °C, and then one cycle consisting of 15 s at 95 °C, 1 min at 60 °C, 15 s at 95 °C and 15 s at 60 °C. To normalize the fluorescent reporter signal was used ROX as the internal passive reference dye. The expression level of each transcript was normalized to the reference gene PP2A used as internal loading control. Three biological replicates were analysed for each time point and the average of the replicates was used to calculate the fold change level. Except, in the 'Elsanta' cultivar at 48 h cold treated samples, a replicate was missing. The analysis for this treatment time point was performed only for two replicates. The relative quantification of a target gene in comparison to a reference gene was calculated according to the method presented by Pfaffl (2001). The calculations were done according to the following equation:

$$(E_{target})^{\Delta CP_{target}\,(control\text{-}sample)} / (E_{PP2A})^{\Delta CP_{\,PP2A}\,(control\text{-}sample)}$$

Where, the ratio of a target gene is expressed in a sample versus a control in comparison to reference (PP2A). E_{target} is the real-time PCR efficiency of target gene transcript; E_{PP2A} is the real-time PCR efficiency of a reference gene transcript; ΔCP_{target} is the CP deviation of control

– sample of the target gene transcript; ΔCP_{PP2A} = CP deviation of control – sample of reference gene transcript.

2.6 Direct sequencing of PCR product

The sequence composition of the amplified RT-qPCR products was verified by sequencing. To perform direct sequencing were selected the PCR product with the lowest Ct value, from each target were taken two samples, one from 'Jonsok' and one from 'Elsanta'. The BigDye® Terminator v 3.1 Cycle Sequencing Kit (Applied Biosystems) was used for sequencing. Prior to sequencing, the PCR amplified products were treated with Exonuclease1 (Exo I) to remove excess primer.

The added amount of PCR product was calculated based on Ct value as follow.

Ct value	Volume µl
20-25	2
26-30	3.5
31-35	6
36-40	7.8

Then, were added 2 µl of 5x sequencing buffer, 0.2 µl of Exo I (20 u/µl) and H2O up to total volume of 10 µl. Samples were incubated at 37 °C for 60 min, 85 °C for 15min and then held at 10 °C in a thermal cycler. Sequencing reactions were performed following St_ep method (Platt, Woodhall, & George, 2007). Amplified fragments were sequenced in both directions (once using the forward primer, and once using the reverse primer) for greater accuracy of the base calls in the overlapping regions (repeated regions). The sequencing product was purified according to the NaOAc/EDTA/EtOH precipitation method as follows. Were added 2 µl 125 EDTA, 2 µl 3M NaAc, and 52 µl 96 % EtOH to the 10 µl product from the sequencing reaction in an Eppendorf tube and incubated this at room temperature (RT) for 15 min. This was centrifuged at maximum speed (14000 rpm) for 30 min at 4 °C, the supernatant was discarded and the pellet was washed twice with 70 µl of 70 % EtOH and centrifuged at max speed for 15 min at RT. The EtOH was carefully removed from the tube and the pellets were centrifuged at max speed for 10 min. Then, the pellets were dried in fume hood approximately 30 min. The precipitated sequencing products were denatured in 10 µl deionized formamide and run in Applied Biosystems 3130xl Genetic Analyzer using BDv3_1_RapidSeq_POP7_1 run module.

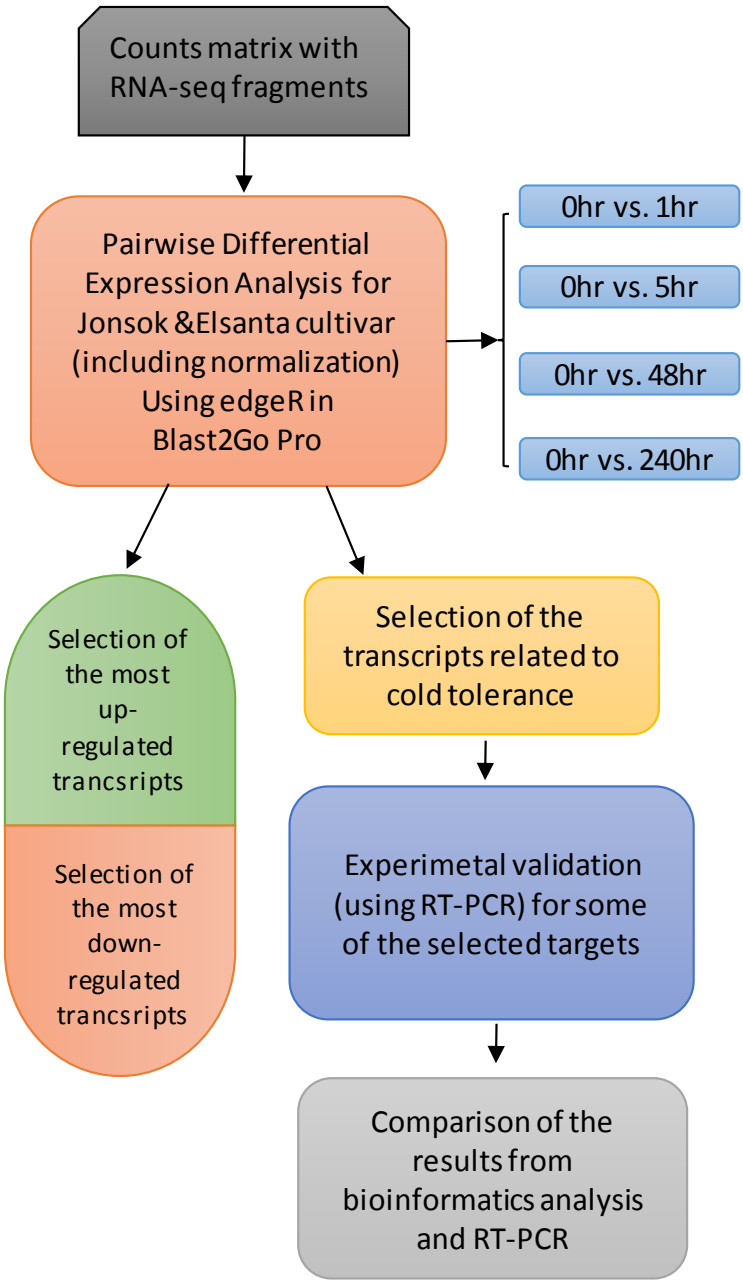

***Figure 5**: Schematic representation of the various steps performed during differential expression analysis of RNA-seq data and experimental validation of target transcripts related to cold tolerance.*

3. Results and discussion

3.1 Pairwise Differential Expression Analysis

The differential expression attributes such as p-values, FDR, and log2 fold change values from count data were calculated using edgeR package, implemented within Blast2GO Pro. By performing pairwise DE analysis we identified various sets of DE transcripts with respect to the 0 h control versus different cold stress time points (1, 5, 48 and 240 h).

The number of DE transcripts in 'Jonsok' cultivar (Figure 6) changes with the cold treatment time points. For Jonsok samples treated at 2 °C for 1 h, 1891 transcripts were up-regulated, whereas 827 transcripts were down-regulated. At 5 h treatment, the number of DE transcripts increased, with 5060 transcripts up-regulated and 1972 transcripts down-regulated. After 48 h, 9744 transcripts were found to be up-regulated and 12214 down-regulated. At 240 h cold treatment, the number of DE transcripts was observed to be the highest, with 9852 transcripts up-regulated and 14446 down-regulated.

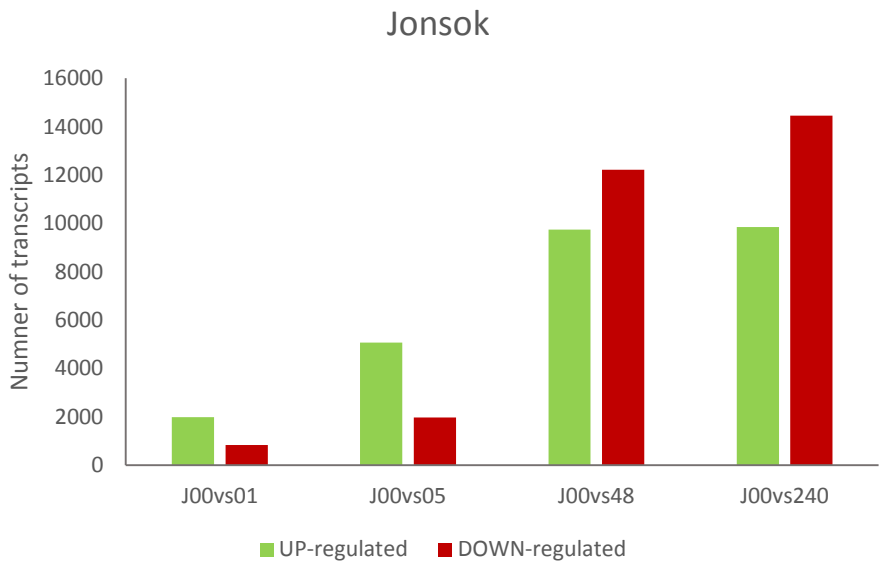

***Figure 6**. Distribution of differentially expressed transcripts (up- and down-regulated) at each time point for 'Jonsok' cultivar. The DE transcripts were identified using a threshold of FDR (false discovery rate) < 0.05 and absolute value of log2 fold change >1 for up-regulated and <-1 for down-regulated transcripts. The J00vs01, J00vs05, J00vs48 and J00vs240 represents four samples treated at 2 °C for 1 h, 5h, 48 h and 240 h in pairwise comparisons with control (0 h).*

The number of up-regulated transcripts exceeded that for those down-regulated at 1 h and 5 h treatment whereas, at 48 and 240 h was the opposite. The most significant change in the number of differentially expressed transcripts was observed between 5 h and 48 h (Figure 6).

The distribution of differentially expressed transcripts at different cold treatment time points in the cultivar 'Elsanta' is shown in Figure 7. At 1 h cold treatment at 2 °C, the number of up-regulated transcripts was found to be 5520 and the number of down-regulated was nearly half of that, with only 2594 transcripts. After 5 h cold treatment, the number of up-regulated transcripts increased in 8492 and of those down-regulated in 4770. The increase in the number of up- and down-regulated transcripts continued also at 48 h treatment, where 11423 transcripts were up-regulated and 12727 down-regulated. However, after 240 h treatment, the number of differentially expressed transcripts is slightly lower, with 9330 up-regulated and 12727 down-regulated transcripts. A linear increasing trend in the number of DE transcripts was observed throughout all cold treatment time points, except the 240 h treatment.

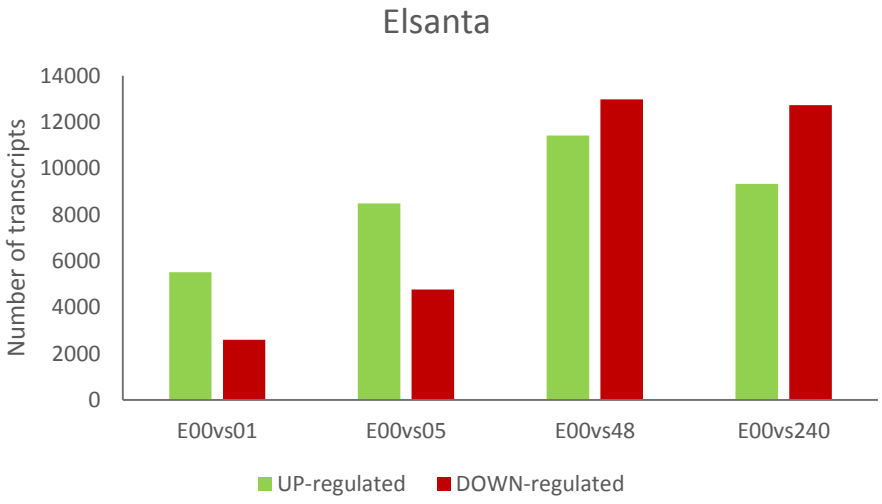

Figure 7*. Distribution of differentially expressed transcripts (up- and down-regulated) in each time point for Elsanta cultivar. The DE transcripts were identified using a threshold of FDR (false discovery rate) < 0.05 and absolute value of log2 fold change >1 for up-regulated and <-1 for down-regulated transcripts. The E00vs01, E00vs05, E00vs48 and E00vs240 represents four samples treated at 2 °C for 1 h, 5 h, 48 h and 240 h in pairwise comparisons with control (0 h).*

The pattern in the number of differentially expressed transcripts was similar among cultivars at respective cold treatment time point. At 1 h and 5 h treatment, the number of up- and down-regulated transcripts in 'Elsanta' were almost the double of the number of transcripts differentially expressed in 'Jonsok'. After, 48 h cold treatment the number of up- and down regulated genes in 'Elsanta' was slightly higher compared to 'Jonsok'. But, this trend was not

followed by 240 h cold treatment since the number of DE transcripts it was greater in ‘Jonsok’ cultivar. For both the ‘Elsanta’ and ‘Jonsok’, the most significant change in the number of DE transcripts was observed between 5 h and 48 h treatment time points (Figure 6 and 7). These results are in agreement with the findings of Peng et al. (2015) in an experiment on paper mulberry treated under 0, 6, 12, 24, 48 and 72 h cold stress. Peng and co-authors reported that the transcriptional level of a large number of genes has been restored after 12 h treatment.

3.2 Selection of most differentially expressed transcripts

The selection of 30 most differentially expressed transcripts of ‘Jonsok’ and ‘Elsanta’ cultivar was done based on their expression level (log2FC). After identifying DE transcripts from four pairwise comparisons of each cultivar, we have selected 15 top most up-regulated and 15 most down-regulated transcripts from each comparison. The expression level of the selected transcripts was identified at all treatment time points (Tables A2-A9 in Appendix).

The Table 2 lists the 10 top most DE (5 up-regulated and 5 down-regulated) transcripts of ‘Jonsok’ cultivar at 48 h cold treatment time point and expression level of these transcripts at other cold treatment time points (1, 5 and 240 h). The transcripts that are presented as NA (not available) were not DE in that cold treatment time point. As most up-regulated transcript (TRINITY_DN293687_c0_g1_i7) was found to be annotated as galactinol synthase 2-like, which is a gene involved in the biosynthesis of raffinose family oligosaccharides (RFOs), that function as osmoprotectants and promotes cold stress tolerance by mediating an increase in levels of the endogenous osmoprotective compounds, galactinol and raffinose (Taji et al., 2002). This transcript was highly expressed only in 48 h (16 log2FC) and 240 h (15 log2FC). Our findings are not in accordance with the study conducted by Taji et al. (2002) in *Arabidopsis thaliana*. The authors reported that galactinol synthase 2 was induced by drought and high-salinity stresses, but not by cold stress. Moreover, they suggested that galactinol synthase 3 was induced by cold stress. However, based on our bioinformatic analysis of cultivated strawberry, we suggest that the galactinol synthase 2-like is most likely to be induced by cold stress. Considering the fact that the expression level of this transcript in ‘Elsanta’ cultivar was half of the expression level observed in ‘Jonsok’.

The transcript (TRINITY_DN302854_c0_g1_i4) annotated as probable galactinol--sucrose galactosyltransferase1 was highly up-regulated at all treatment time points with the highest levels at 48 h (14 log2FC). This transcript may be involved in a ping-pong reaction mechanism as transglycosidase in the synthesis of raffinose (The UniProt Consortium, 2017).

The two other most up-regulated transcripts (TRINITY_DN287924_c1_g1_i1, TRINITY_DN289945_c0_g1_i14) were found to be annotated as embryonic DC-8-like and late embryogenesis abundant 76-like isoform X1, which were not available in 1 h treatment but in other time points the expression level was quite high with 15 log2FC at 48 h for both transcripts. Also, another transcript (TRINITY_DN289945_c0_g1_i5) annotated as late embryogenesis abundant 76-like isoform X1, has almost the same expression profile, with the highest expression level in 240 h treatment time point (15 log2FC). The overexpression of the late embryogenesis abundant genes was reported in the previous findings of Hundertmark & Hincha (2008). The authors identified 51 LEA protein-encoding genes in the *Arabidopsis* genome and most of the genes encoding these proteins had low-temperature response elements in their promoters and were induced by cold stress. Based on the differential expression results of 'Jonsok' and 'Elsanta' this transcript might have an important role in cold tolerance. The detailed information about expression levels of this transcript in both cultivars can be found in the supplementary data.

Table 2. *Details for the 10 most DE transcripts, 5 up-regulated and 5 down-regulated of Jonsok cultivar at 48 hours (J00vs48) cold treatment and expression level (log2 fold change) of these transcripts in other time points (J00vs01- 1 hour, J00vs05- 5 hours, J00vs240- 240 hours).*

Sequence Name	Description	GO IDs	GO Names	J00vs01 (Log2FC)	J00vs05 (Log2FC)	Most DE J00vs48 (Log2FC)	J00vs240 (Log2FC)
TRINITY_DN293687_c0_g1_i7	galactinol synthase 2-like	F:GO:0016757; P:GO:0008152	F:transferase activity, transferring glycosyl groups; P:metabolic process	NA	NA	**16**	15
TRINITY_DN287924_c1_g1_i1	embryonic DC-8-like			NA	10	**15**	14
TRINITY_DN289945_c0_g1_i14	late embryogenesis abundant 76-like isoform X1			NA	8	**15**	15
TRINITY_DN289945_c0_g1_i5	late embryogenesis abundant 76-like isoform X1			NA	10	**14**	15
TRINITY_DN302854_c0_g1_i4	probable galactinol--sucrose galactosyltransferase 1	F:GO:0003824; P:GO:0008152	F:catalytic activity; P:metabolic process	12	10	**14**	13
TRINITY_DN296012_c0_g1_i3	PREDICTED: uncharacterized protein LOC105349822			-4	-5	**-12**	-13
TRINITY_DN299697_c0_g3_i2	Phosphatase 2C family isoform 2 [Theobroma cacao]	F:GO:0004722; F:GO:0046872; P:GO:0006470	F:protein serine/threonine phosphatase activity; F:metal ion binding; P:protein dephosphorylation	-3	-3	**-12**	-6
TRINITY_DN304907_c0_g2_i8	Respiratory burst oxidase D [Theobroma cacao]	P:GO:0007231; C:GO:0005794; P:GO:0043069; C:GO:0005886; P:GO:0042744; F:GO:0004601; P:GO:0009408; F:GO:0005509; F:GO:0016174; C:GO:0016021; P:GO:0033500; P:GO:0098869; P:GO:0055114; P:GO:0050832	P:osmosensory signaling pathway; C:Golgi apparatus; P:negative regulation of programmed cell death; C:plasma membrane; P:hydrogen peroxide catabolic process; F:peroxidase activity; P:response to heat; F:calcium ion binding; F:NAD(P)H oxidase activity; C:integral component of membrane; P:carbohydrate homeostasis; P:cellular oxidant detoxification; P:oxidation-reduction process; P:defense response to fungus	1	1	**-13**	-7
TRINITY_DN293343_c1_g1_i2	PREDICTED: uncharacterized protein LOC101306070			-2	-3	**-13**	-7
TRINITY_DN294967_c1_g1_i8	---NA---			-1	-2	**-13**	-8
TRINITY_DN296507_c0_g3_i2	ethylene-responsive transcription factor ERF017	F:GO:0003677; C:GO:0005634; F:GO:0003700; P:GO:0006351; P:GO:0006355	F:DNA binding; C:nucleus; F:transcription factor activity, sequence-specific DNA binding; P:transcription, DNA-templated; P:regulation of transcription, DNA-templated	-2	-2	**-13**	-11

The five most down-regulated transcript had almost the same expression level at 48 h, approximately -13 log2FC (Table 2). In all transcripts was observed a big difference in expression level between the samples treated at 5 h and 48 h. An interesting example is a transcript (TRINITY_DN304907_c0_g2_i8), which is functionally annotated as respiratory burst oxidase D, it was slightly up-regulated at 1 h and 5 h with 1 log2FC and down-regulated at 48 and 240 h with -13 log2FC and -11 log2FC, respectively. The information in the UniProt database about this transcript are presented as unreviewed. However, is suggested that it may be involved in some biological processes including carbohydrate homeostasis, negative regulation of programmed cell death, osmosensory signaling pathway, reactive oxygen species metabolic process, response to heat, and response to wounding (The UniProt Consortium, 2017). The transcript (TRINITY_DN296507_c0_g3_i2) annotated as ethylene-responsive transcription factor ERF017, may be involved in the regulation of gene expression by stress factors and by components of stress signal transduction pathways (The UniProt Consortium, 2017).

The selected 10 most up and down-regulated transcripts at 48 h in 'Elsanta' cultivar, with functional annotation and their expression profile at all treatment time points are shown in Table 3. All five most up-regulated transcripts at 48 h had the same expression level (13 log2FC). Almost all up-regulated transcripts were highly expressed throughout different treatment time points with their expression level variation from 10 to 13 log2FC. However, some transcripts were not available at specific time points. For example, two transcripts (TRINITY_DN311172_c0_g1_i5 and TRINITY_DN314535_c1_g1_i5) were not DE at the last cold treatment time point, 240 h. The first most up-regulated transcript is integral component of membrane and is highly expressed at all treated samples. The transcript annotated as proteasome activator subunit 4 is an interesting example since it is highly expressed at 1 h (11 log2FC), not DE at 5 h and then again with very high expression level (13 log2FC) at 48 h and 240 h treatments. Based on the information in UniProt database, this gene is involved in DNA damage response by binding to acetylated histones and promotes degradation of histones (The UniProt Consortium, 2017). Another transcript annotated as 2-Cys peroxiredoxin chloroplastic was not DE expressed at first treated sample, but at other time points the expression level was very high. This transcript is a member of the antioxidant defense system of chloroplast (Baier & Dietz, 1997). A study conducted by Dietz et al. (2002) in transgenic Arabidopsis demonstrated that the 2-Cys peroxiredoxin protects chloroplast proteins from oxidative damage.

***Table 3**. Details for the 10 most DE transcripts, 5 up-regulated and 5 down-regulated of 'Elsanta' cultivar at 48 hours (J00vs48) cold treatment and expression level (log$_2$ fold change) of these transcripts in other time points (J00vs01- 1 hour, J00vs05- 5 hours, J00vs240- 240 hours)*

Sequence Name	Description	GO IDs	GO Names	E00vs01 (Log2FC)	E00vs05 (Log2FC)	Most DE E00vs48 (Log2FC)	E00vs240 (Log2FC)
TRINITY_DN314589_c0_g1_i5	uncharacterized membrane At1g16860-like [Fragaria vesca vesca]	C:GO:0016021	C:integral component of membrane	12	13	**13**	12
TRINITY_DN317111_c0_g1_i4	proteasome activator subunit 4			11	NA	**13**	13
TRINITY_DN311172_c0_g1_i5	PREDICTED: phosphoglucomutase, cytoplasmic	F:GO:0000287; P:GO:0005975; F:GO:0016868	F:magnesium ion binding; P:carbohydrate metabolic process; F:intramolecular transferase activity, phosphotransferases	12	11	**13**	NA
TRINITY_DN305130_c0_g1_i1	2-Cys peroxiredoxin chloroplastic	P:GO:0098869; P:GO:0055114; F:GO:0051920	P:cellular oxidant detoxification; P:oxidation-reduction process; F:peroxiredoxin activity	NA	10	**13**	12
TRINITY_DN314535_c1_g1_i5	low-temperature-induced 65 kDa isoform X4			10	13	**13**	NA
TRINITY_DN308694_c0_g1_i2	F-box kelch-repeat At3g27150 [Fragaria vesca vesca]			0	0	**-12**	-3
TRINITY_DN316418_c0_g1_i5	transcription initiation factor TFIID subunit 9 [Fragaria vesca vesca]	F:GO:0046982; P:GO:0006352	F:protein heterodimerization activity; P:DNA-templated transcription, initiation	0	-3	**-12**	-3
TRINITY_DN317424_c2_g1_i2	PREDICTED: uncharacterized protein LOC103968019			1	-2	**-12**	-12
TRINITY_DN314152_c1_g5_i3	PREDICTED: protein BPS1, chloroplastic-like			0	-1	**-12**	-13
TRINITY_DN288725_c0_g1_i1	replication-associated partial	P:GO:0006260	P:DNA replication	0	0	**-19**	-19

Down-regulated transcripts in 'Elsanta' cultivar at 48 h cold treatment had expression level in region of -12 log2FC, except the first most down-regulated transcript (TRINITY_DN288725_c0_g1_i1) which was -19 log2FC (Table 3). A study conducted by Van Norman et al. (2004) showed that the transcript annotated as protein BPS1 chloroplastic-like is required to prevent the constitutive production of a root-derived graft-transmissible signal that is sufficient to inhibit leaf expansion, leaf initiation, and shoot apical meristem activity. The transcript F-box kelch-repeat At3g27150, is suggested to be involved proteasome-mediated ubiquitin-dependent protein catabolic process and regulation of proteolysis (The UniProt Consortium, 2017).

The identification of the most up- and down-regulated transcripts revealed a difference in the function of transcripts that were present in 'Jonsok' and 'Elsanta' cultivar. The available evidence for the transcripts functions gives information that the most of the transcripts present in 'Jonsok' are involved in cold tolerance mechanism. Whereas, most of the transcripts present in 'Elsanta' seems to be involved in the protection and damage response.

3.3 Selection of transcripts associated with cold tolerance

The strawberry cultivars ‘Jonsok’ and ‘Elsanta’ are known to express different response to cold tolerance, our hypothesis was that the same genes will show differences in expression level during cold stress. Besides, the changes in expression level will be expected between samples of the same cultivar among different cold stress exposure.

Table 4 lists the selected isoforms of 21 genes associated with cold tolerance in ‘Jonsok’ and ‘Elsanta’ cultivar. The list contains an isoform of each gene with transcript ID, GO ID-s, GO names and the expression level at all cold treatment time points retrieved from pairwise DE analysis. The selected genes associated with cold tolerance containing all isoform details and the expression level at each treatment time points are listed in Appendix (Tables A10-A31). As anticipated, almost all of the selected transcripts showed variation in expression level between cultivars, as well as between samples exposed to low temperature for the different period of time. The changes in gene expression level during cold stress were observed earlier in *Arabidopsis*. The results of transcriptome profiling of approximately 8000 genes by Fowler & Thomashow (2002) indicate that multiple regulatory pathways are involved in the response to cold. The authors found that the expression of 306 genes identified as being cold responsive during the 7-day experiment, with transcripts for 218 genes increasing and those for 88 genes decreasing. A pathway with a prominent role in gene expression regulation during cold tolerance is the CBF transcriptional cascade. The cold inducible CBF genes are the primary regulators of low temperature stress and overexpression of these genes has been proven to increase cold tolerance in *Arabidopsis* (Gilmour et al., 2000). These genes are regulated by transcription factor ICE1. The activated transcription factor ICE 1 attach to the promoter of CBF3 and induces its expression (Chinnusamy et al., 2006). In the results obtained from pairwise DE analysis (Table 4), we found transcription factor ICE1 down-regulated in both cultivars after 240 h cold treatment, but much lower in Elsanta (-8.5 log2FC) compared to ‘Jonsok’ (-1.6 log2FC). Dong et al. (2006) suggested that the negative regulation of transcription factor ICE1 may be influenced by the high expression of osmotically responsive gene, a ring finger E3 ubiquitin- ligase. In our bioinformatics analysis, the E3 ubiquitin- ligase HOS1 was found to be DE only in ‘Jonsok’ cultivar and was up-regulated at 48 and 240 h treatments. The results about ICE1 and E3 ubiquitin- ligase in present study do not support the assertion of Dong et al. (2006). The transcript E3 SUMO- ligase SIZ1-like is known to regulate plant growth and response to multiple environmental stimuli (Miura et al., 2011). In our analysis this transcript was slightly up-regulated only at 240 h treatment in both cultivars.

The C2H2 zinc finger- type ZAT12- like is a transcription factor that has an important role in increasing freezing tolerance and negatively regulates the expression of CBF1, CBF2, and CBF3 during cold stress (Chinnusamy et al., 2010). In our analysis, this transcript was down-regulated at all cold treatment time points in both cultivars. However, the expression level dropped continuously with the time. ZAT10 is known as a key member of C2H2-type zinc finger transcription factors that contain two distinct C2H2-type fingers and an ERF-associated amphiphilic repression (EAR) domain that is involved in regulation of stress tolerance (Nguyen et al., 2016). The zinc finger ZAT10 transcript in our analysis was down-regulated in both cultivars at 48 and 240 h cold treatments, however, variations in the expression level between cultivars were observed at each of two treatments. In 'Jonsok' the expression level was ~2 log2FC lower than in 'Elsanta'.

While plants are exposed to cold stress, the cell membrane has a crucial role in activating cold-responsive proteins, therefore, often cold temperature resilience is defined by the ability of the cell membranes. In our findings, we selected transcripts that are related to the cell membrane and are DE at various treatment time points. An enzyme that might be necessary to maintain cell wall integrity during cold is cellulose synthase G2 (The UniProt Consortium, 2017). This transcript showed clear differences in expression level between cultivars. In 'Jonsok' was not DE at first two time points, while at 48 h showed high expression level and the level was slightly decreased 240 h. Whilst, in 'Elsanta', was down-regulated at 1 h and up-regulated at 48 h treatment, meanwhile at 5 h and 240 h treatments was not DE at all. The expression pattern of this transcript in 'Jonsok' is similar to the study conducted by Peng et al. (2015) during a cold stress experiment in paper mulberry.

Lipids are known for their structural role in mitigating the effect of low temperatures (Barrero-Sicilia, Silvestre, Haslam, & Michaelson, 2017). We found transcript phosphoinositide phospholipase C 6, as highly up-regulated at last two treatment time points in 'Jonsok', especially at 240 h. Similarly, in 'Elsanta' the phosphoinositide phospholipase C 6 was up-regulated at 48 and 240 h treatments but expression level was half compared to 'Jonsok'.

During the low-temperature stress, through the membrane rigidification or other cellular changes, calcium act as a secondary messenger and activates protein kinases required for cold tolerance (Ray, Agarwal, Arora, Kapoor, & Tyagi, 2007). In our analysis (Table 4), we found different transcripts encoding calcium sensor and receptor, such as calmodulin-binding transcription activator 3-like, calmodulin 3 and CDPK1.

The CDPK1 transcript in our study is present as down-regulated at all treatment time points in 'Jonsok' cultivar. However, in 'Elsanta' is slightly up-regulated in first two treatments,

whereas down-regulated at 48 h, and not DE at 240 h cold treatment. The study from Sheen, (1996) showed a clear demonstration of the involvement of CDPK in stress-responsive gene expression. In an experiment during reproductive development and abiotic stress conditions in rice Ray et al. (2007) found six CDPK genes as induced while the expression of only one gene was down-regulated under stress conditions.

Table 4*. Details for the 21 selected transcripts related to cold tolerance from the pairwise differential expression analysis. The list includes information about transcript ID, description name, GO IDs and GO names for two strawberry cultivars 'Jonsok '(J) and 'Elsanta' (E) and expression level (log2 fold change) of these transcripts at all cold treatment time points (0 vs. 1h- 1 hour, 0 vs. 5h- 5 hours, 0 vs. 48h – 48 hours and 0 vs. 240h- 240 hours)*

Cultivars	Transcript ID	log2 FC 0 vs 1 h	log2 FC 0 vs 5 h	log2 FC 0 vs 48 h	log2 FC 0 vs 240 h	Description	GO IDs	GO Names
J	TRINITY_DN302753_c0_g2_i2	-	1.26101	2.774998	1.1169383	dehydrin COR47-like	P:GO:0006950;	P:response to stress; P:response to
E	TRINITY_DN310505_c0_g6_i1	-	1.28594	3.210931	1.6298551		P:GO:0009415	water
J	TRINITY_DN300514_c1_g4_i1	-	-	-	-1.594223	transcription factor ICE1	F:GO:0032440;	F:2-alkenal reductase [NAD(P)]
E	TRINITY_DN312698_c2_g2_i3	-	-	-	-8.465419		F:GO:0046983;	activity; F:protein dimerization
J	TRINITY_DN290336_c1_g4_i7	-3.0437	-3.981	-5.34494	-6.67714	zinc finger ZAT12-like	F:GO:0046872	F:metal ion binding
E	TRINITY_DN301106_c1_g3_i4	-3.2654	-4.0763	-4.56492	-5.060188			
J	TRINITY_DN306521_c2_g1_i8	-	-	1.409393	1.2853243	E3 ubiquitin- ligase HOS1	P:GO:0016579;	P:protein deubiquitination; P:seed
E	TRINITY_DN316550_c1_g1_i1	-	-	-	-		P:GO:0010162;	dormancy process; P:lipid storage;
J	TRINITY_DN297178_c1_g3_i3	-	-	-4.1606	-4.513627	zinc finger ZAT10	F:GO:0003676;	F:nucleic acid binding; F:metal ion
E	TRINITY_DN306835_c0_g1_i3	-	-	-1.86852	-2.466904		F:GO:0046872	binding
J	TRINITY_DN290899_c0_g1_i4	-	-	-	1.7486687	E3 SUMO- ligase SIZ1-like		
E	TRINITY_DN303579_c0_g1_i3	-	-	-	1.6948777	[Fragaria vesca vesca]		
J	TRINITY_DN299798_c1_g1_i8	-	-	4.333908	2.3959957	cellulose synthase G2		
E	TRINITY_DN313988_c2_g1_i7	-1.8672	-	1.994126	-			
J	TRINITY_DN293071_c0_g1_i4	-	-	9.661879	9.7282481	phosphoinositide	F:GO:0004435;	F:phosphatidylinositol
E	TRINITY_DN309868_c0_g1_i3	-	-	4.200935	3.6082427	phospholipase C 6	P:GO:0016042;	phospholipase C activity; P:lipid
J	TRINITY_DN293238_c3_g1_i5	-	-	-	-1.534203	calmodulin-binding	F:GO:0003677;	F:DNA binding; C:nucleus
E	TRINITY_DN297965_c0_g1_i3	-	-	-1.71787	-1.919735	transcription activator 3-like	C:GO:0005634	
J	TRINITY_DN292755_c0_g1_i3	-	-1.3213	-2.29447	-2.131648	calmodulin 3		
E	TRINITY_DN303217_c0_g1_i2	-	-	-1.86469	-1.4124			
J	TRINITY_DN304860_c1_g5_i6	-1.4484	-2.931	-4.88367	-4.60811	CDPK1 [Fragaria vesca]	F:GO:0005524;	F:ATP binding; F:calcium ion
E	TRINITY_DN313867_c1_g1_i2	1.14984	1.01337	-1.38197	-		F:GO:0005509;	binding; F:protein kinase activity;
J	TRINITY_DN297352_c1_g1_i6	-	5.96873	8.880024	8.8680256	dehydrin Xero 2	P:GO:0006950;	P:response to stress; P:response to
E	TRINITY_DN310904_c1_g5_i10	-	2.14367	7.305525	6.9928305		P:GO:0009415	water
J	TRINITY_DN298252_c3_g3_i5	-	-	-	-1.217827	cytosolic ascorbate peroxidase	P:GO:0006979;	P:response to oxidative stress;
E	TRINITY_DN314524_c1_g3_i1	-	-	-	-1.105632	[Fragaria x ananassa]	P:GO:0098869;	P:cellular oxidant detoxification;
J	TRINITY_DN277097_c0_g1_i3	-	8.85986	10.20421	9.6639824	aldo keto reductase	F:GO:0016491;	F:oxidoreductase activity;
E	NA	-	-	-	-		P:GO:0055114	P:oxidation-reduction process
J	TRINITY_DN298625_c0_g2_i1	-	-	1.799901	1.3258395	glutathione S-transferase-like	C:GO:0009570;	C:chloroplast stroma; C:nucleus;
E	TRINITY_DN303782_c0_g1_i3	-	-	1.701824	1.3193799		C:GO:0005634;	F:glutathione binding; C:stromule;
J	TRINITY_DN306752_c3_g4_i1	-	-	3.553297	2.570411	alcohol dehydrogenase	F:GO:0008270;	F:zinc ion binding;
E	TRINITY_DN316648_c2_g1_i2	1.15515	1.06702	3.753905	3.0233991		F:GO:0016491;	F:oxidoreductase activity;
J	TRINITY_DN306979_c5_g7_i4	-	-	1.235294	-	chalcone synthase	P:GO:0030639;	P:polyketide biosynthetic process;
E	TRINITY_DN300072_c0_g1_i2	-	-1.2113	-	-		P:GO:0080110;	P:sporopollenin biosynthetic
J	TRINITY_DN300034_c0_g1_i1	-	-	-	-	cytosolic aldolase	P:GO:0006096;	P:glycolytic process; F:fructose-
E	TRINITY_DN307161_c2_g2_i1	-	-	-1.01409	-1.668325		F:GO:0004332	bisphosphate aldolase activity
J	TRINITY_DN291493_c2_g5_i1	1.75635	2.46302	-1.15999	-2.465773	Fra a allergen [Fragaria x	P:GO:0009607;	P:response to biotic stimulus;
E	TRINITY_DN302809_c2_g1_i11	-	2.11927	1.68718	-	ananassa ananassa]	P:GO:0006952	P:defense response
J	TRINITY_DN289501_c0_g1_i2	-	-1.7718	-4.04574	-3.051596	cleavage stimulating factor 64-	F:GO:0000166;	F:nucleotide binding; F:nucleic
E	TRINITY_DN299053_c0_g1_i4	-	-	-10.5701	-10.68523	like	F:GO:0003676;	acid binding; P:mRNA 3'-end
J	TRINITY_DN297980_c1_g1_i7	-	7.23981	5.537743	3.8645217	dehydration-responsive	C:GO:0005634;	F:DNA binding; C:nucleus;
E	TRINITY_DN307824_c0_g5_i7	3.62872	5.3266	5.222912	3.5943608	element-binding 1E	F:GO:0003677;	F:transcription factor activity,

3.4 Validation of selected target transcripts by RT-qPCR

In order to confirm the results obtained from RNA-seq data, the RT-qPCR was performed. The purpose of this analysis was to see the variation in expression level of selected target transcripts between samples treated at 2 °C for the different period of time and differences between 'Jonsok' and 'Elsanta'. Therefore, the steady-state of gene expression level was analyzed for the six following target transcripts related to cold tolerance: dehydrin COR47-like, chalcone synthase (CHS), cytosolic aldolase, the transcription factor ICE1, CDPK1, and aldo keto reductase. Data generated from RT-qPCR were analyzed following the principle explained in section 2.5. PP2A was used as a reference transcript. Figure 8 shows the results obtained from the RT-qPCR analysis. The X-axis shows categorical value- first stands for the reference group (0 h) and others are different time points (1, 5, 48 and 240 h). For each point are two bars, the blue bar stands for 'Jonsok' and orange bar for 'Elsanta'.

Dehydrin COR47-like (Figure 8A) in 'Jonsok' showed an increase in expression level until 48 h treatment (6.9-fold), then the expression level dropped at 240 h (2.4-fold). In 'Elsanta' was observed a rapid increase of dehydrin COR47-like until 48 h (16.5-fold), and declining of the expression level at the last treatment (3.3-fold). The accumulation level of this transcript was higher in 'Elsanta' than in 'Jonsok' at all coldly treated samples, in particular at 48 h treatment. In addition, in both cultivars was observed the same expression pattern with an increase until 48 h cold stress, followed by a significant decrease at 240 h.

The results for the transcription factor ICE1 are shown in Figure 8 B. An increase in the expression level of this transcript was observed in 'Jonsok' at 1 h (2-fold) and 5 h (6-fold), then the expression was decreased at 48 and 240 h (4.4-fold). While, in 'Elsanta' the expression level was significantly lower, with an increase after 48 h treatment until 2.4-fold, afterward, at 240 h (0.9-fold) the expression level was under the expression level of control (1-fold). In general, the 'Jonsok' cultivar showed a significantly higher accumulation level.

The observed steady-state level of CHS is presented in the Figure 8C. The CHS is accumulated to a higher level from 48 h, in both cultivars. However, the expression level at this time point in 'Elsanta' is far higher, compared to 'Jonsok'. These results are in accordance with Koehler et al. (2012) findings, whose reported that the CHS was strongly up-regulated in 'Frida' than 'Jonsok', especially at 48 h cold treatment.

The expression level of cytosolic aldolase transcript appeared to be lower than the control plant at almost all cold treatment time points in both cultivars, except at 1 h in 'Jonsok' was slightly higher than control (Figure 8D).

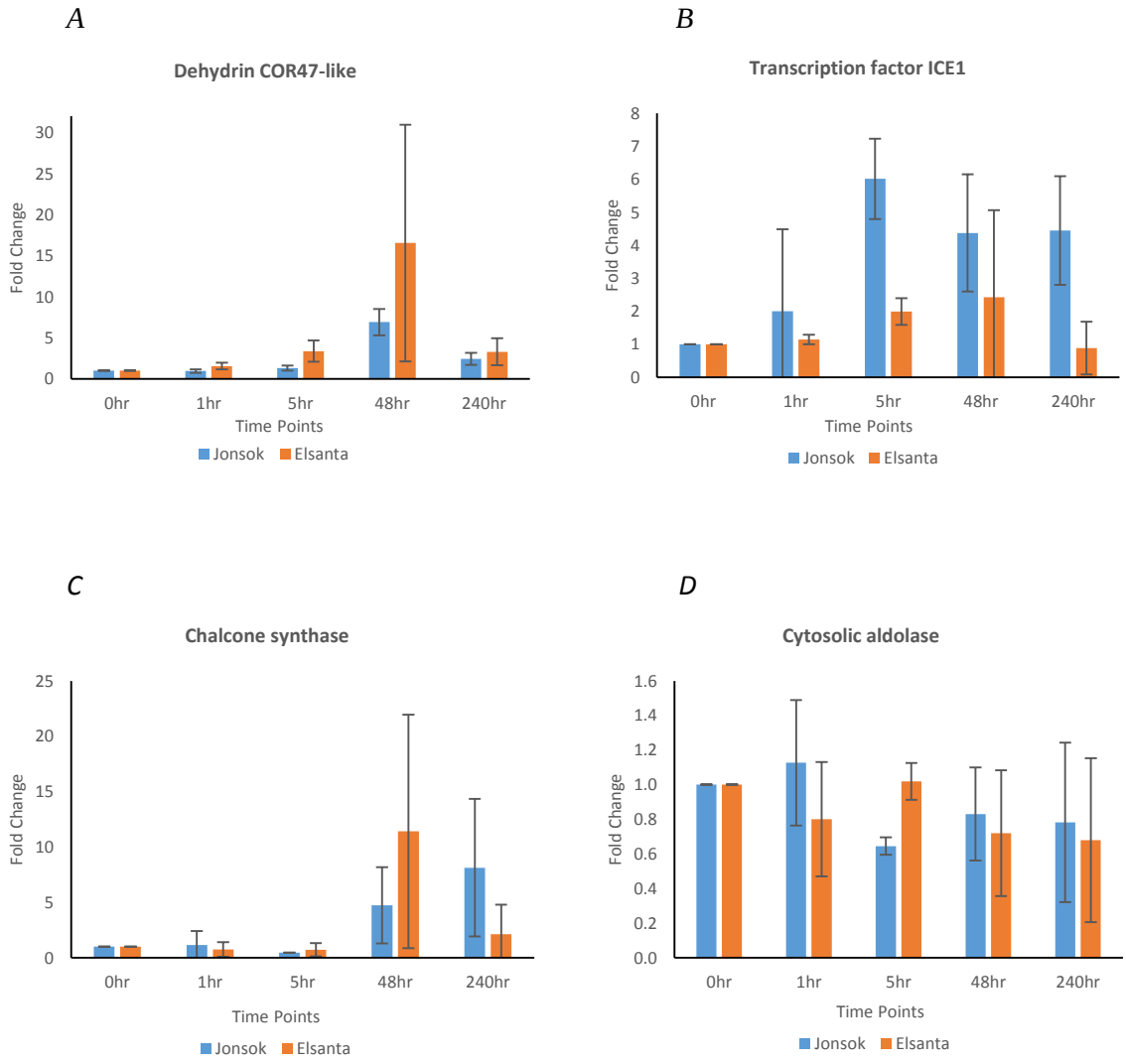

Figure 8*. The relative steady-state transcripts level of dehydrin COR47-like (**A**), transcription factor ICE1(**B**), chalcone synthase (**C**) and cytosolic aldolase (**D**) of the samples treated at 2 °C for the different period of time (1, 5, 48 and 240 h) against control (0 h) in two strawberry cultivars ('Jonsok' and 'Elsanta').*

As it mentioned above the RT-qPCR was performed also for two other targets, aldo keto reductase and CDPK1. However, considering the fact that the transcript aldo keto reductase had a very low number of reads in RNA-seq data, we doubt that poor amplification is the reason that hindered the RT-qPCR reaction to obtain results. McCall et al. (2014) asserted that the samples with a very low copy number of genes fail to produce a detectable signal. Likewise, the CDPK1 target did not produce any data from RT-qPCR reaction. This could be due to large amplicon size (>300 bp) since we tried to design primers specific for one or two isoforms. This gene was very challenging in this context because it has a large number of isoforms.

3.5 Comparative analysis of RNA-seq and RT-qPCR data

The goal of this analysis was to see if the results obtained from pairwise DE analysis of RNA-seq data for some target transcripts are in agreement with the RT-qPCR results. Each type of analysis was performed as the comparison of fold change level from different cold treatment time points (1, 5, 48 and 240 h) with the fold change of control (0 h) for two strawberry cultivars (‘Jonsok’ and ‘Elsanta’), separately. To this end, we compared fold change correlations between RNA-seq and RT-qPCR.

In this section is presented the comparative analysis of eight target transcripts associated with cold tolerance. The four targets are those that the RT-qPCR results are presented in section 3.4, dehydrin COR47-like, transcription factor ICE1, chalcone synthase and cytosolic aldolase. While, the other four target transcripts are: ADH, dehydrin Xero2, E3 ubiquitin-ligase HOS1 and cleavage stimulating factor 64-like. The RT-qPCR analysis for these four transcripts was performed by a fellow master student, who was working on the same project. The RT-qPCR results for these four targets are shown in Appendix (Figure A1).

In following Figures 9-16 is shown the comparative analysis between RNA-seq analysis and RT-qPCR experimental validation. The X-axis shows categorical values that stands for different time points (1, 5, 48 and 240 h). For each point are two bars that shows the expression level of transcripts, the green bar stands for the expression level obtained from RNA-seq analysis and yellow bar for expression level obtained from RT-qPCR analysis.

Dehydrin COR47-like

COR47 belongs to the family of dehydrins that accumulates at high levels in the plasma membrane of cells in the vascular transition area during cold acclimation (P. H. Li & Palva, 2012). Previously, was reported that COR47 and other dehydrins can indeed contribute to freezing tolerance and the authors suggested that it can be due to their function as membrane stabilizers during the low-temperature stress (Puhakainen et al., 2004). The significant expression changes of dehydrin COR47-like transcript are noticed at 48 h cold treatment in both cultivars, however, the ‘Elsanta’ plant showed higher expression level at all treated samples (Figure 9). In general, the influence of cold stress was not so distinctive in this transcript. In the previous study conducted by Badek et al. (2014) on two strawberry cultivars ‘Elsanta’ and ‘Selvik’, the latter shows resistance to freezing temperatures, comparable to ‘Jonsok’, was reported similar variation in expression level of COR47 gene during low temperature stress.

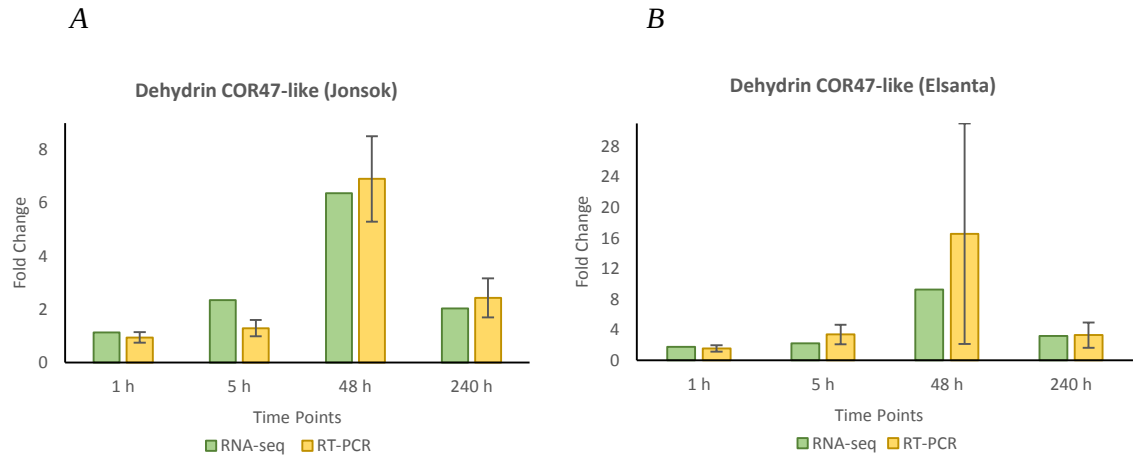

Figure 9. (A) *Relative steady-state transcript level of dehydrin COR47-like in RNA-seq data and RT-qPCR at four different cold treatment time points (1, 5, 48 and 240 h) in 'Jonsok'.* ***(B)*** *Relative steady-state transcript level of dehydrin COR47-like in RNA-seq data and RT-qPCR at four different cold treatment time points (1, 5, 48 and 240 h) in 'Elsanta'.*

COR47 belongs to the group of COR genes which are dependent on their activity on cold-induced transcription factors (CBF). In the previous study was reported that the expression of the CBF1 gene in plants from the genus *Thellungiella* reached the maximum level after 3 hours cold treatment, while the accumulation of COR47 transcripts started after 7 hours (Badek et al., 2014). These results support our findings of CBF transcript (Table 4) and COR47, where CBF reached the maximum level at 5 h cold treatment and COR47 was accumulated highly at 48 h treatment. A similar finding was reported in the proteomic level of COR 47 in two strawberry cultivars 'Jonsok' and 'Frida' showed that the highest accumulation level was reached after 1 day cold treatment, the continuously dropped through the time (Koehler et al., 2012). The authors observed up-regulation of COR47 up to 42 days. Earlier, Zalunskaitė et al. (2008) reported up-regulation of the COR47 gene in strawberry plants even after 30 days of cold acclimation at 2 ° C. Our findings strongly support previous studies, since this transcript was up-regulated even after 10 days (240 h) cold treatment. The expression patterns of dehydrin COR47-like are in concordance between RNA-seq and RT-qPCR data for both cultivars. An observed difference was at 48 h cold treatment of 'Elsanta' plant, in which RT-qPCR showed 7.3-fold higher level than RNA-seq data analysis. As it is mentioned in section 2.5, the RT-qPCR analysis of samples treated for 48 h in 'Elsanta' cultivar was performed only for two biological replicates. The standard deviation between expression levels of these two replicates is very high. Therefore, it is highly likely that this is the reason for the difference in the expression level of this transcript obtained from two analyzed techniques.

Transcription factor ICE1

The ICE1 was identified as an upstream transcription factor that regulates the transcription of CBF genes during the cold stress (Chinnusamy et al., 2003). The results obtained from the RT-qPCR analysis for transcription factor ICE1 in 'Jonsok' cultivar, showed much higher expression level than the results from RNA-seq data at all treatment time points, except at 1 h (Figure 10A). However, the trend of expression across time points is quite similar. In both types of analysis was observed an increase in the expression level from 1 h to 5 h, then the level decreased at 48 h and 240 h treatments. The expression pattern of transcription factor ICE1 in 'Elsanta' varies between RNA-seq and RT-qPCR data (Figure 10B). At first time point, RNA-seq showed higher expression level than RT-qPCR, whereas at other time points was the opposite.

A *B*

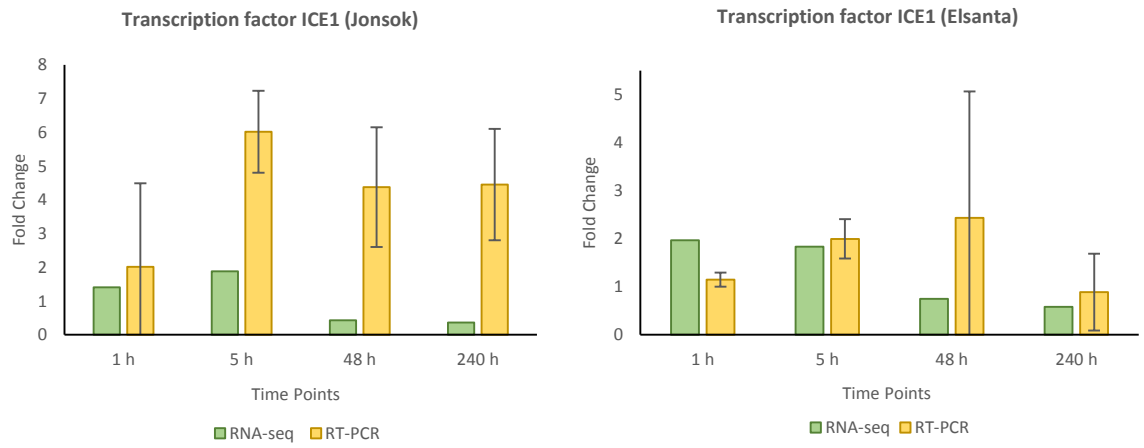

***Figure 10**. **(A)** Relative steady-state transcript level of transcription factor ICE1 in RNA-seq data and RT-qPCR at four different cold treatment time points (1, 5, 48 and 240 h) in 'Jonsok'. **(B)** Relative steady-state transcript level of transcription factor ICE1 in RNA-seq data and RT-qPCR at four different cold treatment time points (1, 5, 48 and 240 h) in 'Elsanta'.*

The data obtained from RNA-seq for 'Jonsok' cultivar showed that the transcription factor ICE1 was DE only at 240 h cold treatment and it was slightly down-regulated. Whereas, in 'Elsanta' the transcript for which the primers were designed is not DE at all treatment time points. Since it was very challenging to design primers for an interested isoform that works in both cultivars.

Chalcone synthase

Chalcone synthase is a key enzyme of the flavonoid biosynthesis pathway (Dao, Linthorst, & Verpoorte, 2011). Previously, Leyva et al. (1995) reported that the CHS accumulate coordinately in response to low temperatures and its expression is light dependent. The study conducted in Arabidopsis plants exposed to 4°C for different times indicated that the steady-state levels of CHS mRNAs started to increase after 10 h of low-temperature exposure, reaching maximum levels after 2 d and declining by the 7th d of exposure (Leyva et al., 1995). These findings are in accordance with the data obtained from RNA-seq in both cultivars.

As is shown in the figure below, the expression level of CHS at 48 h treatment in 'Elsanta' was higher than in 'Jonsok' plant.

A *B*

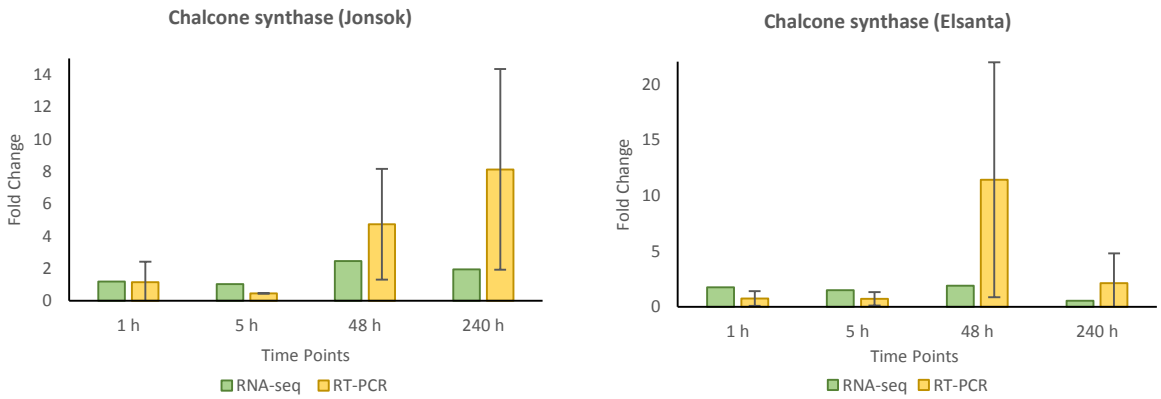

Figure 11. ***(A)*** *Relative steady-state transcript level of chalcone synthase in RNA-seq data and RT-qPCR at four different cold treatment time points (1, 5, 48 and 240 h) in 'Jonsok'.* ***(B)*** *Relative steady-state transcript level of chalcone synthase in RNA-seq data and RT-qPCR at four different cold treatment time points (1, 5, 48 and 240 h) in 'Elsanta'.*

In Figure 11A, expression patterns between RNA-seq and RT-qPCR in 'Jonsok' are quite similar in first two time points. At 240 h treatment the expression level between different types of analyses was almost same, except at 240 h the expression level obtained from RT-qPCR was 6.2-fold higher than from RNA-seq data. In 'Elsanta', the chalcone synthase expression level look alike between RNA-seq and RT-qPCR results (Figure 11B). A big variation was observed at 48 h treatment, where RT-qPCR showed 9.5-fold higher expression level.

In 'Jonsok' cultivar, the primers were designed to amplify two transcripts and the variation in the number of reads between these two transcripts was significant. One of the transcripts was almost not DE at all treatment time points, whereas the other transcript was highly up-regulated throughout all low-temperature treated samples.

Cytosolic aldolase

A study conducted by Schwab et al. (2001) in cultivated strawberry by using microarray and RNA gel blot analyses demonstrated that the cytosolic aldolase gene expression is induced during ripening and during the stress response. However, in our analysis, the expression level of this transcript was under control level at almost all time points in both cultivars (Figure 12). Based on the results, this transcript seems to not have any big effect in the cold tolerance since were no big differences between cultivars.

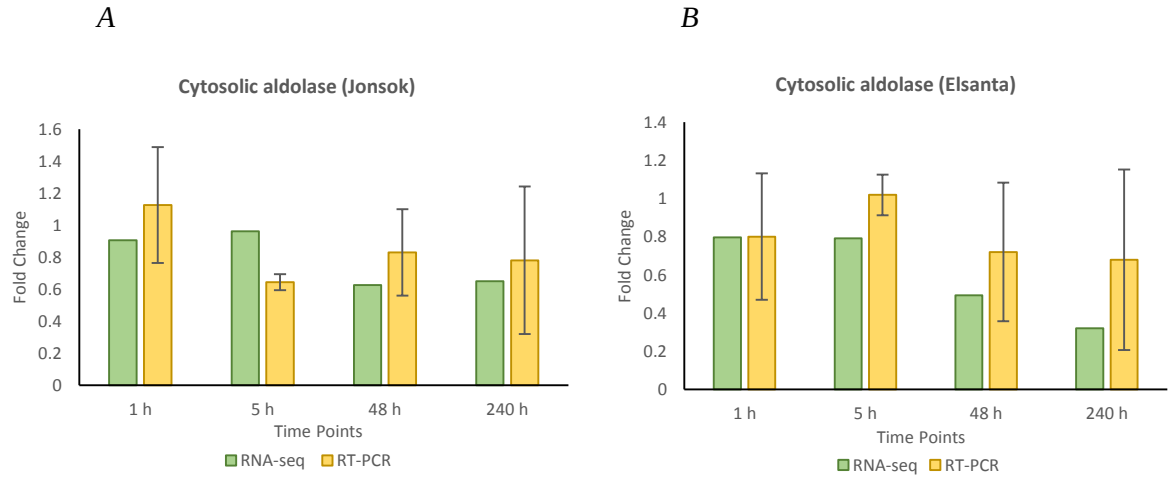

***Figure 12**. **(A)** Relative steady-state transcript level of cytosolic aldolase in RNA-seq data and RT-qPCR at four different cold treatment time points (1, 5, 48 and 240 h) in 'Jonsok'. **(B)** Relative steady-state transcript level of cytosolic aldolase in RNA-seq data and RT-qPCR at four different cold treatment time points (1, 5, 48 and 240 h) in 'Elsanta'.*

The steady-state transcript level of cytosolic aldolase showed quite similar expression pattern between RNA-seq and RT-qPCR data in both cultivars (Figure 12). In 'Jonsok', the RNA-seq data showed almost same expression level at first two time points, followed by a decrease at two other treatment time points. While, in the RT-qPCR data was observed a decrease in expression level from 1 h to 5 h treatment, then a higher level at two other time points.

The cytosolic aldolase level in 'Elsanta' showed almost same expression pattern in both analyses. In RNA-seq data, at first two time points was same expression level, while in RT-qPCR was a slight increase at 5 h treatment, however, at 48 h and 240 h, a lower expression level was observed in both performed analyses.

Alcohol dehydrogenase

Figure 13 shows that ADH transcript was highly up-regulated from 48 h cold treatment in both cultivars. In 'Jonsok', the expression starts to get higher at 48 h treatment and continue with almost the same expression level after 240 h cold treatment with 7.2 fold compared with the 0 h control. While, in 'Elsanta' the expression of ADH is very high at 48 h (10-fold), but after 240 h cold treatment the level decreased (5.5-fold). The previous study from Koehler et al. (2012), showed that ADH isoforms accumulated to higher levels in the 'Jonsok' compared to another strawberry cultivar called 'Frida', during a cold acclimation experiment and protein accumulation peaked after 42 days of CA. These findings are in agreement with the results presented in this work as ADH mRNA accumulated to a high level from 48 h in both cultivars and after 10 days, the 'Jonsok' shows a higher level of ADH accumulation than 'Elsanta'.

The relative steady-state level of transcript ADH obtained from RNA-seq data and RT-qPCR analysis is also shown in Figure 13. In 'Jonsok', both analyses showed almost the same expression level of ADH at all treatment time points (Figure 13A). Expect, at 48 h treatment the RNA-seq showed 5-fold higher expression level than RT-qPCR. Likewise, the results of both analysis for ADH at all treatments in 'Elsanta' indicated the same trend of expression. The 2-fold differences in expression level between RNA-seq and RT-qPCR analysis were at 48 and 240 h treatment time points (Figure 13B). Overall, the expression patterns of ADH between RT-qPCR and RNA-seq results are quite similar in both cultivars.

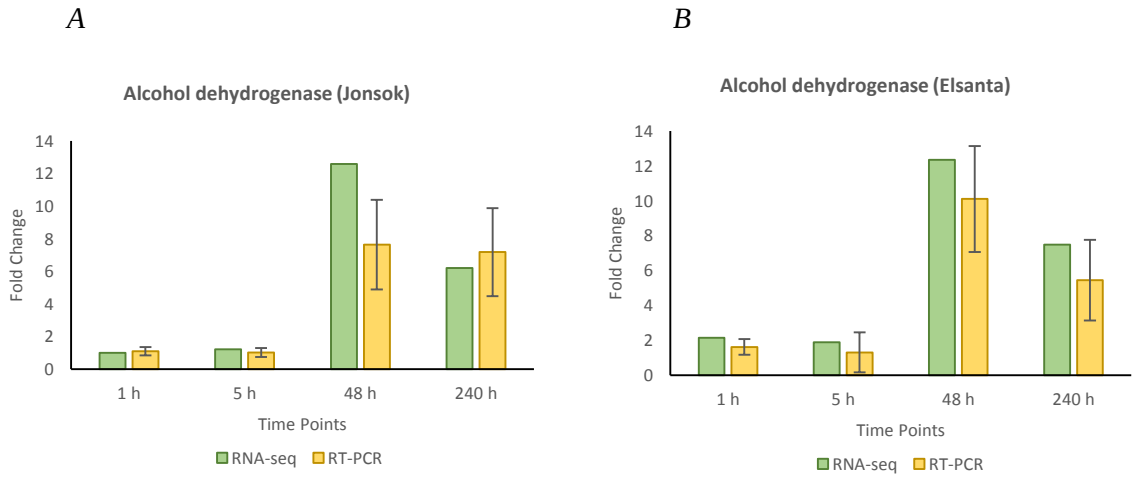

***Figure 13**. **(A)** Relative steady-state transcript level of alcohol dehydrogenase in RNA-seq data and RT-qPCR at four different cold treatment time points (1, 5, 48 and 240 h) in 'Jonsok'. **(B)** Relative steady-state transcript level of alcohol dehydrogenase in RNA-seq data and RT-qPCR at four different cold treatment time points (1, 5, 48 and 240 h) in 'Elsanta'.*

Dehydrin Xero 2

Dehydrin Xero 2 in 'Jonsok' (Figure 14A) showed a strong increase in expression level during the time and the peak of accumulation was at 240 h cold stress with 303-fold compared with the 0 h control. In 'Elsanta' (Figure 14B) was observed a slight increase of Xero 2 until 48 h cold stress at 44-fold, then at 240 h, the level decreased at 35-fold. The accumulation of this transcript was significantly greater in the more cold-tolerant cultivar 'Jonsok' than in 'Elsanta'.

The accumulation level of dehydrin Xero 2 in 'Jonsok' had similar expression pattern between bioinformatics and experimental analysis across treatment time points (Figure 13A). Besides, a significant difference was at 240 h treatment where expression level obtained from the RT-qPCR analysis was 204-fold bigger than expression level from RNA-seq.

The steady-state level of dehydrin Xero 2 in 'Elsanta' showed almost same expression pattern between RNA-seq and RT-qPCR across all treatment time points. The expression level of dehydrin Xero 2 from RNA-seq analysis exceeds the expression level from RT-qPCR at 48 h treatment with 36-fold and at 240 h with the 8-fold difference.

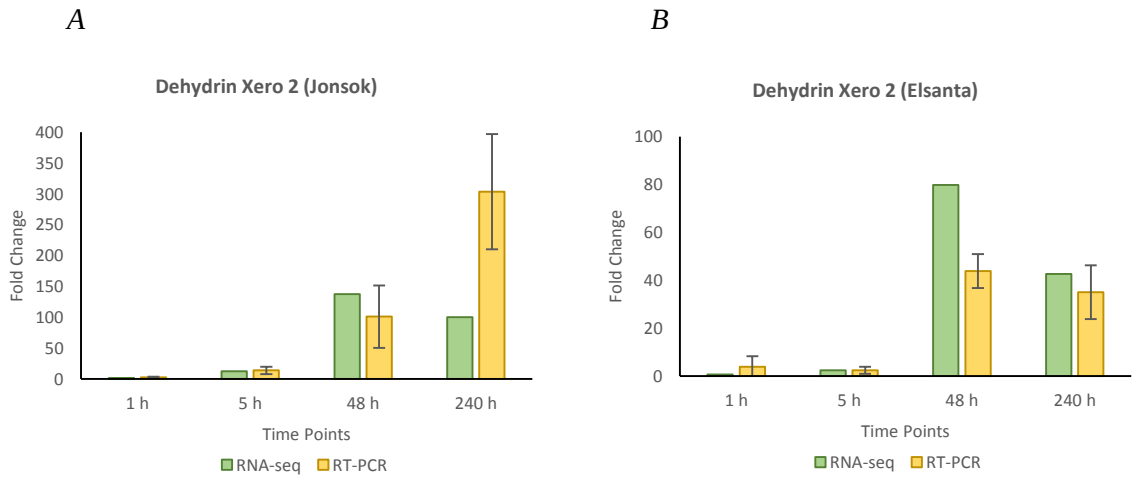

***Figure 14**. **(A)** Relative steady-state transcript level of dehydrin Xero 2 in RNA-seq data and RT-qPCR at four different cold treatment time points (1, 5, 48 and 240 h) in 'Jonsok'. **(B)** Relative steady-state transcript level of dehydrin Xero 2 in RNA-seq data and RT-qPCR at four different cold treatment time points (1, 5, 48 and 240 h) in 'Elsanta'.*

E3 ubiquitin-ligase HOS1

The Figure 15 shows that transcript E3 ubiquitin- ligase HOS1was accumulated in the higher level in 'Jonsok than in 'Elsanta' along all time points. In 'Jonsok', at first two time points were not a big difference compared with 0 h control, however, the changes occur at 48 h cold treatment where the expression level increased (2.6-fold) and continue with the nearly same level at 240 h (2.2-fold). Whereas, in 'Elsanta, at first two time points the transcript was down-regulated compared with 0 h control, then at 48 h and 240 h was up-regulated but not at a level much higher than control.

In Figure 15 is presented the steady-state level analyzed from RNA-seq data and RT-qPCR of E3 ubiquitin- ligase HOS1 in 'Jonsok' and 'Elsanta'. This transcript showed a strong agreement in expression pattern across time points in the comparison of the expression level between RNA-seq and RT-qPCR at each respective treatment time point in both cultivars.

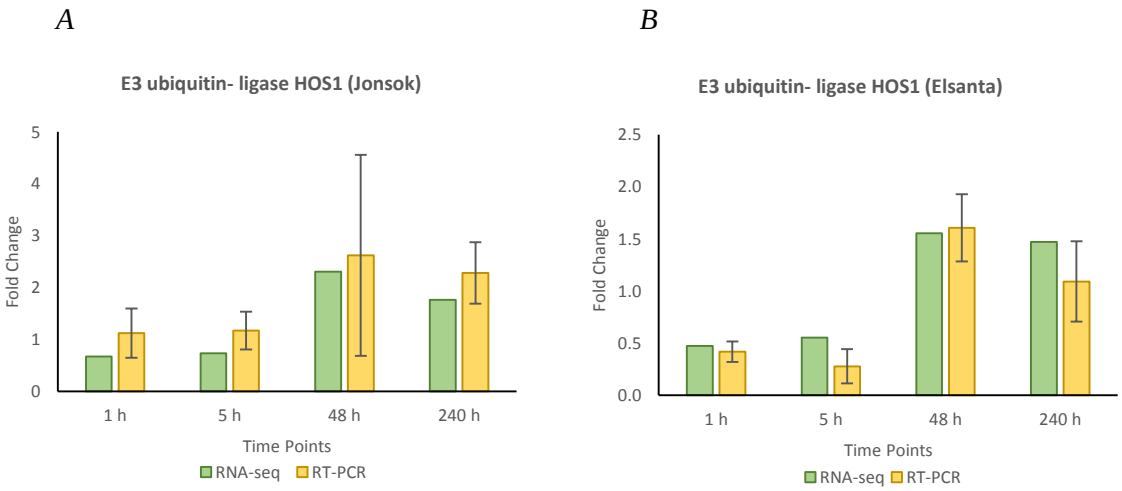

***Figure 15**. **(A)** Relative steady-state transcript level of E3 ubiquitin- ligase HOS1 in RNA-seq data and RT-qPCR at four different cold treatment time points (1, 5, 48 and 240 h) in 'Jonsok'. **(B)** Relative steady-state transcript level of E3 ubiquitin- ligase HOS1 in RNA-seq data and RT-qPCR at four different cold treatment time points (1, 5, 48 and 240 h) in 'Elsanta'.*

Cleavage stimulating factor 64-like

The transcript cleavage stimulating factor 64-like presented in Figure 16 was not accumulated at a high level in all cold treatment time points in both cultivars. In 'Jonsok', the transcript at 1h and 5h was up-regulated, but not with a big difference from 0 h control, whereas, at 48 h and 240 h the transcript was down-regulated. The cleavage stimulating factor 64-like had the same expression patterns also in 'Elsanta' but with greater expression level in all cold treatment time points.

The RNA-seq results of cleavage stimulating factor 64-like (Figure 15) are in compliance with the results taken from RT-qPCR. In Figure 15A, the expression level of this transcript in 'Jonsok' has quite a similar pattern between performed analyses. Also, in 'Elsanta' is shown a high level of similarity between RNA-seq and RT-qPCR results.

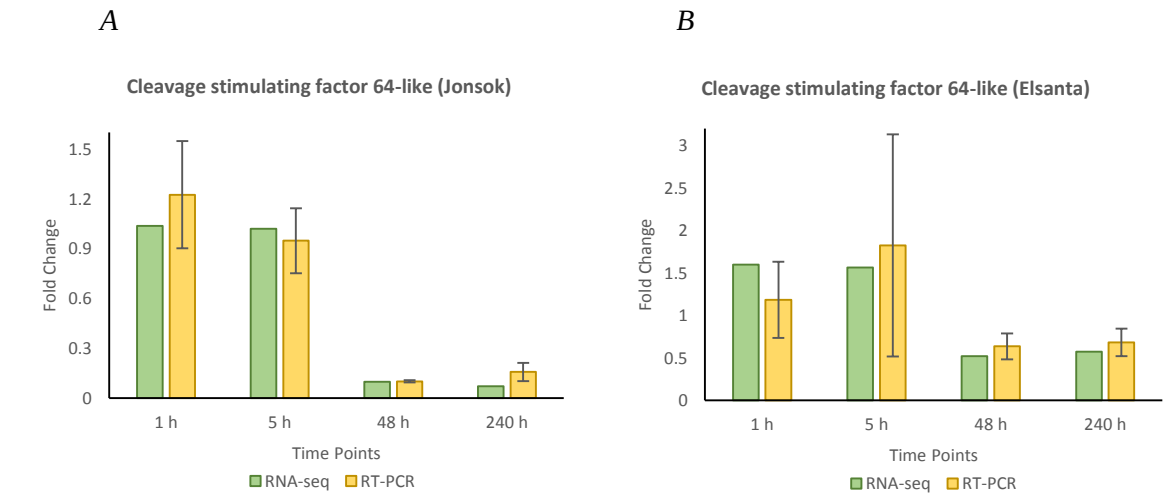

***Figure 16**. **(A)** Relative steady-state transcript level of cleavage stimulating factor 64-like in RNA-seq data and RT-qPCR at four different cold treatment time points (1, 5, 48 and 240 h) in 'Jonsok'. **(B)** Relative steady-state transcript level of cleavage stimulating factor 64-like in RNA-seq data and RT-qPCR at four different cold treatment time points (1, 5, 48 and 240 h) in 'Elsanta'.*

Except the dehydrin Xero 2 that is the only one who gene is strongly induced by cold, most of the selected target genes are expressed only at a slightly higher level than the control during cold stress exposure.

Overall, a high compliance in expression intensities was observed between results obtained from RNA-seq and RT-qPCR for the eight analyzed transcripts. Hence, the results of the experimental validation with RT-qPCR increases reliability in the data obtained from RNA-seq.

3.6 Sequencing of PCR product

Sequencing was performed for the same eight target transcripts that we used in comparative analysis and the reference gene PP2A. The goal was to check the RT-qPCR product if it was amplifying the same target for which the primers were designed. In this analysis participated forward and reverse primers in separate reactions. The sequences were blasted against the *de novo* assemblies of 'Jonsok' and 'Elsanta' (see section 2.2) using CLC genomic workbench 11.0 software. Also, a blast search against National Center for Biotechnology Information (NCBI) database (non-redundant protein sequences) was performed (Altschul et al., 1997). The sequences obtained from sequencing results for all the transcripts, also the alignments against assemblies (JAD and EAD) for some of transcripts are shown in Appendix.

In following figures, are shown the blast results of the transcription factor ICE1 in 'Jonsok' and ADH in 'Elsanta' against the assemblies and against NCBI database. In the alignment (Figure 17) we can see that 93 % of the generated sequence was identity with the transcript in the assembly (target transcript). However, in the alignment is not the full length of the sequence that we wanted to amplify since usually during sequencing in both ends of the sequence the quality is weak.

```
>TRINITY_DN300514_c1_g4_i1 len=465

 Score = 307.9 bits (340), Expect = 2E-82
 Identities = 201/215 (93%), Gaps = 5/215 (2%)
 Strand = Plus/Minus

Query  20   TAGA-ATCCAGCA-GCTGTCATTAGCTGGCTTCAATGGGTTTGCCACGGATAGATTCCGG  77
            |||| |||||||| ||||||||||||||| |||||||||||||||||| ||||| |||||||
Sbjct  358  TAGATATCCAGCAAGCTGTCATTAGCTG-CTTCAATGGGTTTGCCATGGATATATTCCGG  300

Query  78   GCTGAGCAATGCAAGGAAGTCCAAGACGTCCACCCCGAGCATATAAAGGCAGTACTATTG  137
            |||||||||||||||||| ||||||||||||||||||||||||||||||||||||||||||
Sbjct  299  GCTGAGCAATGCAAGGAAGGCCAAGACGTCCACCCCGAGCATATAAAGGCAGTACTATTG  240

Query  138  GATTCAGCTGGCTTCCATGGCATGATATA-GGGGTTGCATCAGAACAACCAAACTGGGGT  196
            |||||||||||||||||||||||||||| |||||||||||||||||| |||||||| ||
Sbjct  239  GATTCAGCTGGCTTCCATGGCATGATATAGGGGGTTGCATCAGAACAA-CAAACTGGAGT  181

Query  197  TGCTTTACCAAGGAAGGGGAGGGGGCGGGGAAATT  231
            |||||||||||  |||||||| | |||| |||||
Sbjct  180  TGCTTTACCAAGATAGGGGAGGAGTCGGGCAAATT  146
```

Figure 17. *The blast results of transcription factor ICE1 sequence obtained from sequencing against the* de novo *assembly of 'Jonsok' (JAD) using CLC. The query is the sequence of RT-qPCR product and the subject is the sequence of ICE transcript present in the assembly.*

The sequencing results were confirmed also by blasting them against the NCBI database (Figure 18). The blast search gave in the first three hits transcription factor ICE1, with query cover 65 % and identity 82 %.

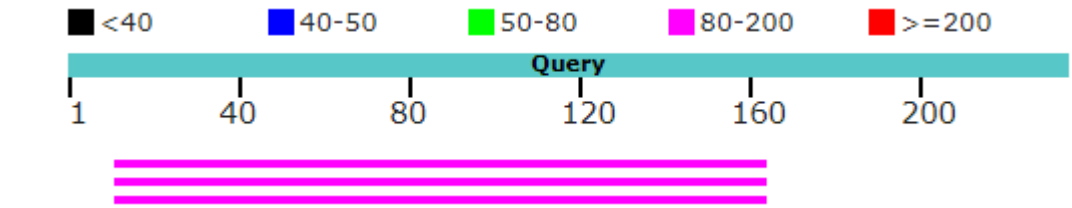

Alignments | Download | GenPept | Graphics

Description	Max score	Total score	Query cover	E value	Ident	Accession
transcription factor ICE1-like [Rosa chinensis]	90.9	90.9	65%	1e-19	82%	XP_024168837.1
PREDICTED: transcription factor ICE1 [Fragaria vesca subsp. vesca]	90.5	90.5	65%	2e-19	82%	XP_004297495.2
transcription factor ICE1-like [Ziziphus jujuba]	87.4	87.4	65%	2e-18	76%	XP_015883400.1

Figure 18. *The blast results from the blast check of transcription factor ICE1 against NCBI database.*

Figure 19 shows the alignment of the ADH target. The primers for this transcript were designed to amplify two isoforms, since it was impossible to design the specific primers. The alignment showed 96 % identity between sequences.

```
>TRINITY_DN316648_c2_g1_i2 len=1865

 Score = 102.3 bits (112),  Expect = 6E-21
 Identities = 61/63 (96%), Gaps = 1/63 (2%)
 Strand = Plus/Plus

Query  2    AAATTCTTTTATACCTCCTTGTGCCATACTGACGTCTACTTCTGGGGAGCCAAGGGACAA  61
            ||||||||| ||||||||||||||||||||||||||||||||| |||||||||||||
Sbjct  564  AAATTCTTT-ATACCTCCTTGTGCCATACTGACGTCTACTTCTGGGAAGCCAAGGGACAA  622

Query  62   AAC  64
            |||
Sbjct  623  AAC  625


>TRINITY_DN316648_c2_g1_i1 len=1880

 Score = 102.3 bits (112),  Expect = 6E-21
 Identities = 61/63 (96%), Gaps = 1/63 (2%)
 Strand = Plus/Plus

Query  2    AAATTCTTTTATACCTCCTTGTGCCATACTGACGTCTACTTCTGGGGAGCCAAGGGACAA  61
            ||||||||| ||||||||||||||||||||||||||||||||| |||||||||||||
Sbjct  564  AAATTCTTT-ATACCTCCTTGTGCCATACTGACGTCTACTTCTGGGAAGCCAAGGGACAA  622

Query  62   AAC  64
            |||
Sbjct  623  AAC  625
```

Figure 19. *The blast results of alcohol dehydrogenase sequence obtained from sequencing against the* de novo *assembly of 'Elsanta' (EAD) using CLC. The query is the sequence of RT-qPCR product and the subject is the sequence of alcohol dehydrogenase present in the assembly.*

The blast check them against the NCBI database confirmed that the amplified sequence is alcohol dehydrogenase (Figure 20). The blast search gave in the first four hits alcohol dehydrogenase, even that the query cover was only 55 % and identity 86 %.

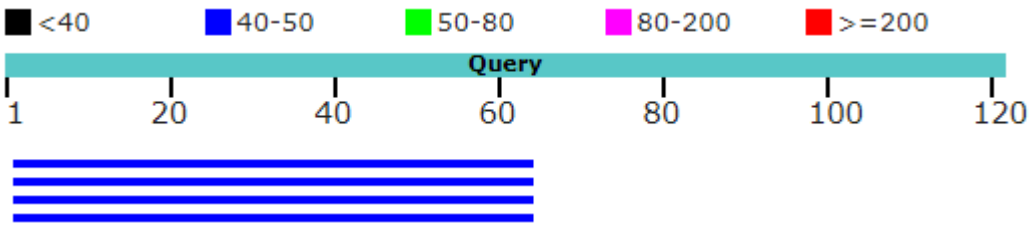

Alignments | Download | GenPept | Graphics

Description	Max score	Total score	Query cover	E value	Ident	Accession
alcohol dehydrogenase [Capsicum annuum]	45.8	45.8	52%	2e-05	86%	BAB17603.1
alcohol dehydrogenase 2 [Nolana confinis]	46.2	46.2	52%	2e-05	86%	AFJ44244.1
alcohol dehydrogenase 2 [Nolana adansonii]	46.2	46.2	52%	2e-05	86%	AFJ44242.1
alcohol dehydrogenase [Solanum habrochaites]	45.4	45.4	52%	4e-05	86%	AAO12183.1

Figure 20. *The blast results from the blast check of alcohol dehydrogenase against NCBI database.*

Analysis of the sequenced PCR products showed that some of the sequences highly match to sequences in the assemblies and the sequences in the NCBI gave the same name as the target. For some targets we did not get results from the sequencing or the sequence was not with the good quality. The sequencing results could have been improved by repeating the experiment, but this was not possible because of the limited time. However, those targets that the sequences had good quality confirmed the RNA-seq results. So, we could confirm that the assembly used in DE analysis has the high quality level.

4. Conclusion

In this study, we successfully determined the number of differentially expressed transcripts at variable time points in response to the low-temperature stress of two strawberry cultivars ('Jonsok' and 'Elsanta'). By analyzing the DE transcripts in detail, we revealed the effects of low-temperature stress on the strawberry plant at the transcriptome level. The most significant change in the number of DE transcripts was observed between 5 h and 48 h cold treatments. Furthermore, we identified the most up- and down regulated transcripts from the results of each pairwise comparison of both cultivars. A difference in the function of transcripts that were most DE at 48 h between Jonsok and Elsanta was observed. The available evidence for most of the transcripts present in Jonsok indicates that these transcripts may be involved in cold tolerance mechanism. Whereas, the most DE transcripts at 48 h in Elsanta are involved in the membrane protection or in the repair damages. From the selection of most DE transcripts at 48 h, we found the transcript galactinol synthase 2-like and late embryogenesis abundant 76-like isoform X1 as highly up-regulated in ‘Jonsok’ compared to ‘Elsanta’ and we suggest that these transcripts might be related to cold tolerance.

The transcriptome data here provide a comprehensive insight into the expression profiles of 21 genes under cold stress. Finally, the expression level of eight selected transcripts was validated by RT-qPCR and sequencing. The experimental and in silico analyses indicated a high concordance in expression patterns in most of the analyzed transcripts.

We assume that these transcriptome data will provide a valuable foundation for further characterizing the molecular mechanisms of freezing stress in cultivated strawberry. Moreover, the transcriptome data of identified genes related to cold tolerance can be used potentially for analysis at the proteomic level.

5. Further research

In the RNA-seq data we have selected information for 21 transcripts related to cold tolerance, however only eight of them are validated experimentally. So, further analysis of transcripts related to cold tolerance is needed. Other transcripts that could be interesting to analyze are galactinol synthase 2-like, late embryogenesis abundant 76-like isoform X1, and some of the transcripts that are present in the selected lists of most up- and down-regulated transcripts at each pairwise comparison, since they might have important role in cold tolerance. Also, these transcriptome data can be used for analysis at the proteomic level.

6. References

Aguan, K., Sugawara, K., Suzuki, N., & Kusano, T. (1993). Low-temperature-dependent expression of a rice gene encoding a protein with a leucine-zipper motif. *Molecular and General Genetics MGG, 240*(1), 1-8.

Akiyama, Y., Yamamoto, Y., Ohmido, N., Ohshima, M., & Fukui, K. (2001). Estimation of the nuclear DNA content of strawberries (Fragaria spp.) compared with Arabidopsis thaliana by using dual-step flow cytometry. *Cytologia, 66*(4), 431-436.

Altschul, S. F., Madden, T. L., Schaffer, A. A., Zhang, J., Zhang, Z., Miller, W., & Lipman, D. J. (1997). Gapped BLAST and PSI-BLAST: a new generation of protein database search programs. *Nucleic Acids Res, 25*(17), 3389-3402.

Anders, S., & Huber, W. (2010). Differential expression analysis for sequence count data. *Genome biology, 11*(10), R106.

Anders, S., McCarthy, D. J., Chen, Y., Okoniewski, M., Smyth, G. K., Huber, W., & Robinson, M. D. (2013). Count-based differential expression analysis of RNA sequencing data using R and Bioconductor. *Nature protocols, 8*(9), 1765.

Badek, B., Napiórkowska, B., Masny, A., & Korbin, M. (2014). Changes In The Expression Of Three Cold-Regulated Genes In 'Elsanta'And 'Selvik'Strawberry (Fragaria× Ananassa) Plants Exposed To Freezing. *Journal of Horticultural Research, 22*(2), 53-61.

Baier, M., & Dietz, K. J. (1997). The plant 2-Cys peroxiredoxin BAS1 is a nuclear-encoded chloroplast protein: its expressional regulation, phylogenetic origin, and implications for its specific physiological function in plants. *The Plant Journal, 12*(1), 179-190.

Barrero-Sicilia, C., Silvestre, S., Haslam, R. P., & Michaelson, L. V. (2017). Lipid remodelling: Unravelling the response to cold stress in Arabidopsis and its extremophile relative Eutrema salsugineum. *Plant Science, 263*, 194-200.

Baudo, M. M., Meza-Zepeda, L. A., Palva, E. T., & Heino, P. (1996). Induction of homologous low temperature and ABA-responsive genes in frost resistant (Solanum commersonii) and frost-sensitive (Solanum tuberosum cv. Bintje) potato species. *Plant molecular biology, 30*(2), 331-336.

Beck, E. H., Fettig, S., Knake, C., Hartig, K., & Bhattarai, T. (2007). Specific and unspecific responses of plants to cold and drought stress. *Journal of biosciences, 32*(3), 501-510.

Bhandari, P. (2016). *Bioinformatic Analysis of RNA-Seq Data from Cultivated Strawberry (Fragaria x ananassa) and Identification of Transcripts Related to Cold Tolerance.* (Master Degree in Applied and Commercial Biotechnology), Inland Norway University of Applied Sciences.

Bio, C. (2012). White Paper on de novo assembly in CLC Assembly Cell 4.0. *CLC bio A/S, Aarhus, Denmark*.

Bita, C. E., & Gerats, T. (2013). Plant tolerance to high temperature in a changing environment: scientific fundamentals and production of heat stress-tolerant crops. *Front Plant Sci, 4*, 273.

Buko, D. H. (2011). *Freezing tolerance and expression of candidate genes in timothy (Phleum pratens L.).* Norwegian University of Life Sciences, Ås.

Bushmanova, E., Antipov, D., Lapidus, A., Suvorov, V., & Prjibelski, A. D. (2016). rnaQUAST: a quality assessment tool for de novo transcriptome assemblies. *Bioinformatics, 32*(14), 2210-2212.

Cavender-Bares, J. (2007). Chilling and freezing stress in live oaks (Quercus section Virentes): intra- and inter-specific variation in PS II sensitivity corresponds to latitude of origin. *Photosynthesis Research, 94*(2-3), 437.

Chaves, M. M., Gil, H. M., & Delrot, S. (2015). *Grapevine in a Changing Environment: A Molecular and Ecophysiological Perspective*: John Wiley & Sons.

Chen, J., Zhang, H., Feng, M., Zuo, D., Hu, Y., & Jiang, T. (2016). Transcriptome analysis of woodland strawberry (Fragaria vesca) response to the infection by Strawberry vein banding virus (SVBV). *Virology journal, 13*(1), 128.

Ching, T., Huang, S., & Garmire, L. X. (2014). Power analysis and sample size estimation for RNA-Seq differential expression. *Rna, 20*(11), 1684-1696.

Chinnusamy, V., Ohta, M., Kanrar, S., Lee, B.-h., Hong, X., Agarwal, M., & Zhu, J.-K. (2003). ICE1: a regulator of cold-induced transcriptome and freezing tolerance in Arabidopsis. *Genes Dev, 17*(8), 1043-1054.

Chinnusamy, V., Zhu, J., & Sunkar, R. (2010). *Gene Regulation During Cold Stress Acclimation in Plants* (Vol. 639).

Chinnusamy, V., Zhu, J., & Zhu, J. K. (2006). Gene regulation during cold acclimation in plants. *Physiologia Plantarum, 126*(1), 52-61.

Ciarmiello, L., Woodrow, P., G, P., & Carillo, P. (2011). *Plant genes for abiotic stress*.

Ciarmiello, L. F., Woodrow, P., Fuggi, A., Pontecorvo, G., & Carillo, P. (2011). Plant genes for abiotic stress *Abiotic Stress in Plants-Mechanisms and Adaptations*: InTech.

Conesa, A., & Götz, S. (2008). Blast2GO: A comprehensive suite for functional analysis in plant genomics. *International Journal of Plant Genomics, 2008*.

Conesa, A., Götz, S., García-Gómez, J. M., Terol, J., Talón, M., & Robles, M. (2005). Blast2GO: a universal tool for annotation, visualization and analysis in functional genomics research. *Bioinformatics, 21*(18), 3674-3676.

Conesa, A., Madrigal, P., Tarazona, S., Gomez-Cabrero, D., Cervera, A., McPherson, A., . . . Mortazavi, A. (2016). A survey of best practices for RNA-seq data analysis. *Genome biology, 17*, 13.

Dao, T. T. H., Linthorst, H. J. M., & Verpoorte, R. (2011). Chalcone synthase and its functions in plant resistance. *Phytochemistry Reviews, 10*(3), 397-412.

Davik, J., Daugaard, H., & Svensson, B. (2000). Strawberry production in the Nordic countries. *Advances in Strawberry Research, 19*, 13-18.

Davik, J., Koehler, G., From, B., Torp, T., Rohloff, J., Eidem, P., . . . Alsheikh, M. (2013). Dehydrin, alcohol dehydrogenase, and central metabolite levels are associated with cold tolerance in diploid strawberry (Fragaria spp.). *Planta, 237*(1), 265-277.

de Magalhães, J. P., Finch, C. E., & Janssens, G. (2010). Next-generation sequencing in aging research: emerging applications, problems, pitfalls and possible solutions. *Ageing research reviews, 9*(3), 315-323.

Dietz, K.-J., Horling, F., Konig, J., & Baier, M. (2002). The function of the chloroplast 2-cysteine peroxiredoxin in peroxide detoxification and its regulation. *Journal of Experimental Botany, 53*(372), 1321-1329.

Dong, C.-H., Agarwal, M., Zhang, Y., Xie, Q., & Zhu, J.-K. (2006). The negative regulator of plant cold responses, HOS1, is a RING E3 ligase that mediates the ubiquitination and degradation of ICE1. *Proceedings of the National Academy of Sciences of the United States of America, 103*(21), 8281-8286.

Finotello, F., & Di Camillo, B. (2015). Measuring differential gene expression with RNA-seq: challenges and strategies for data analysis. *Briefings in Functional Genomics, 14*(2), 130-142.

Fowler, S., & Thomashow, M. F. (2002). Arabidopsis transcriptome profiling indicates that multiple regulatory pathways are activated during cold acclimation in addition to the CBF cold response pathway. *The Plant Cell, 14*(8), 1675-1690.

Frigessi, A., van de Wiel, M. A., Holden, M., Svendsrud, D. H., Glad, I. K., & Lyng, H. (2005). Genome-wide estimation of transcript concentrations from spotted cDNA microarray data. *Nucleic acids research, 33*(17), e143-e143.

Gaafar, R., & Saker, M. (2006). Monitoring of cultivars identity and genetic stability in strawberry varieties grown in Egypt. *World Journal of Agricultural Sciences, 2*(1), 29-36.

Ganeshan, S., Vitamvas, P., Fowler, D. B., & Chibbar, R. N. (2008). Quantitative expression analysis of selected COR genes reveals their differential expression in leaf and crown tissues of wheat (Triticum aestivum L.) during an extended low temperature acclimation regimen. *Journal of Experimental Botany, 59*(9), 2393-2402.

Gilmour, S. J., Artus, N. N., & Thomashow, M. F. (1992). cDNA sequence analysis and expression of two cold-regulated genes ofArabidopsis thaliana. *Plant molecular biology, 18*(1), 13-21.

Gilmour, S. J., Sebolt, A. M., Salazar, M. P., Everard, J. D., & Thomashow, M. F. (2000). Overexpression of the Arabidopsis CBF3transcriptional activator mimics multiple biochemical changes associated with cold acclimation. *Plant physiology, 124*(4), 1854-1865.

Götz, S., García-Gómez, J. M., Terol, J., Williams, T. D., Nagaraj, S. H., Nueda, M. J., . . . Conesa, A. (2008). High-throughput functional annotation and data mining with the Blast2GO suite. *Nucleic acids research, 36*(10), 3420-3435.

Goyal, K., Walton, Laura J., & Tunnacliffe, A. (2005). LEA proteins prevent protein aggregation due to water stress. *Biochemical Journal, 388*(Pt 1), 151-157.

Grabherr, M. G., Haas, B. J., Yassour, M., Levin, J. Z., Thompson, D. A., Amit, I., . . . Zeng, Q. (2011). Full-length transcriptome assembly from RNA-Seq data without a reference genome. *Nature biotechnology, 29*(7), 644.

Guy, C., Niemi, K. J., & Brambl, R. (1985). Altered gene expression during cold acclimation of spinach. *Proceedings of the National Academy of Sciences, 82*(11), 3673-3677.

Haas, B. J., & Zody, M. C. (2010). Advancing RNA-seq analysis. *Nature biotechnology, 28*(5), 421.

Hajela, R. K., Horvath, D. P., Gilmour, S. J., & Thomashow, M. F. (1990). Molecular cloning and expression of cor (cold-regulated) genes in Arabidopsis thaliana. *Plant physiology, 93*(3), 1246-1252.

Han, Y., Gao, S., Muegge, K., Zhang, W., & Zhou, B. (2015). Advanced Applications of RNA Sequencing and Challenges. *Bioinformatics and Biology Insights, 9*(Suppl 1), 29-46.

Hardcastle, T. J., & Kelly, K. A. (2010). baySeq: empirical Bayesian methods for identifying differential expression in sequence count data. *BMC bioinformatics, 11*(1), 422.

Hirakawa, H., Shirasawa, K., Kosugi, S., Tashiro, K., Nakayama, S., Yamada, M., . . . Isobe, S. N. (2014). Dissection of the Octoploid Strawberry Genome by Deep Sequencing of the Genomes of Fragaria Species. *DNA Research, 21*(2), 169-181.

Horvath, D. P., McLarney, B. K., & Thomashow, M. F. (1993). Regulation of Arabidopsis thaliana L.(Heyn) cor78 in response to low temperature. *Plant physiology, 103*(4), 1047-1053.

Hossain, M., Islam, R., Krishna Roy, U., Ahmed, F., Karim, R., & Ara, T. (2018). Varietal Improvement of Strawberry (Fragaria x ananassa Dutch.) Through Somaclonal Variation Using In Vitro Techniques.

Huerta, L., & Burke, M. Functional genomics (II): Common technologies and data analysis methods.

Hummer, K. E., Bassil, N., & Njuguna, W. (2011). Fragaria *Wild crop relatives: Genomic and breeding resources* (pp. 17-44): Springer.

Hundertmark, M., & Hincha, D. K. (2008). LEA (Late Embryogenesis Abundant) proteins and their encoding genes in Arabidopsis thaliana. *BMC genomics, 9*, 118-118.

Hurd, P. J., & Nelson, C. J. (2009). Advantages of next-generation sequencing versus the microarray in epigenetic research. *Briefings in Functional Genomics, 8*(3), 174-183.

Husaini, A. M., & Neri, D. (2016). *Strawberry: Growth, Development and Diseases*: CABI.

Jain, M. (2012). Next-generation sequencing technologies for gene expression profiling in plants. *Briefings in Functional Genomics, 11*(1), 63-70.

Jain, P. (2014). *A study of C-repeat binding factors (CBF) associated with low temperature tolerance locus in winter wheat.* Citeseer.

Jeggari, A. P. (2013). Differential Expression Analysis and Functional Interpretation of Transcriptome Changes in Neural Progenitors under Temporal Switch.

Jensen, E. C. (2012). Real-Time Reverse Transcription Polymerase Chain Reaction to Measure mRNA: Use, Limitations, and Presentation of Results. *The Anatomical Record, 295*(1), 1-3.

John, R., Anjum, N., Sopory, S., Akram, N., & Ashraf, M. (2016). Some key physiological and molecular processes of cold acclimation. *Biologia Plantarum, 60*(4), 603-618.

Kalia, V. C., & Kumar, P. (2017). *Microbial Applications Vol. 1: Bioremediation and Bioenergy*: Springer.

Keogh, M. J., & Chinnery, P. F. (2013). Next generation sequencing for neurological diseases: New hope or new hype? *Clinical Neurology and Neurosurgery, 115*(7), 948-953.

Kim, D., & Salzberg, S. L. (2011). TopHat-Fusion: an algorithm for discovery of novel fusion transcripts. *Genome biology, 12*(8), R72.

Kim, J. C., Lee, S. H., Cheong, Y. H., Yoo, C.-M., Lee, S. I., Chun, H. J., . . . Cho, M. J. (2001). A novel cold-inducible zinc finger protein from soybean, SCOF-1, enhances cold tolerance in transgenic plants. *The Plant Journal, 25*(3), 247-259.

Kim, S. A., Ahn, S.-Y., Han, J. H., Kim, S. H., Noh, J. H., & Yun, H. K. (2013). Differential expression screening of defense related genes in dormant buds of cold-treated grapevines. *Plant Breeding and Biotechnology, 1*(1), 14-23.

Koehler, G., Wilson, R. C., Goodpaster, J. V., Sønsteby, A., Lai, X., Witzmann, F. A., . . . Alsheikh, M. (2012). Proteomic study of low-temperature responses in strawberry cultivars (Fragaria× ananassa) that differ in cold tolerance. *Plant physiology, 159*(4), 1787-1805.

Kumar, V., Dasgupta, N., & Ranjan, S. (2018). *Nanotoxicology: Toxicity Evaluation, Risk Assessment and Management*: CRC Press.

Langmead, B., & Salzberg, S. L. (2012). Fast gapped-read alignment with Bowtie 2. *Nature methods, 9*(4), 357.

Langmead, B., Trapnell, C., Pop, M., & Salzberg, S. L. (2009). Ultrafast and memory-efficient alignment of short DNA sequences to the human genome. *Genome biology, 10*(3), R25-R25.

Lee, B.-h., Henderson, D. A., & Zhu, J.-K. (2005). The Arabidopsis cold-responsive transcriptome and its regulation by ICE1. *The Plant Cell, 17*(11), 3155-3175.

Leyva, A., Jarillo, J. A., Salinas, J., & Martinez-Zapater, J. M. (1995). Low temperature induces the accumulation of phenylalanine ammonia-lyase and chalcone synthase mRNAs of Arabidopsis thaliana in a light-dependent manner. *Plant physiology, 108*(1), 39-46.

Li, B., & Dewey, C. N. (2011). RSEM: accurate transcript quantification from RNA-Seq data with or without a reference genome. *BMC bioinformatics, 12*, 323.

Li, B., Fillmore, N., Bai, Y., Collins, M., Thomson, J. A., Stewart, R., & Dewey, C. N. (2014). Evaluation of de novo transcriptome assemblies from RNA-Seq data. *Genome biology, 15*(12), 553.

Li, H., Handsaker, B., Wysoker, A., Fennell, T., Ruan, J., Homer, N., . . . Durbin, R. (2009). The sequence alignment/map format and SAMtools. *Bioinformatics, 25*(16), 2078-2079.

Li, J., Witten, D. M., Johnstone, I. M., & Tibshirani, R. (2012). Normalization, testing, and false discovery rate estimation for RNA-sequencing data. *Biostatistics, 13*(3), 523-538.

Li, P. H., & Palva, E. T. (2012). *Plant Cold Hardiness: Gene Regulation and Genetic Engineering*: Springer Science & Business Media.

Li, W., Richter, R. A., Jung, Y., Zhu, Q., & Li, R. W. (2016). Web-based bioinformatics workflows for end-to-end RNA-seq data computation and analysis in agricultural animal species. *BMC genomics, 17*, 761.

Lischer, H. E. L., & Shimizu, K. K. (2017). Reference-guided de novo assembly approach improves genome reconstruction for related species. *BMC bioinformatics, 18*, 474.

Liu, Y. (2014). Bioinformatics: The Impact of Accurate Quantification on Proteomic and Genetic Analysis and Research.

Livak, K. J., & Schmittgen, T. D. (2001). Analysis of relative gene expression data using real-time quantitative PCR and the 2− ΔΔCT method. *methods, 25*(4), 402-408.

Lovén, J., Orlando, D. A., Sigova, A. A., Lin, C. Y., Rahl, P. B., Burge, C. B., . . . Young, R. A. (2012). Revisiting global gene expression analysis. *Cell, 151*(3), 476-482.

Lunter, G., & Goodson, M. (2011). Stampy: a statistical algorithm for sensitive and fast mapping of Illumina sequence reads. *Genome Res, 21*(6), 936-939.

Madhava Rao, K. (2006). Introduction. *Physiology and Molecular Biology of Stress Tolerance in Plants*, 1-14.

Martin, J. A., & Wang, Z. (2011). Next-generation transcriptome assembly. *Nature Reviews Genetics, 12*, 671.

McCall, M. N., McMurray, H. R., Land, H., & Almudevar, A. (2014). On non-detects in qPCR data. *Bioinformatics, 30*(16), 2310-2316.

Medina, J., Bargues, M., Terol, J., Pérez-Alonso, M., & Salinas, J. (1999). The Arabidopsis CBF gene family is composed of three genes encoding AP2 domain-containing proteins whose

expression is regulated by low temperature but not by abscisic acid or dehydration. *Plant physiology, 119*(2), 463-470.

Medina, J., Catalá, R., & Salinas, J. (2011). The CBFs: three Arabidopsis transcription factors to cold acclimate. *Plant Science, 180*(1), 3-11.

Miura, K., & Furumoto, T. (2013a). Cold Signaling and Cold Response in Plants. *International Journal of Molecular Sciences, 14*(3), 5312.

Miura, K., & Furumoto, T. (2013b). Cold signaling and cold response in plants. *International Journal of Molecular Sciences, 14*(3), 5312-5337.

Miura, K., Lee, J., Gong, Q., Ma, S., Jin, J. B., Yoo, C. Y., . . . Hasegawa, P. M. (2011). SIZ1 regulation of phosphate starvation-induced root architecture remodeling involves the control of auxin accumulation. *Plant physiology, 155*(2), 1000-1012.

Monroy, A. F., Castonguay, Y., Laberge, S., Sarhan, F., Vezina, L. P., & Dhindsa, R. S. (1993). A new cold-induced alfalfa gene is associated with enhanced hardening at subzero temperature. *Plant physiology, 102*(3), 873-879.

Nes, A., Gullord, M., Alsheikh, M., & Sween, R. (2008). *Strawberry breeding in Norway: progress and future.* Paper presented at the VI International Strawberry Symposium 842.

Nestby, R., & Bjørgum, R. (1999). Freeze injury to strawberry plants as evaluated by crown tissue browning, regrowth and yield parameters. *Scientia horticulturae, 81*(3), 321-329.

Neven, L. G., Haskell, D. W., Hofig, A., Li, Q.-B., & Guy, C. L. (1993). Characterization of a spinach gene responsive to low temperature and water stress. *Plant molecular biology, 21*(2), 291-305.

Nguyen, X. C., Kim, S. H., Hussain, S., An, J., Yoo, Y., Han, H. J., . . . Chung, W. S. (2016). A positive transcription factor in osmotic stress tolerance, ZAT10, is regulated by MAP kinases in Arabidopsis. *Journal of Plant Biology, 59*(1), 55-61.

O'Brien, M. A., Costin, B. N., & Miles, M. F. (2012). Using Genome-Wide Expression Profiling to Define Gene Networks Relevant to the Study of Complex Traits: From RNA Integrity to Network Topology. *International review of neurobiology, 104*, 91-133.

Örvar, B. L., Sangwan, V., Omann, F., & Dhindsa, R. S. (2000). Early steps in cold sensing by plant cells: the role of actin cytoskeleton and membrane fluidity. *The Plant Journal, 23*(6), 785-794.

Oshlack, A., Robinson, M. D., & Young, M. D. (2010). From RNA-seq reads to differential expression results. *Genome biology, 11*(12), 220.

Oshlack, A., & Wakefield, M. J. (2009). Transcript length bias in RNA-seq data confounds systems biology. *Biology direct, 4*, 14-14.

Peng, X., Teng, L., Yan, X., Zhao, M., & Shen, S. (2015). The cold responsive mechanism of the paper mulberry: decreased photosynthesis capacity and increased starch accumulation. *BMC genomics, 16*(1), 898.

Pfaffl, M. W. (2001). A new mathematical model for relative quantification in real-time RT–PCR. *Nucleic acids research, 29*(9), e45-e45.

Phillippy, A. M. (2017). New advances in sequence assembly: Cold Spring Harbor Lab.

Platt, A. R., Woodhall, R. W., & George, A. L. (2007). Improved DNA sequencing quality and efficiency using an optimized fast cycle sequencing protocol. *BioTechniques, 43*(1), 58.

Poling, E. B. (2012). Strawberry plant structure and growth habit. *New York State Berry Growers Association, Berry EXPO*.

Puhakainen, T., Hess, M. W., Mäkelä, P., Svensson, J., Heino, P., & Palva, E. T. (2004). Overexpression of multiple dehydrin genes enhances tolerance to freezing stress in Arabidopsis. *Plant molecular biology, 54*(5), 743-753.

Qiao, Q., Xue, L., Wang, Q., Sun, H., Zhong, Y., Huang, J., . . . Zhang, T. (2016). Comparative Transcriptomics of Strawberries (Fragaria spp.) Provides Insights into Evolutionary Patterns. *Front Plant Sci, 7*, 1839.

Ray, S., Agarwal, P., Arora, R., Kapoor, S., & Tyagi, A. K. (2007). Expression analysis of calcium-dependent protein kinase gene family during reproductive development and abiotic stress conditions in rice (Oryza sativa L. ssp. indica). *Molecular Genetics and Genomics, 278*(5), 493-505.

Robertson, G., Schein, J., Chiu, R., Corbett, R., Field, M., Jackman, S. D., . . . Qian, J. Q. (2010). De novo assembly and analysis of RNA-seq data. *Nature methods, 7*(11), 909.

Robinson, M. D., McCarthy, D. J., & Smyth, G. K. (2010). edgeR: a Bioconductor package for differential expression analysis of digital gene expression data. *Bioinformatics, 26*(1), 139-140.

Robinson, M. D., & Oshlack, A. (2010). A scaling normalization method for differential expression analysis of RNA-seq data. *Genome biology, 11*(3), R25.

Rodriguez, O., Triviño, J. C., Miñambres, R., Zuñiga, S., Santillán, S., Gil, M., . . . Buades, C. (2013). A comprehensive comparison between reference-based and 'de novo'isoform assembly approaches. *EMBnet. journal, 19*(A), p. 76.

Sáez-Vásquez, J., Raynal, M., Meza-Basso, L., & Delseny, M. (1993). Two related, low-temperature-induced genes from Brassica napus are homologous to the human tumour bbc1 (breast basic conserved) gene. *Plant molecular biology, 23*(6), 1211-1221.

Sanger, F., & Coulson, A. R. (1975). A rapid method for determining sequences in DNA by primed synthesis with DNA polymerase. *J Mol Biol, 94*(3), 441-448.

Sanghera, G. S., Wani, S. H., Hussain, W., & Singh, N. B. (2011). Engineering Cold Stress Tolerance in Crop Plants. *Current Genomics, 12*(1), 30-43.

Sangwan, V., Foulds, I., Singh, J., & Dhindsa, R. S. (2001). Cold-activation of Brassica napus BN115 promoter is mediated by structural changes in membranes and cytoskeleton, and requires Ca2+ influx. *The Plant Journal, 27*(1), 1-12.

Schaffer, M. A., & Fischer, R. L. (1988). Analysis of mRNAs that accumulate in response to low temperature identifies a thiol protease gene in tomato. *Plant physiology, 87*(2), 431-436.

Schurch, N. J., Schofield, P., Gierliński, M., Cole, C., Sherstnev, A., Singh, V., . . . Barton, G. J. (2016). How many biological replicates are needed in an RNA-seq experiment and which differential expression tool should you use? *Rna, 22*(6), 839-851.

Schwab, W., Aharoni, A., Raab, T., Pérez, A. G., & Sanz, C. (2001). Cytosolic aldolase is a ripening related enzyme in strawberry fruits (Fragaria× ananassa). *Phytochemistry, 56*(5), 407-415.

Shapshak, P., Levine, A. J., Foley, B. T., Somboonwit, C., Singer, E., Chiappelli, F., & Sinnott, J. T. (2017). *Global Virology II-HIV and NeuroAIDS*: Springer.

Sheen, J. (1996). Ca2+-dependent protein kinases and stress signal transduction in plants. *Science, 274*(5294), 1900-1902.

Shulaev, V., Sargent, D. J., Crowhurst, R. N., Mockler, T. C., Folkerts, O., Delcher, A. L., . . . Mane, S. P. (2011). The genome of woodland strawberry (Fragaria vesca). *Nat Genet, 43*(2), 109.

Singh, K. B., Foley, R. C., & Oñate-Sánchez, L. (2002). Transcription factors in plant defense and stress responses. *Current opinion in plant biology, 5*(5), 430-436.

Smith-Unna, R., Boursnell, C., Patro, R., Hibberd, J. M., & Kelly, S. (2016). TransRate: reference-free quality assessment of de novo transcriptome assemblies. *Genome research, 26*(8), 1134-1144.

Smith, C. J., & Osborn, A. M. (2009). Advantages and limitations of quantitative PCR (Q-PCR)-based approaches in microbial ecology. *FEMS microbiology ecology, 67*(1), 6-20.

Smyth, G. (2004). Linear models and empirical Bayes methods for assessing differential expression in microarray experiments. Stat Appl Gen Mol Biol 3: Article 3.

Sønsteby, A., & Heide, O. M. (2011). Environmental regulation of dormancy and frost hardiness in Norwegian populations of wood strawberry (Fragaria vesca L.). *The European Journal of Plant Science and Biotechnology, 5*, 42-48.

Staudt, G. (1999). *Systematics and geographic distribution of the American strawberry species: Taxonomic studies in the genus Fragaria (Rosaceae: Potentilleae)* (Vol. 81): Univ of California Press.

Taji, T., Ohsumi, C., Iuchi, S., Seki, M., Kasuga, M., Kobayashi, M., . . . Shinozaki, K. (2002). Important roles of drought- and cold-inducible genes for galactinol synthase in stress tolerance in Arabidopsis thaliana. *Plant J, 29*(4), 417-426.

The UniProt Consortium. (2017). UniProt: the universal protein knowledgebase. *Nucleic acids research, 45*(D1), D158-D169.

Thomashow, M. F. (1998). Role of Cold-Responsive Genes in Plant Freezing Tolerance. *Plant physiology, 118*(1), 1-8.

Thomashow, M. F. (2010). Molecular basis of plant cold acclimation: insights gained from studying the CBF cold response pathway. *Plant physiology, 154*(2), 571-577.

Thomashow, M. F., Gilmour, S. J., Stockinger, E. J., Jaglo-Ottosen, K. R., & Zarka, D. G. (2001). Role of the Arabidopsis CBF transcriptional activators in cold acclimation. *Physiologia Plantarum, 112*(2), 171-175.

Tjaden, B. (2015). De novo assembly of bacterial transcriptomes from RNA-seq data. *Genome biology, 16*(1), 1.

Trapnell, C., Hendrickson, D. G., Sauvageau, M., Goff, L., Rinn, J. L., & Pachter, L. (2013). Differential analysis of gene regulation at transcript resolution with RNA-seq. *Nature biotechnology, 31*(1), 46.

Trapnell, C., Pachter, L., & Salzberg, S. L. (2009). TopHat: discovering splice junctions with RNA-Seq. *Bioinformatics, 25*(9), 1105-1111.

Trapnell, C., Roberts, A., Goff, L., Pertea, G., Kim, D., Kelley, D. R., . . . Pachter, L. (2012). Differential gene and transcript expression analysis of RNA-seq experiments with TopHat and Cufflinks. *Nature protocols, 7*(3), 562.

Trejo-Téllez, L. I., & Gómez-Merino, F. (2014). *Nutrient management in strawberry. Effects on yield, quality and plant heath*.

Tuteja, N. (2012). *Improving crop resistance to abiotic stress*: Wiley-VCH.

van Berkel, J., Salamini, F., & Gebhardt, C. (1994). Transcripts accumulating during cold storage of potato (Solanum tuberosum L.) tubers are sequence related to stress-responsive genes. *Plant physiology, 104*(2), 445-452.

Van Norman, J. M., Frederick, R. L., & Sieburth, L. E. (2004). BYPASS1 Negatively Regulates a Root-Derived Signal that Controls Plant Architecture. *Current Biology, 14*(19), 1739-1746.

Venkateswarlu, B., Shanker, A. K., Shanker, C., & Maheswari, M. (2011). *Crop stress and its management: perspectives and strategies*: Springer Science & Business Media.

Wang, W., Vinocur, B., Shoseyov, O., & Altman, A. (2004). Role of plant heat-shock proteins and molecular chaperones in the abiotic stress response. *Trends in plant science, 9*(5), 244-252.

Wang, X., Wang, L., Wang, Y., Liu, H., Hu, D., Zhang, N., . . . Wang, C. (2018). Arabidopsis PCaP2 Plays an Important Role in Chilling Tolerance and ABA Response by Activating CBF- and SnRK2-Mediated Transcriptional Regulatory Network. *Front Plant Sci, 9*, 215.

Wang, Y., Xue, S., Liu, X., Liu, H., Hu, T., Qiu, X., . . . Lei, M. (2016). Analyses of Long Non-Coding RNA and mRNA profiling using RNA sequencing during the pre-implantation phases in pig endometrium. *Scientific Reports, 6*, 20238.

Wang, Z., Gerstein, M., & Snyder, M. (2009). RNA-Seq: a revolutionary tool for transcriptomics. *Nature Reviews Genetics, 10*(1), 57.

Wei, W., Chai, Z., Xie, Y., Gao, K., Cui, M., Jiang, Y., & Feng, J. (2017). Bioinformatics identification and transcript profile analysis of the mitogen-activated protein kinase gene family in the diploid woodland strawberry Fragaria vesca. *PLoS One, 12*(5), e0178596.

Xin, Z., & Browse, J. (2000). Cold comfort farm: the acclimation of plants to freezing temperatures. *Plant, Cell & Environment, 23*(9), 893-902.

Yadav, S. K. (2010). Cold stress tolerance mechanisms in plants. A review. *Agronomy for sustainable development, 30*(3), 515-527.

Yang, I. S., & Kim, S. (2015). Analysis of Whole Transcriptome Sequencing Data: Workflow and Software. *Genomics & Informatics, 13*(4), 119-125.

You, J., & Chan, Z. (2015). ROS Regulation During Abiotic Stress Responses in Crop Plants. *Front Plant Sci, 6*, 1092.

Zalunskaitė, I., Rugienius, R., Vinskienė, J., Bendokas, V., Gelvonauskienė, D., & Stanys, V. (2008). Expression of COR gene homologues in different plants during cold acclimation. *Biologija, 54*(1), 33-35.

Zhang, C., Zhang, B., Lin, L.-L., & Zhao, S. (2017). Evaluation and comparison of computational tools for RNA-seq isoform quantification. *BMC genomics, 18*, 583.

Zhang, X. S., Pei, J. J., Zhao, L. G., Tang, F., & Fang, X. Y. (2018). RNA-Seq analysis and comparison of the enzymes involved in ionone synthesis of three cultivars of Osmanthus. *J Asian Nat Prod Res*, 1-13.

Zhang, Z. H., Jhaveri, D. J., Marshall, V. M., Bauer, D. C., Edson, J., Narayanan, R. K., . . . Zhao, Q.-Y. (2014). A Comparative Study of Techniques for Differential Expression Analysis on RNA-Seq Data. *PLoS One, 9*(8), e103207.

Zhao, Q.-Y., Wang, Y., Kong, Y.-M., Luo, D., Li, X., & Hao, P. (2011). Optimizing de novo transcriptome assembly from short-read RNA-Seq data: a comparative study. *BMC bioinformatics, 12*(Suppl 14), S2-S2.

Zhao, S., Fung-Leung, W.-P., Bittner, A., Ngo, K., & Liu, X. (2014). Comparison of RNA-Seq and Microarray in Transcriptome Profiling of Activated T Cells. *PLoS One, 9*(1), e78644.

Appendix

Table A1. *List of primers designed for ten target transcripts and the reference PP2A*

Oligo Name	Sequence (5' to 3')
FvPP2A SP	AGGACAGAGTACCCAACA
FvPP2A ASP	CTTCTCCACAACCGACT
FaCOR47_SP	GACACAAGAAGCCGGAAGAT
FaCOR47_ASP	CCAATAAACCCTTCTTCTCC
Fa_ICE1_SP	ACAATTTGCCCGACTCCT
Fa_ICE1_ASP	GGTCTGTTGCTCTCCACT
FaAldoKetoReductase_SP	GCTGTCTACCAATGTCCCAAA
FaAlsoKetoReductase_ASP	GGTTAAGCTGTCCGAGGAG
FaCytosolicA_SP	CGCCTGTTTTCCTCAACATT
FaCytosolicA_ASP	ATTGGCACCCCTGGAAAG
FaCDPK1_SP	CCATCACCAAAACCTCTGAAA
FaCDPK1_ASP	ACCTCTCGCTTAACATCCT
FaChalcone_SP	AGAAGATTGAAGGCAGGGA
FaChalcone_ASP	GAATGTTGTGGGAACAGAAG
FvADH_SP	GCACCTCCTCAGGCTAA
FvADH_ASP	GGTTTTGTCCCTTGGCTT
FvXERO2 SP	TACCCCACTCAGTCTCCC
FvXERO2 ASP	GCCTCCGTGACCAGTTC
Fa_E3 Ub ligase At1g63170 SP	ACTCTGGCTGTTTCGGAGAG
Fa_E3 Ub ligase At1g63170 ASP	CGACCAAACAGTAGCAGCAA
Fa_Cleav_simul_fac 64-like SP	TGAAGGGAATTGCGGTAGGG
Fa_Cleav_simul_fac 64-like ASP	CTGCTGGGGCTGGACATTAG

Note: The highlighted primers are borrowed from the fellow student (Shanti Ram Pokhrel).

Selection of most up- and down-regulated transcripts

***Table A2**. Details for the 30 most DE transcripts, 15 up-regulated and 15 down-regulated of Jonsok cultivar at 1 hour cold treatment and expression level (log2 fold change) of these transcripts in other time points (5 h, 48 h and 240 h)*

Name	Description	1 h	5 h	48 h	240 h
TRINITY_DN288259_c0_g4_i4	phospholipid-transporting ATPase 9	12.54660	11.39101		
TRINITY_DN295067_c0_g2_i7	acetyl-acetyltransferase, cytosolic 1-like	12.23070	11.94949		
TRINITY_DN301121_c0_g1_i7	ras-related RABC1	11.97286	10.94354	10.91322	13.05130
TRINITY_DN295052_c1_g2_i6	ocs element-binding factor 1-like	11.75442	10.41477		
TRINITY_DN302854_c0_g1_i4	probable galactinol--sucrose galactosyltransferase 1	11.65207	9.51723	14.26351	13.21789
TRINITY_DN305731_c1_g1_i2	PREDICTED: uncharacterized protein LOC101293408	11.54247	10.78644		
TRINITY_DN298367_c0_g2_i13	pectinesterase pectinesterase inhibitor PPE8B-like	11.24643	10.29452	9.83517	10.74848
TRINITY_DN304600_c0_g6_i2	FAM10 family At4g22670 isoform X4	11.10743	8.62777		11.57733
TRINITY_DN303717_c1_g4_i3	LITAF-like zinc ribbon domain [Medicago truncatula]	11.06439	10.66413	8.79648	8.85273
TRINITY_DN291886_c0_g2_i1	probable glutathione S-transferase	10.87808	11.54230	9.79955	10.34961
TRINITY_DN293362_c0_g3_i7	TMV resistance N-like	10.79592	8.95757		
TRINITY_DN299373_c0_g3_i1	---NA---	10.78518		10.27822	11.06588
TRINITY_DN302887_c0_g2_i4	choline monooxygenase, chloroplastic isoform X2	10.72381	11.27575		
TRINITY_DN299804_c1_g1_i11	ras-related RABD2c	10.70367	11.94703	10.14978	10.65060
TRINITY_DN301939_c2_g2_i8	LOB domain-containing 41-like	10.69714	9.63994	8.12569	
TRINITY_DN302971_c1_g1_i8	multisubstrate pseudouridine synthase 7	-9.71300	-2.19627	-9.56204	-3.33284
TRINITY_DN300980_c1_g1_i3	RNA polymerase sigma factor sigD, chloroplastic	-9.74188	-2.62522	-1.80278	-1.48255
TRINITY_DN302990_c1_g2_i11	receptor-like cytosolic serine threonine-kinase RBK2 isoform X1	-9.75594	-1.62553	-3.68986	-2.34018
TRINITY_DN291326_c0_g2_i6	basic form of pathogenesis-related 1-like	-9.77220	-9.65203	-2.29853	-1.06494
TRINITY_DN295078_c2_g1_i2	stress enhanced 2, chloroplastic	-9.80241	-9.68169	-1.12048	-3.87101
TRINITY_DN293086_c0_g1_i11	Carbohydrate transporter sugar porter transporter isoform 2	-9.80268	-2.57393	-1.41900	-2.07824
TRINITY_DN293376_c0_g3_i9	transmembrane 208 homolog [Pyrus x bretschneideri]	-10.17288	-10.05340	-2.60622	-2.33204
TRINITY_DN298600_c0_g6_i9	probable cinnamyl alcohol dehydrogenase 1	-10.19754	-1.35469	0.25453	-3.18874
TRINITY_DN306850_c3_g1_i4	PREDICTED: uncharacterized protein LOC101294045	-10.39838	-1.46914	-1.05363	-1.10291
TRINITY_DN303221_c3_g1_i9	PREDICTED: uncharacterized protein LOC101295079	-10.60673	-10.48615	-4.85317	-2.88682
TRINITY_DN305523_c1_g1_i10	BTB POZ domain-containing NPY1	-10.97215	-0.25703	-2.15399	-4.31277
TRINITY_DN297911_c1_g2_i4	pectinesterase 1	-11.16131	-1.25326	-1.35306	-11.24837
TRINITY_DN305120_c2_g1_i1	probable phosphatase 2C 34	-11.29611	-1.07348	-1.77896	-2.46683
TRINITY_DN299866_c0_g2_i4	allene oxide cyclase 3, chloroplastic-like	-11.69031	-1.38876	-11.53827	-11.77660
TRINITY_DN301247_c0_g1_i1	probable phosphatase 2C 49	-11.84129	-11.71864	-5.39613	-3.62412

***Note**: Not available transcript = empty cell*

***Table A3**. Details for the 30 most DE transcripts, 15 up-regulated and 15 down-regulated of Jonsok cultivar at 5 hours cold treatment and expression level (log2 fold change) of these transcripts in other time points (1 h, 48 h and 240 h)*

Name	Description	1 h	5 h	48 h	240 h
TRINITY_DN305052_c2_g4_i2	probable folate-biopterin transporter 7		12.0990671322	9.3239752229	8.9236022434
TRINITY_DN304579_c1_g1_i3	RNI-like superfamily , [Theobroma cacao]		12.0454109981		12.2102202628
TRINITY_DN253360_c0_g3_i1	PREDICTED: uncharacterized protein LOC101295191		12.0183573483	13.8282348371	12.6089804931
TRINITY_DN299804_c1_g1_i11	ras-related RABD2c	10.7036714179	11.9470332214	10.1497789773	10.6505965340
TRINITY_DN289409_c1_g1_i1	PREDICTED: uncharacterized protein LOC101300093		11.9071181670	11.1504519069	
TRINITY_DN288624_c0_g3_i23	cyclic nucleotide-gated ion channel 1-like isoform X1	10.0247372282	11.7476354318		7.2836812501
TRINITY_DN289859_c0_g3_i1	allene oxide synthase-like	9.8890890528	11.6682652271		
TRINITY_DN307082_c2_g1_i3	endoglucanase 13-like	9.7964495162	11.5928962231	10.7196715823	10.8898191614
TRINITY_DN291886_c0_g2_i1	probable glutathione S-transferase	10.8780758012	11.5423035862	9.7995520305	10.3496134464
TRINITY_DN305052_c2_g4_i6	probable folate-biopterin transporter 7	8.9553348849	11.5211384154	9.0657072042	9.2835210811
TRINITY_DN306687_c5_g1_i6	probable beta-1,3-galactosyltransferase 19	10.4171376878	11.5019883972	9.9570749361	
TRINITY_DN303391_c1_g3_i8	glutamate dehydrogenase 2	9.7486015852	11.4892355600		
TRINITY_DN305922_c2_g2_i3	copper-transporting ATPase PAA2, chloroplastic	10.4626202267	11.4715381860		7.9762147590
TRINITY_DN302824_c1_g1_i4	40S ribosomal Sa-2	10.0877969391	11.3942509893		11.4100763788
TRINITY_DN288259_c0_g4_i4	phospholipid-transporting ATPase 9	12.5466000000	11.3910061874		
TRINITY_DN293381_c2_g1_i16	cysteine-rich receptor kinase 3 isoform X1	-5.2728022129	-10.2969980412	-5.8811725382	-5.3606395855
TRINITY_DN303221_c3_g1_i9	PREDICTED: uncharacterized protein LOC101295079	-10.6067290203	-10.4861533682	-4.8531741067	-2.8868234315
TRINITY_DN302051_c1_g2_i4	RNA pseudouridine synthase 5	-4.9412784233	-10.4894262697	-10.4592714657	-10.6974575343
TRINITY_DN300289_c2_g1_i8	probable receptor kinase At1g80640 [Fragaria vesca vesca]	-1.2286577168	-10.4985926438	0.0232209460	-0.4469722062
TRINITY_DN302177_c1_g5_i6	glucose-6-phosphate phosphate translocator 1, chloroplastic-like	-0.6302884723	-10.4987109952	-2.0665849841	-4.5685670992
TRINITY_DN302736_c1_g1_i1	TRANSPORT INHIBITOR RESPONSE 1-like	-3.5397156756	-10.5425720957	-0.5514702989	-0.2197540402
TRINITY_DN293381_c2_g1_i18	cysteine-rich receptor kinase 3 isoform X1	-2.7392428228	-10.7797855417	-10.7628834751	-9.1796484103
TRINITY_DN304003_c1_g1_i4	ROOT PRIMORDIUM DEFECTIVE 1	-2.3734259010	-10.7822141035	-2.3094753954	-2.6460119046
TRINITY_DN290854_c0_g2_i10	chaperone dnaJ 8, chloroplastic isoform X2 [Fragaria vesca vesca]	-3.5835624983	-10.9819108118	-10.9529717414	-4.1695074851
TRINITY_DN301100_c0_g1_i8	glycine-rich family [Populus trichocarpa]	-0.2459461142	-11.1269957253	-11.0912965915	-11.3297816244
TRINITY_DN302358_c1_g1_i8	monocopper oxidase SKS1	-4.9987436179	-11.5410267813	-1.6812041615	-1.0859860474
TRINITY_DN300289_c2_g1_i6	probable receptor kinase At1g80640 [Fragaria vesca vesca]	-1.7094065007	-11.7068073757	-0.9861182293	-0.9685640353
TRINITY_DN301247_c0_g1_i1	probable phosphatase 2C 49	-11.8412920945	-11.7186430745	-5.3961258786	-3.6241197089
TRINITY_DN300723_c0_g3_i5	probable steroid-binding 3	-3.0157659019	-12.0468199331	-6.4702398732	-2.3695091624
TRINITY_DN302563_c1_g3_i8	phosphatidylinositol:ceramide inositolphosphotransferase 2-like	0.3712575439	-13.2030308191	-1.9559510501	-2.1756595775

Table A4. *Details for the 30 most DE transcripts, 15 up-regulated and 15 down-regulated of Jonsok cultivar at 48 hours cold treatment and expression level (log2 fold change) of these transcripts in other time points (1 h, 5 h and 240 h)*

Name	Description	1 h	5 h	48 h	240 h
TRINITY_DN293687_c0_g1_i7	galactinol synthase 2-like			16.26489743018	14.94352801011
TRINITY_DN287924_c1_g1_i1	embryonic DC-8-like		9.61813670155	15.49890919045	14.47610063157
TRINITY_DN289945_c0_g1_i14	late embryogenesis abundant 76-like isoform X1		7.92065426022	14.57623304405	14.73606941747
TRINITY_DN289945_c0_g1_i5	late embryogenesis abundant 76-like isoform X1		9.87107631197	14.38623011030	14.72909822329
TRINITY_DN302854_c0_g1_i4	probable galactinol--sucrose galactosyltransferase 1	11.65206714693	9.51722641818	14.26351120535	13.21788801069
TRINITY_DN295378_c1_g1_i1	---NA---		9.59233109586	14.23610798393	14.88112059081
TRINITY_DN253360_c0_g3_i1	PREDICTED: uncharacterized protein LOC101295191		12.01835734828	13.82823483705	12.60898049306
TRINITY_DN276561_c1_g3_i2	beta-amyrin synthase-like [Fragaria vesca vesca]			13.82631767710	11.84440791976
TRINITY_DN287924_c1_g1_i2	embryonic DC-8-like		8.22979140781	13.81488867604	12.10730047518
TRINITY_DN295195_c3_g1_i16	anamorsin homolog			13.09874534457	
TRINITY_DN293687_c0_g1_i1	galactinol synthase 2-like			12.76988815173	9.71759782992
TRINITY_DN284112_c0_g1_i5	embryonic DC-8-like		5.86345649939	12.76768117615	10.99275026995
TRINITY_DN295939_c0_g1_i1	zinc finger CONSTANS-LIKE 2		7.50763065672	12.57697560582	13.45721060142
TRINITY_DN306381_c3_g2_i10	maltose excess 1, chloroplastic-like			12.42879846870	10.64110016322
TRINITY_DN294571_c0_g1_i14	GDT1 4	10.86345697146		12.37772347229	12.69325592124
TRINITY_DN284228_c1_g1_i3	ankyrin repeat-containing At5g02620-like	-2.30283364220	-3.12946274985	-11.56318488662	-8.22418666320
TRINITY_DN305943_c0_g2_i3	translocase subunit , chloroplastic	-0.34602775891	0.01148993270	-11.63117142569	0.83023836053
TRINITY_DN278078_c0_g1_i4	gibberellin 2-beta-dioxygenase 2-like	-1.09093252781	-3.01522026888	-11.67720711761	-4.40222020454
TRINITY_DN296019_c0_g1_i1	glucan endo-1,3-beta-glucosidase 14	-0.15883638092	-0.63699265300	-11.79830889845	-6.11895130818
TRINITY_DN304975_c0_g5_i4	PTI1-like tyrosine- kinase At3g15890	-1.23960516509	-3.03800092250	-11.88163074164	-1.11637013063
TRINITY_DN288337_c2_g1_i5	PREDICTED: uncharacterized protein LOC105350703	-2.13762968836	-2.01596796748	-12.00369855154	-7.42400548240
TRINITY_DN294909_c4_g1_i20	ACT domain-containing ACR12	-1.51339619891	-1.32425021907	-12.06085342420	-12.29924457511
TRINITY_DN301987_c1_g2_i1	ethylene-responsive transcription factor ERF027-like	0.46672444308	0.29265887183	-12.08870475562	-12.32620718079
TRINITY_DN290225_c2_g3_i2	TIFY 5A-like	1.51933554230	1.61565879393	-12.29862832090	-12.53626569431
TRINITY_DN296012_c0_g1_i3	PREDICTED: uncharacterized protein LOC105349822	-3.85828625582	-4.72470616242	-12.41913023863	-12.65715546783
TRINITY_DN299697_c0_g3_i2	Phosphatase 2C family isoform 2 [Theobroma cacao]	-3.42674920137	-3.09676306093	-12.44177826234	-6.31064368003
TRINITY_DN304907_c0_g2_i8	Respiratory burst oxidase D [Theobroma cacao]	0.99384150274	1.01291236930	-12.53811965077	-7.26056772736
TRINITY_DN293343_c1_g1_i2	PREDICTED: uncharacterized protein LOC101306070	-1.63885250718	-3.23494438877	-12.62464747529	-7.35959777622
TRINITY_DN294967_c1_g1_i8	---NA---	-1.46272473709	-2.00577610644	-12.69630973988	-8.43324930381
TRINITY_DN296507_c0_g3_i2	ethylene-responsive transcription factor ERF017	-1.61025475366	-2.45355999758	-13.19151289408	-10.77818627141

***Table A5**. Details for the 30 most DE transcripts, 15 up-regulated and 15 down-regulated of Jonsok cultivar at 240 hours cold treatment and expression level (log2 fold change) of these transcripts in other time points (1 h, 5 h and 240 h)*

Name	Description	1 h	5 h	48 h	240 h
TRINITY_DN293687_c0_g1_i7	galactinol synthase 2-like			16.26489743	14.94352801
TRINITY_DN295378_c1_g1_i1	---NA---		9.59233110	14.23610798	14.88112059
TRINITY_DN289945_c0_g1_i14	late embryogenesis abundant 76-like isoform X1		7.92065426	14.57623304	14.73606942
TRINITY_DN289945_c0_g1_i5	late embryogenesis abundant 76-like isoform X1		9.87107631	14.38623011	14.72909822
TRINITY_DN287924_c1_g1_i1	embryonic DC-8-like		9.61813670	15.49890919	14.47610063
TRINITY_DN303723_c2_g2_i15	PHD finger ALFIN-LIKE 4-like			11.87147678	13.72773224
TRINITY_DN295939_c0_g1_i1	zinc finger CONSTANS-LIKE 2		7.50763066	12.57697561	13.45721060
TRINITY_DN302854_c0_g1_i4	probable galactinol--sucrose galactosyltransferase 1	11.65206715	9.51722642	14.26351121	13.21788801
TRINITY_DN301121_c0_g1_i7	ras-related RABC1	11.97285706	10.94354351	10.91321689	13.05130360
TRINITY_DN306978_c0_g1_i8	asparagine synthetase [glutamine-hydrolyzing]	9.33778993	7.82908429	7.90687273	12.78003539
TRINITY_DN294571_c0_g1_i14	GDT1 4	10.86345697		12.37772347	12.69325592
TRINITY_DN302743_c1_g1_i12	serine threonine- kinase HT1 [Fragaria vesca vesca]			11.87199607	12.64487469
TRINITY_DN253360_c0_g3_i1	PREDICTED: uncharacterized protein LOC101295191		12.01835735	13.82823484	12.60898049
TRINITY_DN303047_c2_g4_i6	RING-H2 finger ATL56-like			11.47775094	12.33631517
TRINITY_DN304579_c1_g1_i3	RNI-like superfamily , [Theobroma cacao]		12.04541100		12.21022026
TRINITY_DN290225_c2_g3_i2	TIFY 5A-like	1.51933554	1.61565879	-12.29862832	-12.53626569
TRINITY_DN303225_c0_g3_i7	PREDICTED: uncharacterized protein LOC101305073	-0.67912605	-0.86221802	-3.18947802	-12.63987933
TRINITY_DN296012_c0_g1_i3	PREDICTED: uncharacterized protein LOC105349822	-3.85828626	-4.72470616	-12.41913024	-12.65715547
TRINITY_DN287758_c0_g1_i6	transcription factor bHLH92	0.49482036	0.69761943	-9.16425631	-12.67993582
TRINITY_DN301868_c1_g1_i5	PREDICTED: uncharacterized protein LOC101315183	0.25797816	0.14653808	-2.48835841	-12.90214904
TRINITY_DN302262_c0_g1_i22	omega-3 fatty acid desaturase, chloroplastic	1.25727708	0.95066144	-8.63562719	-12.91014945
TRINITY_DN306832_c5_g1_i9	pentatricopeptide repeat-containing At3g42630 [Prunus mume]	-0.77387892	-3.36408583	-4.09437360	-13.05943726
TRINITY_DN293026_c0_g1_i2	ethylene-responsive transcription factor ERF109-like	-0.55793586	-0.79628178	-10.17651140	-13.22367905
TRINITY_DN294967_c1_g1_i10	---NA---	0.23776915	-1.97831955	-10.25831814	-13.31570558
TRINITY_DN305112_c3_g1_i15	probable calcium-binding CML27	2.08310026	2.31479712	-2.68751109	-13.35432344
TRINITY_DN293026_c0_g1_i1	ethylene-responsive transcription factor ERF109-like	-1.16436560	-1.29037789	-9.35315612	-13.52927780
TRINITY_DN293026_c0_g1_i3	ethylene-responsive transcription factor ERF109-like	-0.38445888	-0.24059036	-9.12815984	-13.60926739
TRINITY_DN298821_c0_g2_i4	transcription factor bHLH14-like isoform X1	1.33909692	1.69227821	-7.67738258	-13.72420040
TRINITY_DN297575_c2_g1_i3	dehydration-responsive element-binding 1B-like	-0.58820759	-1.88375640	-9.50434639	-14.00323839
TRINITY_DN293026_c0_g1_i7	ethylene-responsive transcription factor ERF109-like	-0.74784153	-0.74850853	-10.24835410	-14.43310989

***Table A6**. Details for the 30 most DE transcripts, 15 up-regulated and 15 down-regulated of Elsanta cultivar at 1 hour cold treatment and expression level (log2 fold change) of these transcripts in other time points (5 h, 48 h and 240 h)*

Name	Description	1 h	5 h	48 h	240 h
TRINITY_DN306505_c0_g3_i1	xyloglucan endotransglucosylase hydrolase 9	12.65447	10.81811		10.61280
TRINITY_DN309623_c0_g2_i9	IAA-amino acid hydrolase ILR1-like 1	12.07047	12.76854		
TRINITY_DN314561_c1_g3_i1	mitogen-activated kinase 20	12.00337	11.28049		
TRINITY_DN311172_c0_g1_i5	PREDICTED: phosphoglucomutase, cytoplasmic	11.82698	10.94941	12.70129	
TRINITY_DN314589_c0_g1_i5	uncharacterized membrane At1g16860-like [Fragaria vesca vesca]	11.82324	12.76027	12.86271	12.25161
TRINITY_DN317011_c2_g2_i10	RING finger and CHY zinc finger domain-containing 1	11.78121	10.96013		
TRINITY_DN309623_c0_g2_i6	IAA-amino acid hydrolase ILR1-like 1	11.65469	11.53897		
TRINITY_DN310629_c0_g1_i13	methionine gamma-lyase	11.62488	10.61958	11.47862	11.68384
TRINITY_DN317108_c4_g4_i5	ubiquitin receptor RAD23b	11.58180	10.53506	11.37683	
TRINITY_DN311526_c0_g1_i3	PREDICTED: uncharacterized protein LOC101303095	11.43921	10.61713		10.42753
TRINITY_DN311329_c2_g4_i12	PREDICTED: uncharacterized protein LOC101315048	11.32271			
TRINITY_DN311065_c0_g3_i3	mediator of RNA polymerase II transcription subunit 1 isoform X1	11.31267	12.08289	12.49217	12.26349
TRINITY_DN317111_c0_g1_i4	proteasome activator subunit 4	11.30131		12.82647	12.52513
TRINITY_DN317177_c3_g1_i6	auxin response factor partial	11.30040	11.19276		
TRINITY_DN307080_c1_g1_i2	glutathione gamma-glutamylcysteinyltransferase 1-like isoform X1	11.23057	12.42255		
TRINITY_DN305747_c0_g2_i10	nudC domain-containing 2	-10.20370	-0.83971	-1.06356	-0.16504
TRINITY_DN300138_c1_g1_i2	PREDICTED: ankyrin-3	-10.24167	-0.09597	-0.30597	-0.17955
TRINITY_DN314533_c0_g1_i8	myosin-1 [Prunus mume]	-10.25980	-10.21098	-0.14698	-1.62890
TRINITY_DN316636_c0_g1_i11	DNA-directed RNA polymerase chloroplastic	-10.26813	-2.24431	0.76539	-4.33703
TRINITY_DN315874_c4_g1_i2	PREDICTED: metacaspase-1-like	-10.41445	-10.36626	-1.76882	-0.00191
TRINITY_DN316939_c2_g2_i5	DNA-directed RNA polymerases IV and V subunit 11	-10.48708	-10.44111	-0.32206	0.34086
TRINITY_DN305198_c1_g3_i2	Translocon at the outer envelope membrane of chloroplasts	-10.51578	-1.91266	-6.52033	-3.80849
TRINITY_DN309993_c0_g3_i16	homeobox knotted-1-like 6	-10.55144	-3.26969	-1.25422	-3.92675
TRINITY_DN309567_c0_g1_i4	PREDICTED: uncharacterized protein At4g06744	-10.63734	-10.58865	-3.60795	-10.65590
TRINITY_DN300393_c7_g2_i1	receptor kinase FERONIA isoform X1	-10.79563	-10.74757	-4.69116	-10.81517
TRINITY_DN315254_c1_g1_i6	PREDICTED: uncharacterized protein LOC101304894	-10.82781	-4.24912	-5.35485	-5.19704
TRINITY_DN306571_c3_g2_i5	PREDICTED: protein YLS9-like	-11.22757	-2.86433	0.68069	0.49813
TRINITY_DN313908_c1_g1_i7	lipid phosphate phosphatase 2-like isoform X1	-11.57999	-11.53142	-11.48850	-4.77428
TRINITY_DN315087_c1_g3_i5	interferon-related developmental regulator 1	-12.132010	-6.063257	0.350973	0.289603
TRINITY_DN315882_c1_g3_i7	patatin 6 [Fragaria vesca vesca]	-12.611269	-4.085163	-2.302454	-3.906719

***Table A7**. Details for the 30 most DE transcripts, 15 up-regulated and 15 down-regulated of Elsanta cultivar at 5 hour cold treatment and expression level (log2 fold change) of these transcripts in other time points (1 h, 48 h and 240 h)*

Name	Description	1 h	5 h	48 h	240 h
TRINITY_DN309623_c0_g2_i9	IAA-amino acid hydrolase ILR1-like 1	12.0704681611	12.7685381700		
TRINITY_DN314589_c0_g1_i5	uncharacterized membrane At1g16860-like	11.8232386210	12.7602709436	12.8627093427	12.2516120425
TRINITY_DN312997_c0_g1_i9	PREDICTED: uncharacterized protein LOC101297897		12.7087256751		
TRINITY_DN317011_c2_g2_i7	RING finger and CHY zinc finger domain-containing 1		12.5644081178		
TRINITY_DN314535_c1_g1_i5	low-temperature-induced 65 kDa isoform X4	10.4824893147	12.5214781112	12.5356035003	
TRINITY_DN307080_c1_g1_i2	glutathione gamma-glutamylcysteinyltransferase 1	11.2305681770	12.4225457984		
TRINITY_DN315584_c3_g1_i9	26S proteasome non-ATPase regulatory subunit 6 homolog	10.5740715854	12.3867347881	9.8238622413	
TRINITY_DN312056_c2_g1_i1	12-oxophytodienoate reductase 3-like	10.3685170473	12.2956994695		
TRINITY_DN311065_c0_g3_i3	mediator of RNA polymerase II transcription subunit 1	11.3126673927	12.0828912179	12.4921670561	12.2634862898
TRINITY_DN277572_c0_g1_i2	7-deoxyloganetin glucosyltransferase-like	10.2572224521	12.0745874775		
TRINITY_DN316642_c3_g3_i1	adagio 3	9.5299618721	11.9189728322	10.6102944657	8.8215579559
TRINITY_DN307336_c1_g1_i2	zinc finger CONSTANS-LIKE 2	10.6102077298	11.8427590945	11.9064587808	11.5908830901
TRINITY_DN303050_c0_g1_i6	PREDICTED: uncharacterized protein At1g66480-like		11.8232057756		
TRINITY_DN286546_c0_g1_i6	bark storage A-like	10.7594529661	11.7194184693		
TRINITY_DN309623_c0_g2_i6	IAA-amino acid hydrolase ILR1-like 1	11.6546943233	11.5389734799		
TRINITY_DN296902_c2_g1_i6	probable ADP-ribosylation factor GTPase-activating AGD11	-4.1386600430	-10.4440934517	-10.4001741623	-7.3282338197
TRINITY_DN316173_c2_g2_i5	pentatricopeptide repeat-containing chloroplastic	0.0661815785	-10.4506982351	-0.0587681190	0.4809777072
TRINITY_DN303846_c4_g1_i1	NADPH:quinone oxidoreductase	0.1853044183	-10.5147484186	-0.0840433454	-2.0004461429
TRINITY_DN309567_c0_g1_i4	PREDICTED: uncharacterized protein At4g06744	-10.6373363481	-10.5886479279	-3.6079528231	-10.6558966173
TRINITY_DN295438_c0_g1_i7	---NA---	-4.4648541547	-10.6684106111	-5.6202935753	-7.1865612727
TRINITY_DN300393_c7_g2_i1	receptor kinase FERONIA isoform X1	-10.7956306861	-10.7475738074	-4.6911582497	-10.8151749487
TRINITY_DN297033_c3_g3_i4	PREDICTED: uncharacterized protein LOC101296587	0.4482485990	-10.8249233972	-1.8815591527	-10.8916971890
TRINITY_DN316328_c1_g1_i7	PREDICTED: uncharacterized protein LOC101308870	-8.9620870086	-10.8353594795	-2.1758075147	-1.9471803215
TRINITY_DN306539_c1_g2_i3	3-oxoacyl-[acyl-carrier-] chloroplastic-like	-1.6273488985	-11.1581165766	-1.0670586240	0.1019367161
TRINITY_DN296306_c4_g2_i3	---NA---	-3.3384998834	-11.4246436714	0.0468552541	-0.8788840388
TRINITY_DN309894_c0_g2_i2	LOB domain-containing 37-like	-0.9397035181	-11.4990387018	-11.4544828507	-4.1374497154
TRINITY_DN313908_c1_g1_i7	lipid phosphate phosphatase 2-like isoform X1 [Prunus mume]	-11.5799883111	-11.5314226094	-11.4885011003	-4.7742778031
TRINITY_DN299928_c0_g1_i5	PREDICTED: uncharacterized protein LOC101297173	0.6100859221	-12.2852600904	-0.0176848467	-7.1855811825
TRINITY_DN312089_c3_g2_i9	vicianin hydrolase-like	-3.0150922344	-12.3088444541	-3.6782347844	-2.6431780679
TRINITY_DN312089_c3_g2_i25	vicianin hydrolase-like	-3.3750674526	-12.7476504927	-3.9887082101	-1.3751892547

***Table A8**. Details for the 30 most DE transcripts, 15 up-regulated and 15 down-regulated of Elsanta cultivar at 48 hours cold treatment and expression level (log2 fold change) of these transcripts in other time points (1 h, 5 h and 240 h)*

Name	Description	1 h	5 h	48 h	240 h
TRINITY_DN314589_c0_g1_i5	uncharacterized membrane At1g16860-like [Fragaria vesca vesca]	11.8232386210	12.7602709436	12.8627093427	12.2516120425
TRINITY_DN317111_c0_g1_i4	proteasome activator subunit 4	11.3013084887		12.8264727055	12.5251256961
TRINITY_DN311172_c0_g1_i5	PREDICTED: phosphoglucomutase, cytoplasmic	11.8269770756	10.9494140737	12.7012902975	
TRINITY_DN305130_c0_g1_i1	2-Cys peroxiredoxin chloroplastic		9.5041668280	12.6011821955	11.6980740197
TRINITY_DN314535_c1_g1_i5	low-temperature-induced 65 kDa isoform X4	10.4824893147	12.5214781112	12.5356035003	
TRINITY_DN311065_c0_g3_i3	mediator of RNA polymerase II transcription subunit 1 isoform X1	11.3126673927	12.0828912179	12.4921670561	12.2634862898
TRINITY_DN308841_c1_g4_i2	40S ribosomal S2-1-like		10.7089156366	12.2011851654	11.5759368561
TRINITY_DN312042_c3_g1_i14	PREDICTED: uncharacterized protein LOC105350894			12.1766726930	11.4447692685
TRINITY_DN312943_c2_g3_i3	inorganic phosphate transporter 2- chloroplastic			12.1765079822	11.4233951825
TRINITY_DN314975_c0_g1_i15	PREDICTED: uncharacterized protein LOC101291352		9.6920775401	12.1613684743	10.8328251939
TRINITY_DN307336_c1_g1_i2	zinc finger CONSTANS-LIKE 2	10.6102077298	11.8427590945	11.9064587808	11.5908830901
TRINITY_DN295296_c1_g2_i4	unnamed protein product		10.8062792398	11.8348353697	
TRINITY_DN310904_c1_g5_i7	dehydrin Xero 2			11.7821156092	9.1794986411
TRINITY_DN309484_c1_g2_i2	transcription repressor OFP12-like			11.7671465117	
TRINITY_DN301916_c2_g2_i7	probable phosphatase 2C 34		8.1902902851	11.6546699883	9.4504947450
TRINITY_DN315646_c1_g1_i4	linolenate hydroperoxide chloroplastic	-0.3477854610	-4.5040209727	-11.1541637602	-0.7671967854
TRINITY_DN311944_c0_g1_i7	photosystem I reaction center subunit chloroplastic	-3.5787108074	-5.2124997249	-11.2064201825	-2.2830254144
TRINITY_DN317061_c1_g1_i13	F-box At3g58530 isoform X1	-0.0906164849	-1.4077948251	-11.3468164573	-3.6336737280
TRINITY_DN317633_c2_g1_i1	CHROMATIN REMODELING 4 isoform X2	-2.0564682954	0.2073631876	-11.3610162251	-11.4718141045
TRINITY_DN309281_c3_g3_i1	ethylene-responsive transcription factor ERF109-like	0.8541569441	0.2126361634	-11.3709909934	-11.4864708275
TRINITY_DN309894_c0_g2_i2	LOB domain-containing 37-like	-0.9397035181	-11.4990387018	-11.4544828507	-4.1374497154
TRINITY_DN313908_c1_g1_i7	lipid phosphate phosphatase 2-like isoform X1 [Prunus mume]	-11.5799883111	-11.5314226094	-11.4885011003	-4.7742778031
TRINITY_DN310384_c3_g1_i17	probable receptor kinase At5g15080	-1.6803900058	-0.9882664891	-11.6873757770	-0.3288910006
TRINITY_DN315882_c1_g3_i3	nudix hydrolase mitochondrial-like	-0.8660165588	-6.0482832635	-11.8116040407	-11.9272746966
TRINITY_DN309049_c0_g1_i1	dehydration-responsive element-binding 1B-like	1.4084797767	-1.3033395861	-11.8631823079	-6.1283049088
TRINITY_DN308694_c0_g1_i2	F-box kelch-repeat At3g27150 [Fragaria vesca vesca]	-0.3415545681	-0.2320374868	-11.8676091871	-3.3063138302
TRINITY_DN316418_c0_g1_i5	transcription initiation factor TFIID subunit 9 [Fragaria vesca vesca]	-0.4297298473	-3.1367042763	-12.0356710939	-3.2639609055
TRINITY_DN317424_c2_g1_i2	PREDICTED: uncharacterized protein LOC103968019	1.0150613731	-2.2794562104	-12.2631390413	-12.3787871433
TRINITY_DN314152_c1_g5_i3	PREDICTED: protein BPS1, chloroplastic-like	-0.4573989063	-0.5632121686	-12.4558089646	-12.5709892173
TRINITY_DN288725_c0_g1_i1	replication-associated partial	-0.1755219085	0.2660218302	-19.0413887557	-19.1528611933

***Table A9**. Details for the 30 most DE transcripts, 15 up-regulated and 15 down-regulated of Elsanta cultivar at 240 hours cold treatment and expression level (log2 fold change) of these transcripts in other time points (1 h, 5 h and 48 h)*

Name	Description	1 h	5 h	48 h	240 h
TRINITY_DN317111_c0_g1_i4	proteasome activator subunit 4	11.30130848872		12.82647270554	12.52512569607
TRINITY_DN311065_c0_g3_i3	mediator of RNA polymerase II transcription subunit 1 isoform X1	11.31266739273	12.08289121787	12.49216705607	12.26348628979
TRINITY_DN314589_c0_g1_i5	uncharacterized membrane At1g16860-like [Fragaria vesca vesca]	11.82323862098	12.76027094361	12.86270934267	12.25161204247
TRINITY_DN305130_c0_g1_i1	2-Cys peroxiredoxin chloroplastic		9.50416682802	12.60118219546	11.69807401969
TRINITY_DN310629_c0_g1_i13	methionine gamma-lyase	11.62488302707	10.61957600750	11.47862043383	11.68384430125
TRINITY_DN309017_c1_g3_i4	hypothetical protein GLYMA_19G2530001, partial				11.66421932276
TRINITY_DN307336_c1_g1_i2	zinc finger CONSTANS-LIKE 2	10.61020772976	11.84275909450	11.90645878075	11.59088309013
TRINITY_DN314152_c1_g5_i9	PREDICTED: protein BPS1, chloroplastic-like			10.47499712238	11.57708027801
TRINITY_DN308841_c1_g4_i2	40S ribosomal S2-1-like		10.70891563663	12.20118516545	11.57593685608
TRINITY_DN300733_c0_g1_i7	trichome birefringence-like 36 isoform X1		10.02657415206	10.47552813944	11.53969018384
TRINITY_DN296610_c2_g1_i6	probable xyloglucan endotransglucosylase hydrolase 6			9.98246789341	11.53946793162
TRINITY_DN300144_c0_g3_i13	PREDICTED: uncharacterized protein LOC101292509 isoform X2		9.88503807582	10.12699734463	11.50510547905
TRINITY_DN312042_c3_g1_i14	PREDICTED: uncharacterized protein LOC105350894			12.17667269296	11.44476926846
TRINITY_DN312943_c2_g3_i3	inorganic phosphate transporter 2-chloroplastic			12.17650798222	11.42339518248
TRINITY_DN306767_c2_g2_i4	serine threonine- kinase SAPK2-like				11.37569515667
TRINITY_DN303505_c7_g1_i5	acyl-[acyl-carrier-] desaturase chloroplastic	1.33793710498	0.01062296780	-6.41997046886	-11.71994044541
TRINITY_DN303553_c0_g1_i2	2-aminoethanethiol dioxygenase-like	0.09676917949	-2.78610532794	-9.70140180130	-11.81575399271
TRINITY_DN246508_c0_g3_i2	PREDICTED: uncharacterized protein LOC101300623	1.95874104300	1.01403061847	-3.96099399250	-11.81643762863
TRINITY_DN309644_c0_g1_i8	transcription factor bHLH14-like isoform X2	1.43166886605	3.06067120586	-5.84256296423	-11.91112044606
TRINITY_DN315882_c1_g3_i3	nudix hydrolase mitochondrial-like	-0.86601655879	-6.04828326345	-11.81160404074	-11.92727469656
TRINITY_DN310742_c2_g4_i4	glycine-rich RNA-binding mitochondrial	-0.19678776169	-1.18448059960	-0.71579189493	-12.06992883823
TRINITY_DN311697_c2_g2_i8	cytochrome P450 71D9-like	-0.68390523383	0.36420629577	-5.06606223734	-12.09973748042
TRINITY_DN310293_c0_g1_i8	signal recognition particle 54 kDa chloroplastic	-1.70251425974	-0.09177394963	-1.18310128104	-12.23125294964
TRINITY_DN315254_c1_g1_i3	PREDICTED: uncharacterized protein LOC101304894	-0.06108555795	-1.28141724236	-7.18237471222	-12.23488451429
TRINITY_DN310464_c1_g2_i3	nucleosome assembly 1 4-like	-0.30087265690	-1.49678166127	-2.25537216276	-12.33723977278
TRINITY_DN317424_c2_g1_i2	PREDICTED: uncharacterized protein LOC103968019	1.01506137309	-2.27945621042	-12.26313904126	-12.37878714326
TRINITY_DN314152_c1_g5_i3	PREDICTED: protein BPS1, chloroplastic-like	-0.45739890630	-0.56321216855	-12.45580896459	-12.57098921735
TRINITY_DN309281_c3_g3_i4	ethylene-responsive transcription factor ERF109-like	1.29703381343	0.77309376874	-10.69129918458	-12.78103893101
TRINITY_DN301346_c2_g1_i1	salicylic acid-binding 2-like	-2.53939843267	-1.20733211164	-4.18661244384	-13.27123541769
TRINITY_DN288725_c0_g1_i1	replication-associated partial	-0.17552190855	0.26602183020	-19.04138875571	-19.15286119333

Selection of genes related to cold tolerance

Table A10. *Details for the all DE isoforms of dehydrin COR47-like at each treatment time point in 'Jonsok' and 'Elsanta'. The highlighted transcripts are the transcripts that are presented in the final table in result section. The NA (not available) stands for the transcripts which were not DE in that particular treatment.*

	Tags	SeqName	Description	Length	#Hits	e-Value	sim mean	#GO	GO IDs	GO Names	logFC	logCPM	PValue	FDR
J00vs01		NA												
J00vs05	[BLASTED]	TRINITY_DN302753_c0_g3_i4	dehydrin COR47-like	551	1	4.89E-04	95				2.20298107	2.278978	1.13E-08	8.51E-07
	[BLASTED, MAP	TRINITY_DN302753_c0_g2_i2	dehydrin COR47-like	687	3	1.87E-32	75.33	2	P:GO:0006950; P:	P:response to stress; P:respo	1.261008158	9.677999	2.51E-12	3.60E-10
	[BLASTED, MAP	TRINITY_DN302753_c0_g2_i1	dehydrin COR47-like	701	3	2.24E-37	75.67	2	P:GO:0006950; P:	P:response to stress; P:respo	1.053595522	10.1114	9.44E-09	7.23E-07
J00vs48	[BLASTED, MAP	TRINITY_DN302753_c0_g2_i2	dehydrin COR47-like	687	3	1.87E-32	75.33	2	P:GO:0006950; P:	P:response to stress; P:respo	2.774998076	10.97948	2.57E-46	1.27E-43
	[BLASTED, MAP	TRINITY_DN302753_c0_g2_i1	dehydrin COR47-like	701	3	2.24E-37	75.67	2	P:GO:0006950; P:	P:response to stress; P:respo	2.395028834	11.23053	2.82E-40	1.10E-37
	[BLASTED]	TRINITY_DN302753_c0_g3_i2	dehydrin COR47-like	397	1	2.57E-04	95				2.158486617	8.053652	1.04E-28	2.25E-26
	[BLASTED]	TRINITY_DN302753_c0_g3_i4	dehydrin COR47-like	551	1	4.89E-04	95				2.085987952	2.184094	6.33E-08	1.37E-06
J00vs240	[BLASTED]	TRINITY_DN302753_c0_g3_i4	dehydrin COR47-like	551	1	4.89E-04	95				1.340055217	1.678366	0.000793	0.005188
	[BLASTED, MAP	TRINITY_DN302753_c0_g2_i2	dehydrin COR47-like	687	3	1.87E-32	75.33	2	P:GO:0006950; P:	P:response to stress; P:respo	1.11693828	9.681944	4.61E-09	1.10E-07
	[BLASTED, MAP	TRINITY_DN288018_c0_g1_i3	dehydrin COR47-like	822	3	8.15E-33	78.33	2	P:GO:0006950; P:	P:response to stress; P:respo	-3.356319384	0.094887	2.12E-08	4.44E-07
	[BLASTED, MAP	TRINITY_DN288018_c0_g1_i1	dehydrin COR47-like	600	3	1.27E-57	81	1	P:GO:0050896	P:response to stimulus	-3.862041609	-1.37403	2.82E-04	0.002158
E00vs01		NA												
E00vs05	[BLASTED, MAP	TRINITY_DN310505_c0_g6_i1	dehydrin COR47-like	496	3	9.02E-29	76.33	2	P:GO:0006950; P:	P:response to stress; P:respo	1.285938357	9.700372	1.48E-10	6.38E-09
E00vs48	[BLASTED, MAP	TRINITY_DN310505_c0_g6_i1	dehydrin COR47-like	496	3	9.02E-29	76.33	2	P:GO:0006950; P:	P:response to stress; P:respo	3.210931215	11.27732	8.08E-86	8.45E-83
E00vs240	[BLASTED, MAP	TRINITY_DN310505_c0_g6_i1	dehydrin COR47-like	496	3	9.02E-29	76.33	2	P:GO:0006950; P:	P:response to stress; P:respo	1.629855063	10.04077	3.66E-31	5.78E-29

Table A11. *Details for the all DE isoforms of transcription factor ICE1*

	Tags	SeqName	Description	Length	#Hits	e-Value	sim mean	#GO	GO IDs	GO Names	logFC	logCPM	PValue	FDR
J00vs01		NA												
J00vs05		NA												
J00vs48		NA												
J00vs240	[BLASTED,	TRINITY_DN300514_c1_g4_i1	transcription factor ICE1	465	3	4.24E-52	98	1	F:GO:0046983	F:protein dimerization activity	-1.59422	0.144759	0.000718	0.004776
E00vs01		NA												
E00vs05		NA												
E00vs48		NA												
E00vs240	[BLASTED,	TRINITY_DN312698_c2_g2_i3	transcription factor ICE1	701	3	7.69E-66	98.67	3	F:GO:0032440; F:GO:0046983; P:GO:0055114	F:2-alkenal reductase [NAD(P)] activity; F:protein dimerization activity; P:oxidation-reduction process	-8.46542	-0.92565	0.004619	0.019979

Table A12. *Details for the all DE isoforms of E3 ubiquitin- ligase HOS1*

	Tags	SeqName	Description	Length	#Hits	e-Value	sim mean	#GO	GO IDs	GO Names	logFC	logCPM	PValue	FDR
J00vs01		NA												
J00vs05		NA												
J00vs48	[BLASTED]	TRINITY_DN306521_c2_g1_i8	E3 ubiquitin- ligase HOS1	2460	3	0	87.67				1.409393	2.24787	0.002064	0.012644
	[BLASTED]	TRINITY_DN306521_c2_g1_i1	E3 ubiquitin- ligase HOS1	482	1	3.19E-07	100				1.011788	1.97692	0.002511	0.014862
J00vs240	[BLASTED, N	TRINITY_DN298257_c0_g7_i3	E3 ubiquitin- ligase HOS1	884	3	2E-156	81.33	23	P:GO:0016579; P:GO:0010162; P:GO:0019915; P	P:protein deubiqui	1.58752	0.394499	0.001173	0.00722
	[BLASTED]	TRINITY_DN306521_c2_g1_i8	E3 ubiquitin- ligase HOS1	2460	3	0	87.67				1.285324	2.257426	0.004065	0.020241
E00vs01	[BLASTED]	TRINITY_DN316550_c1_g1_i1	E3 ubiquitin- ligase HOS1	3680	3	0E	88.67				-			
E00vs05		NA												
E00vs48		NA												
E00vs240		NA												

Table A13. *Details for the all DE isoforms of zinc finger ZAT12-like*

	Tags	SeqName	Description	Length	#Hits	e-Value	sim mean	#GO	GO IDs	GO Names	logFC	logCPM	PValue	FDR
J00vs01	[BLASTED]	TRINITY_DN290336_c0_g1_i1	zinc finger ZAT12-like	209	3	6.29E-14	90.67				-2.21798	-0.24521	0.000816	0.031755
	[BLASTED]	TRINITY_DN290336_c1_g4_i10	zinc finger ZAT12-like	699	3	1.83E-90	95				-2.38255	3.058606	1.44E-05	0.001237
	[BLASTED]	TRINITY_DN290336_c1_g4_i5	zinc finger ZAT12-like	976	3	3.78E-94	84.33				-2.56502	3.238975	3.54E-09	9.26E-07
	[BLASTED]	TRINITY_DN290336_c1_g4_i1	zinc finger ZAT12-like	505	3	5.21E-66	88.33				-2.72515	2.565176	1.14E-06	0.000137
	[BLASTED]	TRINITY_DN290336_c1_g4_i7	zinc finger ZAT12-like	965	3	8.66E-84	94.67				-3.04372	3.901198	1.27E-08	2.87E-06
	[BLASTED]	TRINITY_DN290336_c1_g4_i2	zinc finger ZAT12-like	888	3	2.6E-108	92				-3.14679	4.454774	1.31E-08	2.96E-06
J00vs05	[BLASTED]	TRINITY_DN290336_c1_g4_i10	zinc finger ZAT12-like	699	3	1.83E-90	95				-2.7157	2.975198	1.5E-06	7.01E-05
	[BLASTED]	TRINITY_DN290336_c0_g1_i1	zinc finger ZAT12-like	209	3	6.29E-14	90.67				-2.90449	-0.37015	9.74E-05	0.002694
	[BLASTED]	TRINITY_DN290336_c1_g4_i4	zinc finger ZAT12-like	887	5	3.54E-91	80.2				-2.92724	-0.02413	0.001309	0.023512
	[BLASTED]	TRINITY_DN290336_c1_g4_i5	zinc finger ZAT12-like	976	3	3.78E-94	84.33				-3.15844	3.122581	4.96E-12	6.84E-10
	[BLASTED]	TRINITY_DN290336_c1_g4_i1	zinc finger ZAT12-like	505	3	5.21E-66	88.33				-3.35113	2.456375	4.79E-16	1.11E-13
	[BLASTED]	TRINITY_DN290336_c1_g4_i2	zinc finger ZAT12-like	888	3	2.6E-108	92				-3.35419	4.409702	4.13E-23	1.92E-20
	[BLASTED]	TRINITY_DN290336_c1_g4_i7	zinc finger ZAT12-like	965	3	8.66E-84	94.67				-3.98099	3.775071	7.1E-16	1.63E-13
J00vs48	[BLASTED,	TRINITY_DN286910_c0_g3_i3	zinc finger ZAT12-like	804	3	3.9E-128	82	1	F:GO:0046872	F:metal ion binding	-1.38357	1.956824	0.002666	0.015611
	[BLASTED]	TRINITY_DN290336_c0_g1_i1	zinc finger ZAT12-like	209	3	6.29E-14	90.67				-3.38704	-0.42518	0.00019	0.001695
	[BLASTED]	TRINITY_DN290336_c1_g4_i10	zinc finger ZAT12-like	699	3	1.83E-90	95				-3.81116	2.840206	2.37E-12	1.09E-10
	[BLASTED]	TRINITY_DN290336_c1_g4_i4	zinc finger ZAT12-like	887	5	3.54E-91	80.2				-4.1544	-0.14458	0.002413	0.014389
	[BLASTED]	TRINITY_DN290336_c1_g4_i2	zinc finger ZAT12-like	888	3	2.6E-108	92				-4.59584	4.310927	2.95E-35	9.33E-33
	[BLASTED]	TRINITY_DN290336_c1_g4_i1	zinc finger ZAT12-like	505	3	5.21E-66	88.33				-4.79486	2.345857	9.2E-14	5.13E-12
	[BLASTED]	TRINITY_DN290336_c1_g4_i5	zinc finger ZAT12-like	976	3	3.78E-94	84.33				-5.05841	2.975693	3.53E-19	3.52E-17
	[BLASTED]	TRINITY_DN290336_c1_g4_i7	zinc finger ZAT12-like	965	3	8.66E-84	94.67				-5.34494	3.709514	5.29E-12	2.31E-10
J00vs240	[BLASTED]	TRINITY_DN290336_c1_g4_i4	zinc finger ZAT12-like	887	5	3.54E-91	80.2				-3.2651	0.020909	0.000777	0.005103
	[BLASTED]	TRINITY_DN290336_c1_g4_i10	zinc finger ZAT12-like	699	3	1.83E-90	95				-3.8975	2.935537	3.84E-13	1.74E-11
	[BLASTED]	TRINITY_DN290336_c0_g1_i1	zinc finger ZAT12-like	209	3	6.29E-14	90.67				-4.12867	-0.4218	4.17E-07	6.69E-06
	[BLASTED]	TRINITY_DN290336_c1_g4_i2	zinc finger ZAT12-like	888	3	2.6E-108	92				-4.79471	4.406116	9.48E-43	4.05E-40
	[BLASTED]	TRINITY_DN290336_c1_g4_i1	zinc finger ZAT12-like	505	3	5.21E-66	88.33				-5.03047	2.435117	6.39E-24	8.88E-22
	[BLASTED]	TRINITY_DN290336_c1_g4_i5	zinc finger ZAT12-like	976	3	3.78E-94	84.33				-5.51853	3.062453	6.2E-25	9.4E-23
	[BLASTED]	TRINITY_DN290336_c1_g4_i7	zinc finger ZAT12-like	965	3	8.66E-84	94.67				-6.67714	3.783085	9.59E-17	6.9E-15
E00vs01	[BLASTED,	TRINITY_DN289738_c0_g1_i4	zinc finger ZAT12-like	986	3	3.8E-132	81.33	1	F:GO:0046872	F:metal ion binding	-1.11591	2.823898	1.81E-08	8.94E-07
	[BLASTED]	TRINITY_DN301106_c1_g3_i1	zinc finger ZAT12-like	852	3	2.1E-110	92.33				-1.55554	3.8525	0.005386	0.049453
	[BLASTED]	TRINITY_DN301106_c1_g3_i4	zinc finger ZAT12-like	1011	3	5.5E-112	93				-3.26542	3.51238	2.79E-09	1.61E-07
	[BLASTED]	TRINITY_DN301106_c1_g8_i1	zinc finger ZAT12-like	724	3	3.29E-95	95				-1.98518	2.818505	0.000173	0.003055
E00vs05	[BLASTED]	TRINITY_DN301106_c1_g3_i3	zinc finger ZAT12-like	966	3	6.9E-71	91				-2.75208	-0.42096	0.000105	0.001348
	[BLASTED]	TRINITY_DN301106_c1_g3_i5	zinc finger ZAT12-like	806	3	2.85E-94	89				-2.7612	2.413915	0.000217	0.002517
	[BLASTED]	TRINITY_DN301106_c1_g8_i1	zinc finger ZAT12-like	724	3	3.29E-95	95				-3.14353	2.620094	3.6E-08	1.02E-06
	[BLASTED]	TRINITY_DN301106_c1_g3_i1	zinc finger ZAT12-like	852	3	2.1E-110	92.33				-3.33855	3.536941	1.74E-07	4.33E-06
	[BLASTED]	TRINITY_DN301106_c1_g3_i4	zinc finger ZAT12-like	1011	3	5.5E-112	93				-4.07628	3.422965	8.16E-12	4.21E-10
E00vs48	[BLASTED]	TRINITY_DN301106_c1_g8_i1	zinc finger ZAT12-like	724	3	3.29E-95	95				-3.03939	2.632565	1.09E-06	1.22E-05
	[BLASTED]	TRINITY_DN301106_c1_g3_i1	zinc finger ZAT12-like	852	3	2.1E-110	92.33				-4.54569	3.463231	2.11E-12	6.19E-11
	[BLASTED]	TRINITY_DN301106_c1_g3_i3	zinc finger ZAT12-like	966	3	6.9E-71	91				-2.86737	-0.42601	0.00559	0.021623
	[BLASTED]	TRINITY_DN301106_c1_g3_i4	zinc finger ZAT12-like	1011	3	5.5E-112	93				-4.56492	3.400951	1.92E-13	6.41E-12
	[BLASTED]	TRINITY_DN301106_c1_g3_i5	zinc finger ZAT12-like	806	3	2.85E-94	89				-3.32307	2.356112	9.27E-06	8.49E-05
	[BLASTED,	TRINITY_DN289738_c0_g1_i4	zinc finger ZAT12-like	986	3	3.8E-132	81.33	1	F:GO:0046872	F:metal ion binding	-1.12744	2.790782	3.53E-05	0.00028
	[BLASTED]	TRINITY_DN289738_c0_g1_i3	zinc finger ZAT12-like	798	3	5.7E-126	77.33				-1.15702	1.117689	0.000326	0.001969
E00vs240	[BLASTED]	TRINITY_DN301106_c1_g3_i5	zinc finger ZAT12-like	806	3	2.85E-94	89				-3.34673	2.440599	1.77E-06	2.09E-05
	[BLASTED]	TRINITY_DN301106_c1_g8_i1	zinc finger ZAT12-like	724	3	3.29E-95	95				-3.96803	2.64452	6.94E-10	1.55E-08
	[BLASTED]	TRINITY_DN301106_c1_g3_i4	zinc finger ZAT12-like	1011	3	5.5E-112	93				-5.06019	3.472437	5.57E-16	2.75E-14
	[BLASTED]	TRINITY_DN301106_c1_g3_i1	zinc finger ZAT12-like	852	3	2.1E-110	92.33				-5.3894	3.525406	1.88E-16	9.79E-15
	[BLASTED]	TRINITY_DN301106_c1_g3_i3	zinc finger ZAT12-like	966	3	6.9E-71	91				-5.71356	-0.50647	4.92E-08	7.89E-07

Table A14. *Details for the all DE isoforms of zinc finger ZAT10*

	Tags	SeqName	Description	Length	#Hits	e-Value	sim mean	#GO	GO IDs	GO Names	logFC	logCPM	PValue	FDR
J00vs01		NA												
J00vs05		NA												
J00vs48	[BLASTED,	TRINITY_DN300151_c0_g5_i1	zinc finger ZAT10	374	2	2.15E-22	94.5	1	F:GO:0046872	F:metal ion binding	-1.97464	0.134997	0.006357	0.031604
	[BLASTED,	TRINITY_DN297178_c1_g3_i1	zinc finger ZAT10	466	3	6.41E-65	83	1	F:GO:0046872	F:metal ion binding	-2.08852	4.441307	1.67E-08	4.06E-07
	[BLASTED]	TRINITY_DN297178_c1_g4_i1	zinc finger ZAT10	372	3	5E-38	77.33				-2.18824	3.448486	3.73E-07	6.79E-06
	[BLASTED]	TRINITY_DN297178_c1_g3_i6	zinc finger ZAT10	243	3	6.8E-39	78				-2.19025	2.164884	4.38E-07	7.84E-06
	[BLASTED,	TRINITY_DN300151_c0_g2_i4	zinc finger ZAT10	308	3	9.12E-40	83	1	F:GO:0046872	F:metal ion binding	-2.21148	1.274025	0.001882	0.011723
	[BLASTED,	TRINITY_DN297178_c1_g4_i2	zinc finger ZAT10	219	3	1.16E-16	73.67	1	F:GO:0046872	F:metal ion binding	-2.24694	2.094765	4.95E-05	0.000525
	[BLASTED,	TRINITY_DN297178_c1_g3_i2	zinc finger ZAT10	504	3	1.42E-89	77.33	1	F:GO:0046872	F:metal ion binding	-2.43048	3.336945	4.52E-07	8.08E-06
	[BLASTED]	TRINITY_DN300151_c0_g3_i4	zinc finger ZAT10	858	1	7.8E-24	98				-2.54102	1.166378	0.002015	0.012394
	[BLASTED]	TRINITY_DN297178_c1_g3_i4	zinc finger ZAT10-like	244	3	4.76E-36	79				-2.60227	0.782324	3.83E-09	1.05E-07
	[BLASTED,	TRINITY_DN297178_c1_g3_i5	zinc finger ZAT10	576	3	4.84E-72	82.33	2	F:GO:0003676;	F:nucleic acid binding; I	-2.76987	4.437907	3.04E-10	1.01E-08
	[BLASTED,	TRINITY_DN300151_c0_g2_i2	zinc finger ZAT10-like	598	5	9.9E-109	73	1	F:GO:0046872	F:metal ion binding	-3.15827	3.34639	2.33E-05	0.000271
	[BLASTED,	TRINITY_DN297178_c1_g4_i3	zinc finger ZAT10	381	3	1.71E-38	78.67	1	F:GO:0046872	F:metal ion binding	-3.39496	4.764221	1.52E-11	6.21E-10
	[BLASTED,	TRINITY_DN297178_c1_g3_i3	zinc finger ZAT10	493	3	7.79E-90	77.33	1	F:GO:0046872	F:metal ion binding	-4.1606	4.827798	1.84E-11	7.44E-10
J00vs240	[BLASTED,	TRINITY_DN300151_c0_g2_i4	zinc finger ZAT10	308	3	9.12E-40	83	1	F:GO:0046872	F:metal ion binding	-1.7446	1.498638	0.007647	0.033842
	[BLASTED,	TRINITY_DN300151_c0_g5_i1	zinc finger ZAT10	374	2	2.15E-22	94.5	1	F:GO:0046872	F:metal ion binding	-2.11808	0.185352	0.001079	0.006732
	[BLASTED,	TRINITY_DN300151_c0_g2_i2	zinc finger ZAT10-like	598	5	9.9E-109	73	1	F:GO:0046872	F:metal ion binding	-2.73077	3.520486	0.000215	0.001701
	[BLASTED,	TRINITY_DN297178_c1_g3_i1	zinc finger ZAT10	466	3	6.41E-65	83	1	F:GO:0046872	F:metal ion binding	-2.75864	4.401188	3.99E-12	1.57E-10
	[BLASTED]	TRINITY_DN297178_c1_g3_i4	zinc finger ZAT10-like	244	3	4.76E-36	79				-2.80911	0.840329	6.77E-07	1.04E-05
	[BLASTED,	TRINITY_DN297178_c1_g3_i2	zinc finger ZAT10	504	3	1.42E-89	77.33	1	F:GO:0046872	F:metal ion binding	-2.86325	3.35847	1.51E-11	5.43E-10
	[BLASTED]	TRINITY_DN297178_c1_g4_i1	zinc finger ZAT10	372	3	5E-38	77.33				-2.87336	3.412497	4.81E-10	1.36E-08
	[BLASTED]	TRINITY_DN297178_c1_g3_i6	zinc finger ZAT10	243	3	6.8E-39	78				-2.98805	2.109458	1.69E-11	6.04E-10
	[BLASTED,	TRINITY_DN297178_c1_g3_i5	zinc finger ZAT10	576	3	4.84E-72	82.33	2	F:GO:0003676;	F:nucleic acid binding; I	-3.59166	4.426883	2.99E-15	1.78E-13
	[BLASTED,	TRINITY_DN297178_c1_g4_i2	zinc finger ZAT10	219	3	1.16E-16	73.67	1	F:GO:0046872	F:metal ion binding	-3.77086	1.953635	4.19E-13	1.89E-11
	[BLASTED]	TRINITY_DN300151_c0_g3_i4	zinc finger ZAT10	858	1	7.8E-24	98				-3.88344	1.074782	0.007139	0.032016
	[BLASTED,	TRINITY_DN297178_c1_g4_i3	zinc finger ZAT10	381	3	1.71E-38	78.67	1	F:GO:0046872	F:metal ion binding	-3.93341	4.813495	3.28E-13	1.5E-11
	[BLASTED,	TRINITY_DN297178_c1_g3_i3	zinc finger ZAT10	493	3	7.79E-90	77.33	1	F:GO:0046872	F:metal ion binding	-4.51363	4.90972	2.25E-18	1.94E-16
E00vs01	[BLASTED]	TRINITY_DN309059_c0_g1_i1	zinc finger ZAT10-like	822	3	1.48E-89	82				1.803369	2.031704	2.91E-10	2.05E-08
	[BLASTED]	TRINITY_DN309059_c0_g1_i3	zinc finger ZAT10-like	1569	3	2E-137	77.67				1.391224	4.068014	0.000818	0.011195
	[BLASTED]	TRINITY_DN309059_c0_g1_i4	zinc finger ZAT10-like	1514	3	2.3E-134	76.33				1.847852	2.669727	7.98E-10	5.12E-08
	[BLASTED,	TRINITY_DN309059_c0_g1_i6	zinc finger ZAT10	850	3	5.8E-101	81.67	1	F:GO:0046872	F:metal ion binding	1.213093	1.893505	0.002433	0.026824
E00vs05	[BLASTED]	TRINITY_DN309059_c0_g1_i1	zinc finger ZAT10-like	822	3	1.48E-89	82				1.097984	1.491978	0.000508	0.00518
E00vs48	[BLASTED]	TRINITY_DN306835_c0_g1_i1	zinc finger ZAT10	1143	3	3.4E-132	74.33				-1.46308	6.40943	4.9E-05	0.000375
	[BLASTED]	TRINITY_DN306835_c0_g1_i2	zinc finger ZAT10	967	3	2.5E-142	76.67				-1.26057	6.392585	0.001787	0.008426
	[BLASTED]	TRINITY_DN306835_c0_g1_i3	zinc finger ZAT10	963	3	7E-142	76.67				-1.86852	6.47619	4.66E-07	5.63E-06
	[BLASTED]	TRINITY_DN309059_c0_g1_i3	zinc finger ZAT10-like	1569	3	2E-137	77.67				-1.28996	2.682159	0.010936	0.037276
E00vs240	[BLASTED]	TRINITY_DN309059_c0_g1_i3	zinc finger ZAT10-like	1569	3	2E-137	77.67				-1.46563	2.721762	0.001238	0.00666
	[BLASTED]	TRINITY_DN306835_c0_g1_i2	zinc finger ZAT10	967	3	2.5E-142	76.67				-1.92059	6.317472	1.03E-05	0.000102
	[BLASTED]	TRINITY_DN306835_c0_g1_i1	zinc finger ZAT10	1143	3	3.4E-132	74.33				-2.08359	6.358246	7.73E-08	1.19E-06
	[BLASTED]	TRINITY_DN306835_c0_g1_i3	zinc finger ZAT10	963	3	7E-142	76.67				-2.4669	6.456557	3.07E-10	7.25E-09

Table A15. *Details for the all DE isoforms of cellulose synthase G2*

	Tags	SeqName	Description	Length	#Hits	e-Value	sim mean	#GO	GO IDs	GO Names	logFC	logCPM	PValue	FDR
J00vs01		NA												
J00vs05		NA												
J00vs48	[BLASTED]	TRINITY_DN299798_c1_g1_i2	cellulose synthase G2	467	3	3.17E-69	89.67				5.214014	-0.06246	3.43E-10	1.13E-08
	[BLASTED]	TRINITY_DN299798_c1_g1_i10	cellulose synthase G2	781	3	1.9E-155	87.67				5.003801	-0.59844	1.52E-05	0.000186
	[BLASTED]	TRINITY_DN299798_c1_g1_i8	cellulose synthase G2	2919	3	0	90				4.333908	1.365065	1.22E-13	6.73E-12
	[BLASTED]	TRINITY_DN299798_c1_g1_i7	cellulose synthase G2	2023	3	0	89.33				-8.80556	-0.832	2.02E-09	5.85E-08
J00vs240	[BLASTED]	TRINITY_DN299798_c1_g1_i7	cellulose synthase G2	2023	3	0	89.33				-9.04259	-0.77641	5.36E-11	1.76E-09
	[BLASTED]	TRINITY_DN299798_c1_g1_i8	cellulose synthase G2	2919	3	0	90				2.395996	-0.29145	0.000259	0.001998
E00vs01	[BLASTED]	TRINITY_DN313988_c2_g1_i7	cellulose synthase G2	2495	3	0	88.33				-1.86716	-0.63354	0.002362	0.026226
E00vs05		NA												
E00vs48	[BLASTED]	TRINITY_DN313988_c2_g1_i7	cellulose synthase G2	2495	3	0	88.33				1.994126	1.227045	6.13E-08	8.78E-07
	[BLASTED]	TRINITY_DN313988_c2_g1_i4	cellulose synthase G2	1490	3	0	90.33				2.966167	-1.10907	0.001228	0.006155
E00vs240		NA												

Table A16. *Details for the all DE isoforms of phosphoinositide phospholipase C6*

	Tags	SeqName	Description	Length	#Hits	e-Value	sim mean	#GO	GO IDs	GO Names	logFC	logCPM	PValue	FDR
J00vs01		NA												
J00vs05	[BLASTED,	TRINITY_DN300259_c1_g1_i2	phosphoinositide phospholipase C 6	2279	3	0	91	5	F:GO:0004435; P:GO:00160	F:phospha	8.70768	-0.49895	1.06E-07	6.46E-06
J00vs48	[BLASTED,	TRINITY_DN300259_c1_g1_i2	phosphoinositide phospholipase C 6	2279	3	0	91	5	F:GO:0004435; P:GO:00160	F:phospha	10.71949	1.528107	3.06E-18	2.78E-16
	[BLASTED]	TRINITY_DN293071_c0_g1_i4	phosphoinositide phospholipase C 6-like	1159	3	3.5E-113	82.67				9.661879	0.486705	2.7E-06	3.97E-05
	[BLASTED]	TRINITY_DN300259_c1_g1_i14	phosphoinositide phospholipase C 6-like	1917	3	0	90.33				4.526292	2.188073	4.58E-05	0.000491
	[BLASTED,	TRINITY_DN300259_c1_g1_i8	phosphoinositide phospholipase C 6	1616	3	5.4E-107	92	5	F:GO:0004435; P:GO:00160	F:phospha	4.24209	0.844123	0.000219	0.001916
	[BLASTED,	TRINITY_DN293071_c0_g1_i11	phosphoinositide phospholipase C 6	1503	3	7.9E-59	92	5	F:GO:0004435; P:GO:00160	F:phospha	4.193227	0.885155	4.66E-11	1.76E-09
	[BLASTED,	TRINITY_DN300259_c1_g1_i6	phosphoinositide phospholipase C 6	2258	3	0	83	3	P:GO:0007165; P:GO:00066	P:signal tr	3.640565	2.789083	2.75E-22	3.69E-20
	[BLASTED]	TRINITY_DN293071_c0_g1_i6	phosphoinositide phospholipase C 6-like	1270	3	1.2E-124	83.67				3.286452	1.604459	1.9E-08	4.57E-07
	[BLASTED]	TRINITY_DN300259_c1_g1_i7	phosphoinositide phospholipase C 6-like	2101	3	0	85				2.894648	2.453466	2.74E-11	1.08E-09
	[BLASTED]	TRINITY_DN293071_c0_g1_i10	phosphoinositide phospholipase C 6-like	1345	3	1.1E-114	82.33				2.818098	2.325236	1.31E-15	9.18E-14
	[BLASTED]	TRINITY_DN300259_c1_g1_i5	phosphoinositide phospholipase C 6-like	2156	3	0	86.67				2.564244	3.833739	8.62E-19	8.26E-17
	[BLASTED]	TRINITY_DN293071_c0_g1_i9	phosphoinositide phospholipase C 6-like	1011	3	7.4E-125	83				2.466289	1.061848	0.001408	0.009228
	[BLASTED]	TRINITY_DN300259_c1_g1_i12	phosphoinositide phospholipase C 6-like	1101	3	1.18E-78	92.67				2.242901	1.981073	5.25E-09	1.4E-07
	[BLASTED]	TRINITY_DN293071_c0_g1_i7	phosphoinositide phospholipase C 6-like	1086	3	1.5E-113	82.67				2.228267	1.096499	0.000174	0.001568
J00vs240	[BLASTED]	TRINITY_DN293071_c0_g1_i4	phosphoinositide phospholipase C 6-like	1159	3	3.5E-113	82.67				9.728248	0.431537	2.32E-12	9.38E-11
	[BLASTED]	TRINITY_DN300259_c1_g1_i14	phosphoinositide phospholipase C 6-like	1917	3	0	90.33				4.255268	2.034365	0.000182	0.001473
	[BLASTED]	TRINITY_DN293071_c0_g1_i6	phosphoinositide phospholipase C 6-like	1270	3	1.2E-124	83.67				3.548609	1.959894	5.43E-13	2.41E-11
	[BLASTED]	TRINITY_DN300259_c1_g1_i7	phosphoinositide phospholipase C 6-like	2101	3	0	85				3.248457	2.8877	3.81E-14	1.99E-12
	[BLASTED]	TRINITY_DN293071_c0_g1_i10	phosphoinositide phospholipase C 6-like	1345	3	1.1E-114	82.33				2.742893	2.365713	1.68E-16	1.18E-14
	[BLASTED]	TRINITY_DN300259_c1_g1_i5	phosphoinositide phospholipase C 6-like	2156	3	0	86.67				2.521789	3.904051	2.75E-27	5.08E-25
	[BLASTED]	TRINITY_DN293071_c0_g1_i9	phosphoinositide phospholipase C 6-like	1011	3	7.4E-125	83				2.449643	1.159053	1.26E-05	0.000141
	[BLASTED]	TRINITY_DN300259_c1_g1_i12	phosphoinositide phospholipase C 6-like	1101	3	1.18E-78	92.67				2.400961	2.226891	1.51E-13	7.3E-12
	[BLASTED,	TRINITY_DN300259_c1_g1_i11	phosphoinositide phospholipase C 6-like	1161	5	9.16E-50	91.4	5	F:GO:0004435; P:GO:00160	F:phospha	1.564754	0.557707	0.008533	0.036939
E00vs01		NA												
E00vs05		NA												
E00vs48	[BLASTED,	TRINITY_DN309868_c0_g1_i11	phosphoinositide phospholipase C 6	1136	3	2.07E-91	93.33	5	F:GO:0004435; P:GO:00160	F:phospha	1.826606	0.846693	2.82E-05	0.000229
	[BLASTED]	TRINITY_DN309868_c0_g1_i10	phosphoinositide phospholipase C 6-like	951	3	2.61E-81	92				1.74268	0.366635	3.17E-06	3.21E-05
	[BLASTED,	TRINITY_DN309868_c0_g1_i12	phosphoinositide phospholipase C 6	2823	3	0	84.33	3	P:GO:0007165; P:GO:00066	P:signal tr	4.233868	0.856754	1.01E-17	5.38E-16
	[BLASTED]	TRINITY_DN309868_c0_g1_i2	phosphoinositide phospholipase C 6-like	3661	3	0	84.33				3.201936	3.773468	1.96E-37	3.9E-35
	[BLASTED]	TRINITY_DN309868_c0_g1_i5	phosphoinositide phospholipase C 6-like	2432	3	0	85				2.044359	2.595616	2.76E-21	2.01E-19
	[BLASTED]	TRINITY_DN309868_c0_g1_i4	phosphoinositide phospholipase C 6-like	3761	3	0	81.67				2.519819	2.616956	1.13E-16	5.42E-15
	[BLASTED]	TRINITY_DN309868_c0_g1_i3	phosphoinositide phospholipase C 6-like	931	3	2.11E-81	92				4.200935	0.859664	1.49E-19	9.47E-18
E00vs240	[BLASTED]	TRINITY_DN309868_c0_g1_i1	phosphoinositide phospholipase C 6-like	1157	3	2.66E-80	92				4.381634	0.544346	0.000178	0.001263
	[BLASTED]	TRINITY_DN309868_c0_g1_i3	phosphoinositide phospholipase C 6-like	931	3	2.11E-81	92				3.608243	0.407695	1.11E-10	2.81E-09
	[BLASTED]	TRINITY_DN309868_c0_g1_i2	phosphoinositide phospholipase C 6-like	3661	3	0	84.33				2.958812	3.645014	3.55E-50	1.34E-47
	[BLASTED,	TRINITY_DN309868_c0_g1_i12	phosphoinositide phospholipase C 6	2823	3	0	84.33	3	P:GO:0007165; P:GO:00066	P:signal tr	2.769262	-0.35017	0.001302	0.006951
	[BLASTED]	TRINITY_DN309868_c0_g1_i4	phosphoinositide phospholipase C 6-like	3761	3	0	81.67				2.279711	2.505415	4.26E-18	2.62E-16
	[BLASTED]	TRINITY_DN309868_c0_g1_i5	phosphoinositide phospholipase C 6-like	2432	3	0	85				2.143381	2.763668	1.23E-20	9.58E-19
	[BLASTED,	TRINITY_DN309868_c0_g1_i11	phosphoinositide phospholipase C 6	1136	3	2.07E-91	93.33	5	F:GO:0004435; P:GO:00160	F:phospha	1.490541	0.687235	2.22E-05	0.000201
	[BLASTED]	TRINITY_DN309868_c0_g1_i10	phosphoinositide phospholipase C 6-like	951	3	2.61E-81	92				1.421252	0.223667	0.001849	0.009361

Table A17. *Details for the all DE isoforms of calmodulin 3*

	Tags	SeqName	Description	Length	#Hits	e-Value	sim mean	#GO	GO IDs	GO Names	logFC	logCPM	PValue	FDR
J00vs01		NA												
J00vs05	[BLASTED]	TRINITY_DN292755_c0_g1_i3	calmodulin 3	1203	3	1.3E-120	82				-1.32132	3.357062	7.27E-06	0.000281
J00vs48	[BLASTED]	TRINITY_DN292755_c0_g1_i2	calmodulin 3	1203	5	1.8E-122	80.8				-1.90064	3.720257	5.47E-07	9.58E-06
	[BLASTED]	TRINITY_DN292755_c0_g1_i1	calmodulin 3	1136	3	1.6E-123	84				-1.96045	4.088912	3.88E-06	5.5E-05
	[BLASTED]	TRINITY_DN292755_c0_g1_i3	calmodulin 3	1203	3	1.3E-120	82				-2.29447	3.076237	1.05E-12	5.05E-11
J00vs240	[BLASTED]	TRINITY_DN292755_c0_g1_i1	calmodulin 3	1136	3	1.6E-123	84				-1.8519	4.226051	6.2E-06	7.53E-05
	[BLASTED]	TRINITY_DN292755_c0_g1_i3	calmodulin 3	1203	3	1.3E-120	82				-2.13165	3.220879	6E-13	2.64E-11
	[BLASTED]	TRINITY_DN292755_c0_g1_i2	calmodulin 3	1203	5	1.8E-122	80.8				-2.21091	3.744209	1.95E-09	4.95E-08
E00vs01		NA												
E00vs05		NA												
E00vs48	[BLASTED]	TRINITY_DN303217_c0_g1_i3	calmodulin 3	1295	3	7.1E-120	84				-1.13471	2.805412	1.68E-05	0.000144
	[BLASTED]	TRINITY_DN303217_c0_g1_i1	calmodulin 3	1295	3	9E-126	84				-1.28154	3.444824	1.9E-05	0.000162
	[BLASTED]	TRINITY_DN303217_c0_g1_i2	calmodulin 3	1227	3	4.1E-126	84				-1.86469	2.472703	3.66E-07	4.52E-06
E00vs240	[BLASTED]	TRINITY_DN303217_c0_g1_i1	calmodulin 3	1295	3	9E-126	84				-1.23638	3.546354	1.06E-06	1.31E-05
	[BLASTED]	TRINITY_DN303217_c0_g1_i2	calmodulin 3	1227	3	4.1E-126	84				-1.4124	2.66874	4.89E-05	0.000406

Table A18. *Details for the all DE isoforms of CDPK1 [Fragaria vesca]*

	Tags	SeqName	Description	Length	#Hits	e-Value	sim mean	#GO	GO IDs	GO Names	logFC	logCPM	PValue	FDR
J00vs01	[BLASTED,	TRINITY_DN304860_c1_g5_i6	CDPK1 [Fragaria vesca]	2059	3	0	95.33	4	F:GO:0005	F:ATP binding; F:(	-1.44836	1.664106	0.000326	0.015619
J00vs05	[BLASTED,	TRINITY_DN304860_c1_g5_i6	CDPK1 [Fragaria vesca]	2059	3	0	95.33	4	F:GO:0005	F:ATP binding; F:(	-2.93102	1.287257	4.79E-06	0.000194
J00vs48	[BLASTED,	TRINITY_DN304860_c1_g5_i5	CDPK1 [Fragaria vesca]	1934	3	0	96	4	F:GO:0005	F:ATP binding; F:(	-1.39961	4.892937	5.35E-09	1.43E-07
	[BLASTED,	TRINITY_DN304860_c1_g5_i6	CDPK1 [Fragaria vesca]	2059	3	0	95.33	4	F:GO:0005	F:ATP binding; F:(	-4.88367	1.11797	1.98E-05	0.000235
J00vs240	[BLASTED,	TRINITY_DN304860_c1_g5_i6	CDPK1 [Fragaria vesca]	2059	3	0	95.33	4	F:GO:0005	F:ATP binding; F:(	-4.60811	1.226141	1.45E-11	5.23E-10
	[BLASTED,	TRINITY_DN304860_c1_g5_i5	CDPK1 [Fragaria vesca]	1934	3	0	96	4	F:GO:0005	F:ATP binding; F:(	-1.35465	5.01665	3.3E-08	6.67E-07
	[BLASTED,	TRINITY_DN304860_c1_g5_i4	CDPK1 [Fragaria vesca]	526	3	9.73E-81	90.33	4	F:GO:0005	F:ATP binding; F:(	-1.44994	1.659512	0.003034	0.015944
	[BLASTED,	TRINITY_DN304860_c1_g5_i8	CDPK1 [Fragaria vesca]	871	3	1.52E-76	87.33	4	F:GO:0005	F:ATP binding; F:(	-1.70246	1.864058	0.002531	0.013707
E00vs01	[BLASTED,	TRINITY_DN313867_c1_g1_i2	CDPK1 [Fragaria vesca]	852	3	8.9E-167	89.67	4	F:GO:0005	F:ATP binding; F:(	1.149838	4.449746	4.22E-11	3.46E-09
	[BLASTED,	TRINITY_DN313867_c1_g2_i3	CDPK1 [Fragaria vesca]	720	3	2.09E-44	95.67	4	F:GO:0005	F:ATP binding; F:(	1.306647	4.047673	1.43E-16	2.65E-14
	[BLASTED,	TRINITY_DN313867_c1_g2_i4	CDPK1 [Fragaria vesca]	847	3	1.56E-44	95.67	4	F:GO:0005	F:ATP binding; F:(	1.11087	3.688929	2.45E-10	1.75E-08
E00vs05	[BLASTED,	TRINITY_DN313867_c1_g1_i2	CDPK1 [Fragaria vesca]	852	3	8.9E-167	89.67	4	F:GO:0005	F:ATP binding; F:(	1.013371	4.3272	1.57E-08	4.82E-07
E00vs48	[BLASTED,	TRINITY_DN313867_c1_g2_i3	CDPK1 [Fragaria vesca]	720	3	2.09E-44	95.67	4	F:GO:0005	F:ATP binding; F:(	-2.02144	2.547519	4.21E-20	2.8E-18
	[BLASTED,	TRINITY_DN313867_c1_g2_i4	CDPK1 [Fragaria vesca]	847	3	1.56E-44	95.67	4	F:GO:0005	F:ATP binding; F:(	-1.04737	2.575366	1.51E-07	2.01E-06
	[BLASTED,	TRINITY_DN313867_c1_g1_i4	CDPK1 [Fragaria vesca]	840	3	4.2E-135	98.33	4	F:GO:0005	F:ATP binding; F:(	-1.17476	3.45006	1.46E-13	4.94E-12
	[BLASTED,	TRINITY_DN313867_c1_g1_i5	CDPK1 [Fragaria vesca]	605	3	1.6E-119	99.33	4	F:GO:0005	F:ATP binding; F:(	-1.31532	1.336839	0.008243	0.029616
	[BLASTED,	TRINITY_DN313867_c1_g1_i1	CDPK1 [Fragaria vesca]	743	3	4.5E-178	99.33	4	F:GO:0005	F:ATP binding; F:(	-1.22022	3.779926	1.99E-14	7.52E-13
	[BLASTED,	TRINITY_DN313867_c1_g1_i2	CDPK1 [Fragaria vesca]	852	3	8.9E-167	89.67	4	F:GO:0005	F:ATP binding; F:(	-1.38197	3.207006	2.28E-11	5.78E-10
	[BLASTED,	TRINITY_DN313867_c1_g4_i4	CDPK1 [Fragaria vesca]	1100	3	5.8E-157	93	8	F:GO:0000	F:nucleotide binc	-1.44074	3.48192	4.07E-14	1.47E-12
E00vs240	[BLASTED,	TRINITY_DN313867_c1_g1_i1	CDPK1 [Fragaria vesca]	743	3	4.5E-178	99.33	4	F:GO:0005	F:ATP binding; F:(	-1.06474	3.915189	4.18E-11	1.12E-09
	[BLASTED,	TRINITY_DN313867_c1_g1_i4	CDPK1 [Fragaria vesca]	840	3	4.2E-135	98.33	4	F:GO:0005	F:ATP binding; F:(	-1.16773	3.538486	6.28E-11	1.64E-09
	[BLASTED,	TRINITY_DN313867_c1_g2_i3	CDPK1 [Fragaria vesca]	720	3	2.09E-44	95.67	4	F:GO:0005	F:ATP binding; F:(	-1.19586	2.836485	4.15E-10	9.59E-09
	[BLASTED,	TRINITY_DN313867_c1_g4_i4	CDPK1 [Fragaria vesca]	1100	3	5.8E-157	93	8	F:GO:0000	F:nucleotide binc	-1.2187	3.630497	9.37E-12	2.77E-10
	[BLASTED,	TRINITY_DN313867_c1_g1_i6	CDPK1 [Fragaria vesca]	494	3	6.57E-90	97.33	4	F:GO:0005	F:ATP binding; F:(	-1.79288	-0.32373	0.003623	0.016384

Table A19. *Details for the all DE isoforms of dehydrin Xero 2*

	Tags	SeqName	Description	Length	#Hits	e-Value	sim mean	#GO	GO IDs	GO Names	logFC	logCPM	PValue	FDR
J00vs01		NA												
J00vs05	[BLASTED]	TRINITY_DN297352_c1_g1_i6	dehydrin Xero 2	363	3	8.47E-45	89				5.968728	0.97076	4.11E-16	9.65E-14
	[BLASTED,	TRINITY_DN295378_c1_g2_i5	dehydrin Xero 2	579	3	1.07E-15	86.33	2	P:GO:0006950;	P:respons	5.076119	5.697596	7.27E-61	3.24E-57
	[BLASTED,	TRINITY_DN297352_c1_g1_i12	dehydrin Xero 2	221	5	5.43E-36	83.2	1	P:GO:0050896	P:respons	4.962118	3.643462	4.43E-35	5.51E-32
	[BLASTED,	TRINITY_DN297352_c1_g1_i11	dehydrin Xero 2	280	3	1.03E-45	83.67	2	P:GO:0006950;	P:respons	4.844588	4.871417	1E-78	9.28E-75
	[BLASTED,	TRINITY_DN297352_c1_g1_i3	dehydrin Xero 2	241	3	5.88E-32	84	1	P:GO:0050896	P:respons	4.71182	3.236276	2.84E-42	5.04E-39
	[BLASTED]	TRINITY_DN297352_c1_g4_i1	dehydrin Xero 2	237	3	3.57E-40	84.33				4.706398	3.735045	8.78E-32	8.61E-29
	[BLASTED]	TRINITY_DN297352_c1_g1_i14	dehydrin Xero 2	346	3	7.15E-46	89.33				4.697767	4.028896	1.66E-50	5E-47
	[BLASTED]	TRINITY_DN297352_c1_g1_i1	dehydrin Xero 2	535	2	3.1E-10	96				4.665787	4.158688	4.13E-66	2.37E-62
	[BLASTED]	TRINITY_DN297352_c1_g1_i2	dehydrin Xero 2	402	2	2.3E-10	96				4.592074	5.286755	8.46E-72	6.37E-68
	[BLASTED,	TRINITY_DN295378_c1_g2_i4	dehydrin Xero 2	381	3	5.98E-25	90	2	P:GO:0006950;	P:respons	4.501852	4.64083	6.48E-69	4.34E-65
	[BLASTED]	TRINITY_DN297352_c1_g1_i9	dehydrin Xero 2	504	2	5.93E-10	96				4.325028	0.950154	0.000371	0.008276
	[BLASTED,	TRINITY_DN297352_c1_g1_i7	dehydrin Xero 2	231	3	1.94E-42	85.33	2	P:GO:0006950;	P:respons	4.118184	2.500678	6.91E-26	4.16E-23
	[BLASTED,	TRINITY_DN295378_c1_g2_i3	dehydrin Xero 2	376	3	5.59E-25	90	2	P:GO:0006950;	P:respons	3.947106	4.959451	7.99E-59	3.21E-55
	[BLASTED]	TRINITY_DN297352_c1_g1_i4	dehydrin Xero 2	1667	5	1.07E-58	74.6				3.800542	5.765299	5.05E-52	1.56E-48
	[BLASTED]	TRINITY_DN295378_c1_g2_i1	dehydrin Xero 2	289	1	0.000521	92				3.76019	3.492046	6.54E-30	5.56E-27
	[BLASTED]	TRINITY_DN297352_c1_g1_i5	dehydrin Xero 2	480	2	2.46E-37	95.5				3.634504	4.917168	2.47E-33	2.83E-30
	[BLASTED,	TRINITY_DN295378_c1_g2_i2	dehydrin Xero 2	890	3	1.5E-11	85	2	P:GO:0006950;	P:respons	3.59761	5.471735	4.66E-57	1.76E-53
	[BLASTED]	TRINITY_DN297352_c1_g1_i8	dehydrin Xero 2	657	3	1.12E-68	83.67				2.896958	3.699258	9.81E-15	1.95E-12
J00vs48	[BLASTED]	TRINITY_DN297352_c1_g1_i6	dehydrin Xero 2	363	3	8.47E-45	89				8.880024	3.852302	1.19E-92	2.15E-89
	[BLASTED,	TRINITY_DN295378_c1_g2_i4	dehydrin Xero 2	381	3	5.98E-25	90	2	P:GO:0006950;	P:respons	8.705479	8.810324	1.4E-207	2.9E-203
	[BLASTED]	TRINITY_DN297352_c1_g1_i14	dehydrin Xero 2	346	3	7.15E-46	89.33				8.528808	7.830799	3.2E-215	3.8E-210
	[BLASTED]	TRINITY_DN297352_c1_g1_i2	dehydrin Xero 2	402	2	2.3E-10	96				8.425168	9.090225	5.1E-207	8.9E-203
	[BLASTED,	TRINITY_DN297352_c1_g1_i3	dehydrin Xero 2	241	3	5.88E-32	84	1	P:GO:0050896	P:respons	8.380528	6.874935	6.2E-156	3.3E-152
	[BLASTED]	TRINITY_DN297352_c1_g1_i1	dehydrin Xero 2	535	2	3.1E-10	96				8.283986	7.747461	3.3E-185	2.5E-181
	[BLASTED]	TRINITY_DN297352_c1_g4_i1	dehydrin Xero 2	237	3	3.57E-40	84.33				8.248406	7.247139	9.4E-110	2.2E-106
	[BLASTED,	TRINITY_DN297352_c1_g1_i12	dehydrin Xero 2	221	5	5.43E-36	83.2	1	P:GO:0050896	P:respons	8.080608	6.740384	1.79E-88	2.89E-85
	[BLASTED,	TRINITY_DN295378_c1_g2_i5	dehydrin Xero 2	579	3	1.07E-15	86.33	2	P:GO:0006950;	P:respons	7.82537	8.432263	8.6E-101	1.84E-97
	[BLASTED,	TRINITY_DN297352_c1_g1_i11	dehydrin Xero 2	280	3	1.03E-45	83.67	2	P:GO:0006950;	P:respons	7.703779	7.709005	2.4E-176	1.6E-172
	[BLASTED,	TRINITY_DN295378_c1_g2_i3	dehydrin Xero 2	376	3	5.59E-25	90	2	P:GO:0006950;	P:respons	7.624193	8.586008	5.5E-206	8.4E-202
	[BLASTED]	TRINITY_DN295378_c1_g2_i1	dehydrin Xero 2	289	1	0.000521	92				7.512758	7.182672	4.8E-147	2.2E-143
	[BLASTED]	TRINITY_DN297352_c1_g1_i4	dehydrin Xero 2	1667	5	1.07E-58	74.6				7.36166	9.271269	1.5E-191	1.7E-187
	[BLASTED]	TRINITY_DN297352_c1_g1_i9	dehydrin Xero 2	504	2	5.93E-10	96				7.202081	3.77869	5.04E-13	2.55E-11
	[BLASTED,	TRINITY_DN297352_c1_g1_i7	dehydrin Xero 2	231	3	1.94E-42	85.33	2	P:GO:0006950;	P:respons	7.108946	5.442613	1.3E-103	2.7E-100
	[BLASTED]	TRINITY_DN297352_c1_g1_i5	dehydrin Xero 2	480	2	2.46E-37	95.5				6.820312	8.040459	9.59E-98	1.97E-94
	[BLASTED,	TRINITY_DN295378_c1_g2_i2	dehydrin Xero 2	890	3	1.5E-11	85	2	P:GO:0006950;	P:respons	6.799565	8.61126	1.7E-126	6.7E-123
	[BLASTED]	TRINITY_DN297352_c1_g1_i8	dehydrin Xero 2	657	3	1.12E-68	83.67				5.171553	5.883022	3.52E-29	7.86E-27

J00vs240	[BLASTED,	TRINITY_DN295378_c1_g2_i4	dehydrin Xero 2	381	3	5.98E-25	90	2	P:GO:0006950;	P:respons	8.959155	9.17153	3.8E-255	4.7E-250
	[BLASTED]	TRINITY_DN297352_c1_g1_i6	dehydrin Xero 2	363	3	8.47E-45	89				8.868026	3.936315	1.15E-98	2.61E-95
	[BLASTED]	TRINITY_DN297352_c1_g1_i14	dehydrin Xero 2	346	3	7.15E-46	89.33				8.600591	8.00992	1.1E-226	6.9E-222
	[BLASTED]	TRINITY_DN297352_c1_g1_i1	dehydrin Xero 2	535	2	3.1E-10	96				8.253236	7.823798	1.7E-225	7.1E-221
	[BLASTED,	TRINITY_DN297352_c1_g1_i3	dehydrin Xero 2	241	3	5.88E-32	84	1	P:GO:0050896	P:respons	8.232437	6.834521	1.3E-172	1.5E-168
	[BLASTED]	TRINITY_DN297352_c1_g1_i2	dehydrin Xero 2	402	2	2.3E-10	96				7.931737	8.705544	5.4E-194	1.4E-189
	[BLASTED,	TRINITY_DN297352_c1_g1_i12	dehydrin Xero 2	221	5	5.43E-36	83.2	1	P:GO:0050896	P:respons	7.874205	6.641794	4.47E-83	6.99E-80
	[BLASTED]	TRINITY_DN297352_c1_g4_i1	dehydrin Xero 2	237	3	3.57E-40	84.33				7.639103	6.74864	1.13E-81	1.67E-78
	[BLASTED]	TRINITY_DN295378_c1_g2_i1	dehydrin Xero 2	289	1	0.000521	92				7.376326	7.15381	2E-171	2.1E-167
	[BLASTED,	TRINITY_DN295378_c1_g2_i5	dehydrin Xero 2	579	3	1.07E-15	86.33	2	P:GO:0006950;	P:respons	7.095058	7.811578	9.3E-108	2.6E-104
	[BLASTED,	TRINITY_DN297352_c1_g1_i11	dehydrin Xero 2	280	3	1.03E-45	83.67	2	P:GO:0006950;	P:respons	6.943395	7.0592	1.9E-176	2.4E-172
	[BLASTED,	TRINITY_DN295378_c1_g2_i3	dehydrin Xero 2	376	3	5.59E-25	90	2	P:GO:0006950;	P:respons	6.927625	8.000254	8.8E-187	1.6E-182
	[BLASTED,	TRINITY_DN297352_c1_g1_i7	dehydrin Xero 2	231	3	1.94E-42	85.33	2	P:GO:0006950;	P:respons	6.880236	5.321148	1.2E-132	6E-129
	[BLASTED]	TRINITY_DN297352_c1_g1_i4	dehydrin Xero 2	1667	5	1.07E-58	74.6				6.87836	8.898048	4.3E-190	8.9E-186
	[BLASTED]	TRINITY_DN297352_c1_g1_i9	dehydrin Xero 2	504	2	5.93E-10	96				6.783263	3.476468	2.22E-08	4.63E-07
	[BLASTED]	TRINITY_DN297352_c1_g1_i5	dehydrin Xero 2	480	2	2.46E-37	95.5				6.545112	7.875443	5.5E-112	1.8E-108
	[BLASTED,	TRINITY_DN295378_c1_g2_i2	dehydrin Xero 2	890	3	1.5E-11	85	2	P:GO:0006950;	P:respons	6.448214	8.370042	1.9E-162	1.4E-158
	[BLASTED]	TRINITY_DN297352_c1_g1_i8	dehydrin Xero 2	657	3	1.12E-68	83.67				5.084012	5.902416	1.84E-81	2.64E-78
E00vs01		NA												
E00vs05	[BLASTED,	TRINITY_DN310904_c1_g5_i10	dehydrin Xero 2	868	3	2.31E-46	84.33	2	P:GO:0006950;	P:respons	2.143668	5.272126	8.64E-11	3.85E-09
	[BLASTED]	TRINITY_DN310904_c1_g5_i3	dehydrin Xero 2	594	3	4.94E-30	89.33				1.651328	3.784786	1.65E-08	5.04E-07
	[BLASTED,	TRINITY_DN310904_c1_g5_i1	dehydrin Xero 2	522	3	5.43E-48	83.33	2	P:GO:0006950;	P:respons	1.594945	4.974421	2.21E-08	6.56E-07
	[BLASTED,	TRINITY_DN310904_c1_g5_i12	dehydrin Xero 2	490	3	2.63E-47	82.33	2	P:GO:0006950;	P:respons	1.363498	4.149244	2.63E-05	0.000404
	[BLASTED,	TRINITY_DN310904_c1_g5_i13	dehydrin Xero 2	700	3	3.61E-38	84	2	P:GO:0006950;	P:respons	1.168232	0.577262	0.005745	0.037168
E00vs48	[BLASTED,	TRINITY_DN310904_c1_g5_i10	dehydrin Xero 2	868	3	2.31E-46	84.33	2	P:GO:0006950;	P:respons	7.305525	10.14686	9.5E-263	2.8E-258
	[BLASTED,	TRINITY_DN310904_c1_g5_i13	dehydrin Xero 2	700	3	3.61E-38	84	2	P:GO:0006950;	P:respons	5.989094	4.851049	9.43E-66	5.74E-63
	[BLASTED,	TRINITY_DN310904_c1_g5_i12	dehydrin Xero 2	490	3	2.63E-47	82.33	2	P:GO:0006950;	P:respons	6.579018	8.903216	3E-134	9.1E-131
	[BLASTED,	TRINITY_DN310904_c1_g5_i7	dehydrin Xero 2	915	3	3.72E-46	84.33	2	P:GO:0006950;	P:respons	11.78212	2.311015	2.17E-27	2.46E-25
	[BLASTED]	TRINITY_DN310904_c1_g5_i4	dehydrin Xero 2	423	3	1.25E-43	92				5.47943	6.699426	2.31E-45	6.58E-43
	[BLASTED]	TRINITY_DN310904_c1_g5_i3	dehydrin Xero 2	594	3	4.94E-30	89.33				6.736033	8.479711	3.3E-248	7.7E-244
	[BLASTED,	TRINITY_DN310904_c1_g5_i1	dehydrin Xero 2	522	3	5.43E-48	83.33	2	P:GO:0006950;	P:respons	6.579018	8.903216	3E-134	9.1E-131
E00vs240	[BLASTED,	TRINITY_DN310904_c1_g5_i7	dehydrin Xero 2	915	3	3.72E-46	84.33	2	P:GO:0006950;	P:respons	9.179499	-0.24313	0.001198	0.006481
	[BLASTED,	TRINITY_DN310904_c1_g5_i10	dehydrin Xero 2	868	3	2.31E-46	84.33	2	P:GO:0006950;	P:respons	6.992831	9.924573	0	0
	[BLASTED]	TRINITY_DN310904_c1_g5_i3	dehydrin Xero 2	594	3	4.94E-30	89.33				5.907216	7.749377	1.2E-255	1.5E-251
	[BLASTED,	TRINITY_DN310904_c1_g5_i12	dehydrin Xero 2	490	3	2.63E-47	82.33	2	P:GO:0006950;	P:respons	5.751802	8.175171	1.8E-143	8E-140
	[BLASTED,	TRINITY_DN310904_c1_g5_i1	dehydrin Xero 2	522	3	5.43E-48	83.33	2	P:GO:0006950;	P:respons	5.593175	8.67572	4.5E-189	3E-185
	[BLASTED,	TRINITY_DN310904_c1_g5_i13	dehydrin Xero 2	700	3	3.61E-38	84	2	P:GO:0006950;	P:respons	4.735108	3.715485	1.29E-73	1.16E-70
	[BLASTED]	TRINITY_DN310904_c1_g5_i4	dehydrin Xero 2	423	3	1.25E-43	92				3.923543	5.291841	2.77E-35	5.38E-33

Table A20. *Details for the all DE isoforms of cytosolic ascorbate peroxidase [Fragaria x ananassa]*

	Tags	SeqName	Description	Length	#Hits	e-Value	sim mean	#GO	GO IDs	GO Names	logFC	logCPM	PValue	FDR
J00vs01		NA												
J00vs05		NA												
J00vs48		NA												
J00vs240	[BLASTED,	TRINITY_DN298252_c3_g4_i3	cytosolic ascorbate peroxidase [Fragaria x ananassa]	248	3	2.01E-36	100	5	P:GO:0006979	P:response to oxidative stress;	-1.10068	6.141017	4.67E-09	1.11E-07
	[BLASTED,	TRINITY_DN298252_c3_g3_i5	cytosolic ascorbate peroxidase [Fragaria x ananassa]	633	3	7.1E-118	99	5	P:GO:0006979	P:response to oxidative stress;	-1.21783	4.972461	1.67E-09	4.29E-08
E00vs01		NA												
E00vs05		NA												
E00vs48		NA												
E00vs240	[BLASTED,	TRINITY_DN314524_c1_g4_i6	cytosolic ascorbate peroxidase [Fragaria x ananassa]	369	3	1.22E-26	100	5	P:GO:0006979	P:response to oxidative stress;	-1.0114	2.753627	5.35E-05	0.000439
	[BLASTED,	TRINITY_DN314524_c1_g6_i1	cytosolic ascorbate peroxidase [Fragaria x ananassa]	281	3	1.38E-61	100	5	P:GO:0006979	P:response to oxidative stress;	-1.05909	4.670218	1.91E-11	5.37E-10
	[BLASTED,	TRINITY_DN314524_c1_g4_i2	cytosolic ascorbate peroxidase [Fragaria x ananassa]	749	3	7.5E-123	99.33	5	P:GO:0006979	P:response to oxidative stress;	-1.07999	7.322472	1.1E-15	5.25E-14
	[BLASTED,	TRINITY_DN314524_c1_g3_i1	cytosolic ascorbate peroxidase [Fragaria x ananassa]	229	3	4.06E-45	100	5	P:GO:0006979	P:response to oxidative stress;	-1.10563	3.52587	1.15E-10	2.9E-09

Table A21. *Details for the all DE isoforms of aldo keto reductase*

	Tags	SeqName	Description	Length	#Hits	e-Value	sim mean	#GO	GO IDs	GO Names	logFC	logCPM	PValue	FDR
J00vs01		NA												
J00vs05	[BLASTED	TRINITY_DN277097_c0_g1_i3	aldo keto reductase	881	3	2.16E-25	96	2	F:GO:0016491; P:GO:0055114	F:oxidoreductase activity,	8.859857	-0.31336	1.86E-08	1.33E-06
	[BLASTED	TRINITY_DN277097_c0_g1_i8	aldo keto reductase	881	5	2.16E-25	96	2	F:GO:0016491; P:GO:0055114	F:oxidoreductase activity	7.778136	-1.38454	5.96E-05	0.001763
J00vs48	[BLASTED	TRINITY_DN277097_c0_g1_i3	aldo keto reductase	881	3	2.16E-25	96	2	F:GO:0016491; P:GO:0055114	F:oxidoreductase activity,	10.20421	1.019946	1.04E-23	1.56E-21
	[BLASTED	TRINITY_DN277097_c0_g1_i8	aldo keto reductase	881	5	2.16E-25	96	2	F:GO:0016491; P:GO:0055114	F:oxidoreductase activity	9.192248	0.031214	2.35E-10	7.9E-09
J00vs240	[BLASTED	TRINITY_DN277097_c0_g1_i3	aldo keto reductase	881	3	2.16E-25	96	2	F:GO:0016491; P:GO:0055114	F:oxidoreductase activity,	9.663982	0.370185	1.48E-18	1.3E-16
E00vs01		NA												
E00vs05		NA												
E00vs48		NA												
E00vs240		NA												

Table A22. *Details for the all DE isoforms of alcohol dehydrogenase*

	Tags	SeqName	Description	Length	#Hits	e-Value	sim mean	#GO	GO IDs	GO Names	logFC	logCPM	PValue	FDR
J00vs01		NA												
J00vs05		NA												
J00vs48	[BLASTED	TRINITY_DN260958_c0_g1_i1	alcohol dehydrogenase	206	3	2.71E-08	84	4	F:GO:0008270	F:zinc ion binding;	7.840583	-1.24333	2.37E-05	0.000275
	[BLASTED	TRINITY_DN306752_c3_g4_i1	alcohol dehydrogenase	553	3	7.96E-97	98.67	4	F:GO:0008270	F:zinc ion binding;	3.553297	8.417776	1.51E-72	1.58E-69
	[BLASTED	TRINITY_DN306752_c3_g3_i1	alcohol dehydrogenase	970	3	9.5E-153	98	4	F:GO:0008270	F:zinc ion binding;	3.49027	8.699994	3.74E-76	4.3E-73
	[BLASTED	TRINITY_DN306752_c3_g3_i2	alcohol dehydrogenase	984	3	1.2E-152	98	4	F:GO:0008270	F:zinc ion binding;	3.361353	8.556766	1.26E-53	7.82E-51
	[BLASTED	TRINITY_DN296777_c1_g1_i1	alcohol dehydrogenase	401	3	2.58E-07	82.33	3	F:GO:0008270	F:zinc ion binding;	-1.0698	1.910769	0.001915	0.011895
J00vs240	[BLASTED	TRINITY_DN306752_c3_g3_i2	alcohol dehydrogenase	984	3	1.2E-152	98	4	F:GO:0008270	F:zinc ion binding;	2.628067	7.988616	1.53E-31	3.8E-29
	[BLASTED	TRINITY_DN306752_c3_g4_i1	alcohol dehydrogenase	553	3	7.96E-97	98.67	4	F:GO:0008270	F:zinc ion binding;	2.570411	7.616761	3.1E-38	1.07E-35
	[BLASTED	TRINITY_DN306752_c3_g3_i1	alcohol dehydrogenase	970	3	9.5E-153	98	4	F:GO:0008270	F:zinc ion binding;	2.435216	7.837536	8.48E-36	2.59E-33
E00vs01	[BLASTED	TRINITY_DN316648_c2_g1_i1	alcohol dehydrogenase	1880	3	0	98.33	4	F:GO:0008270	F:zinc ion binding;	1.128677	5.959713	3.96E-09	2.22E-07
	[BLASTED	TRINITY_DN316648_c2_g1_i2	alcohol dehydrogenase	1865	3	0	98.33	4	F:GO:0008270	F:zinc ion binding;	1.155155	6.361117	4.82E-08	2.18E-06
E00vs05	[BLASTED	TRINITY_DN316648_c2_g1_i2	alcohol dehydrogenase	1865	3	0	98.33	4	F:GO:0008270	F:zinc ion binding;	1.067019	6.270935	2.1E-08	6.27E-07
	[BLASTED	TRINITY_DN316648_c2_g1_i1	alcohol dehydrogenase	1880	3	0	98.33	4	F:GO:0008270	F:zinc ion binding;	1.015521	5.852805	2.69E-08	7.86E-07
E00vs48	[BLASTED	TRINITY_DN316648_c2_g1_i1	alcohol dehydrogenase	1880	3	0	98.33	4	F:GO:0008270	F:zinc ion binding;	3.422286	7.807492	1.55E-77	1.32E-74
	[BLASTED	TRINITY_DN316648_c2_g1_i2	alcohol dehydrogenase	1865	3	0	98.33	4	F:GO:0008270	F:zinc ion binding;	3.753905	8.497313	7.98E-73	6.16E-70
E00vs240	[BLASTED	TRINITY_DN316648_c2_g1_i2	alcohol dehydrogenase	1865	3	0	98.33	4	F:GO:0008270	F:zinc ion binding;	3.023399	7.919778	1.31E-64	8.68E-62
	[BLASTED	TRINITY_DN316648_c2_g1_i1	alcohol dehydrogenase	1880	3	0	98.33	4	F:GO:0008270	F:zinc ion binding;	2.613659	7.177416	2.21E-54	1.01E-51

Table A23. *Details for the all DE isoforms of chalcone synthase*

	Tags	SeqName	Description	Length	#Hits	e-Value	sim mean	#GO	GO IDs	GO Names	logFC	logCPM	PValue	FDR
J00vs01		NA												
J00vs05		NA												
J00vs48	[BLASTED,	TRINITY_DN306979_c5_g7_i4	chalcone synthase	784	3	3.1E-10	100	2	F:GO:0016210	F:naringenin-chalcone synthase activity;	1.235294	4.911737	0.002951	0.016957
J00vs240		NA												
E00vs01		NA												
E00vs05	[BLASTED,	TRINITY_DN300072_c0_g1_i2	chalcone synthase	2166	3	0	94	4	P:GO:0030639	P:polyketide biosynthetic process; P:spo	-1.21126	0.402293	0.003823	0.027035
E00vs48		NA												
E00vs240	[BLASTED	TRINITY_DN313783_c2_g5_i4	chalcone synthase	344	3	1.72E-33	99.33	2	F:GO:0016210	F:naringenin-chalcone synthase activity;	-1.06683	5.22572	0.006409	0.026038
	[BLASTED	TRINITY_DN313783_c2_g2_i2	chalcone synthase	341	3	3.41E-74	100	2	F:GO:0016747	F:transferase activity, transferring acyl g	-1.22027	4.397385	0.001382	0.007315

Table A24. *Details for the all DE isoforms of cleavage stimulating factor 64-like*

	Tags	SeqName	Description	Length	#Hits	e-Value	sim mean	#GO	GO IDs	GO Names	logFC	logCPM	PValue	FDR
J00vs01		NA												
J00vs05	[BLASTED	TRINITY_DN289501_c0_g1_i2	cleavage stimulating factor 64-like	372	3	4.86E-32	69.67	3	F:GO:0000166,	F:nucleotide binding;	-1.7718	0.742286	6.62E-05	0.001931
J00vs48	[BLASTED	TRINITY_DN289501_c0_g1_i6	cleavage stimulating factor 64-like	1233	5	1.7E-152	77.4	3	F:GO:0000166,	F:nucleotide binding;	-2.418	2.92358	7.23E-08	1.54E-06
	[BLASTED	TRINITY_DN289501_c0_g1_i7	cleavage stimulating factor 64-like	544	5	1.57E-32	91.8				-2.95188	2.020147	3.41E-11	1.32E-09
	[BLASTED	TRINITY_DN289501_c0_g1_i9	cleavage stimulating factor 64-like	1237	3	1.7E-152	86.33	3	F:GO:0000166,	F:nucleotide binding;	-3.13366	2.983042	2.84E-13	1.49E-11
	[BLASTED	TRINITY_DN289501_c0_g1_i5	cleavage stimulating factor 64-like	1255	3	1.4E-155	85.33	3	F:GO:0000166,	F:nucleotide binding;	-3.29534	2.9426	8.88E-10	2.74E-08
	[BLASTED	TRINITY_DN289501_c0_g1_i2	cleavage stimulating factor 64-like	372	3	4.86E-32	69.67	3	F:GO:0000166,	F:nucleotide binding;	-4.04574	0.373785	5.94E-11	2.21E-09
	[BLASTED	TRINITY_DN289501_c0_g1_i4	cleavage stimulating factor 64-like	1270	3	2.1E-156	86	3	F:GO:0000166,	F:nucleotide binding;	-4.15966	2.442416	6.07E-15	3.95E-13
	[BLASTED	TRINITY_DN289501_c0_g1_i8	cleavage stimulating factor 64-like	761	3	2.77E-63	94.67				-4.68309	1.843226	0.000182	0.001627
J00vs240	[BLASTED	TRINITY_DN306411_c3_g1_i1	cleavage stimulating factor 64	1352	3	6.2E-178	81.67				-1.09616	3.277042	2.8E-07	4.67E-06
	[BLASTED	TRINITY_DN289501_c0_g1_i1	cleavage stimulating factor 64-like	779	5	1.05E-66	92.4	3	F:GO:0000166,	F:nucleotide binding;	-1.39081	1.431162	0.009405	0.03987
	[BLASTED	TRINITY_DN289501_c0_g1_i6	cleavage stimulating factor 64-like	1233	5	1.7E-152	77.4	3	F:GO:0000166,	F:nucleotide binding;	-2.55527	2.998987	0.00043	0.003086
	[BLASTED	TRINITY_DN289501_c0_g1_i2	cleavage stimulating factor 64-like	372	3	4.86E-32	69.67	3	F:GO:0000166,	F:nucleotide binding;	-3.0516	0.574903	1.35E-07	2.41E-06
	[BLASTED	TRINITY_DN289501_c0_g1_i7	cleavage stimulating factor 64-like	544	5	1.57E-32	91.8				-3.59919	2.034641	8.92E-16	5.73E-14
	[BLASTED	TRINITY_DN289501_c0_g1_i5	cleavage stimulating factor 64-like	1255	3	1.4E-155	85.33	3	F:GO:0000166,	F:nucleotide binding;	-4.21714	2.952941	2.05E-16	1.43E-14
	[BLASTED	TRINITY_DN289501_c0_g1_i8	cleavage stimulating factor 64-like	761	3	2.77E-63	94.67				-4.53099	1.950876	0.002102	0.011768
	[BLASTED	TRINITY_DN289501_c0_g1_i4	cleavage stimulating factor 64-like	1270	3	2.1E-156	86	3	F:GO:0000166,	F:nucleotide binding;	-4.79799	2.504401	1.09E-15	6.95E-14
E00vs01		NA												
E00vs05	[BLASTED	TRINITY_DN299053_c0_g1_i7	cleavage stimulating factor 64-like	1326	3	7.81E-160	86.67	3	F:GO:0000166,	F:nucleotide binding;	1.320953	3.664117	2.98E-05	4.50E-04
E00vs48	[BLASTED	TRINITY_DN299053_c0_g1_i2	cleavage stimulating factor 64-like	1251	3	9.4E-121	86.67	3	F:GO:0000166,	F:nucleotide binding;	-1.7411	3.109573	2.48E-07	3.17E-06
	[BLASTED	TRINITY_DN299053_c0_g1_i1	cleavage stimulating factor 64-like	1310	3	1.1E-158	86.67	3	F:GO:0000166,	F:nucleotide binding;	-2.04425	2.290738	7E-06	6.58E-05
	[BLASTED	TRINITY_DN299053_c0_g1_i9	cleavage stimulating factor 64-like	1328	3	2.9E-158	86.33	3	F:GO:0000166,	F:nucleotide binding;	-2.48368	0.710919	0.000146	0.000981
	[BLASTED	TRINITY_DN299053_c0_g1_i4	cleavage stimulating factor 64-like	1342	3	3.4E-160	86.67	3	F:GO:0000166,	F:nucleotide binding;	-10.5701	1.126106	5.12E-10	1.06E-08
E00vs240	[BLASTED	TRINITY_DN299053_c0_g1_i2	cleavage stimulating factor 64-like	1251	3	9.4E-121	86.67	3	F:GO:0000166,	F:nucleotide binding;	-1.68229	3.210603	2.2E-05	0.000199
	[BLASTED	TRINITY_DN299053_c0_g1_i1	cleavage stimulating factor 64-like	1310	3	1.1E-158	86.67	3	F:GO:0000166,	F:nucleotide binding;	-2.29274	2.332743	1.79E-07	2.59E-06
	[BLASTED	TRINITY_DN299053_c0_g1_i4	cleavage stimulating factor 64-like	1342	3	3.4E-160	86.67	3	F:GO:0000166,	F:nucleotide binding;	-10.6852	1.207245	5.5E-10	1.25E-08
	[BLASTED	TRINITY_DN299053_c0_g1_i9	cleavage stimulating factor 64-like	1328	3	2.9E-158	86.33	3	F:GO:0000166,	F:nucleotide binding;	-3.31308	0.694746	8.16E-08	1.26E-06

Table A25. *Details for the all DE isoforms of dehydration-responsive element-binding 1E (CBF)*

	Tags	SeqName	Description	Length	#Hits	e-Value	sim mean	#GO	GO IDs	GO Names	logFC	logCPM	PValue	FDR
J00vs01		NA												
J00vs05	[BLASTED,	TRINITY_DN297980_c1_g1_i7	dehydration-responsive element-binding 1E (CBF)	1257	3	2.8E-138	84.67	5	C:GO:0005634	C:nucleus; F:DN	7.239806	5.641429	3.04E-44	6.11E-41
	[BLASTED,	TRINITY_DN297980_c1_g1_i3	dehydration-responsive element-binding 1E (CBF)	600	3	4.22E-82	81.33	5	F:GO:0003677	F:DNA binding;	5.802151	4.128645	6.7E-07	3.43E-05
	[BLASTED,	TRINITY_DN297980_c1_g1_i2	dehydration-responsive element-binding 1E (CBF)	293	3	1.96E-51	94	5	C:GO:0005634	C:nucleus; F:DN	5.301175	2.401638	1.2E-14	2.36E-12
	[BLASTED,	TRINITY_DN297980_c1_g1_i1	dehydration-responsive element-binding 1E (CBF)	637	3	5.7E-109	83.67	5	C:GO:0005634	C:nucleus; F:DN	4.478282	3.464432	1.43E-07	8.43E-06
	[BLASTED,	TRINITY_DN297980_c1_g1_i6	dehydration-responsive element-binding 1E (CBF)	1185	3	2.3E-122	82	5	F:GO:0003677	F:DNA binding;	4.386529	5.06564	0.000106	0.002886
	[BLASTED,	TRINITY_DN297980_c1_g1_i4	dehydration-responsive element-binding 1E (CBF)	478	5	1.89E-77	77.2	5	F:GO:0003677	F:DNA binding;	4.088038	3.296723	0.002003	0.033181
	[BLASTED,	TRINITY_DN297980_c1_g2_i1	dehydration-responsive element-binding 1E (CBF)	297	3	4.2E-39	95	5	C:GO:0005634	C:nucleus; F:DN	3.938296	2.649191	3.61E-11	4.32E-09
	[BLASTED,	TRINITY_DN297980_c1_g3_i1	dehydration-responsive element-binding 1E (CBF)	249	1	2.17E-05	96				3.80272	1.474179	6.24E-12	8.48E-10
J00vs48	[BLASTED,	TRINITY_DN297980_c1_g1_i7	dehydration-responsive element-binding 1E (CBF)	1257	3	2.8E-138	84.67	5	C:GO:0005634	C:nucleus; F:DN	5.537743	3.964184	1.67E-38	6.07E-36
	[BLASTED,	TRINITY_DN297980_c1_g1_i3	dehydration-responsive element-binding 1E (CBF)	600	3	4.22E-82	81.33	5	F:GO:0003677	F:DNA binding;	3.441708	1.866024	0.001406	0.009215
	[BLASTED,	TRINITY_DN297980_c1_g1_i2	dehydration-responsive element-binding 1E (CBF)	293	3	1.96E-51	94	5	C:GO:0005634	C:nucleus; F:DN	3.136967	0.373551	0.000527	0.004044
	[BLASTED,	TRINITY_DN297980_c1_g1_i1	dehydration-responsive element-binding 1E (CBF)	637	3	5.7E-109	83.67	5	C:GO:0005634	C:nucleus; F:DN	2.194388	1.366886	0.007529	0.036143
	[BLASTED,	TRINITY_DN297980_c1_g2_i1	dehydration-responsive element-binding 1E (CBF)	297	3	4.2E-39	95	5	C:GO:0005634	C:nucleus; F:DN	1.928108	0.849289	0.004046	0.021946
J00vs240	[BLASTED,	TRINITY_DN297980_c1_g1_i7	dehydration-responsive element-binding 1E (CBF)	1257	3	2.8E-138	84.67	5	C:GO:0005634	C:nucleus; F:DN	3.864522	2.453657	2.79E-15	1.68E-13
E00vs01	[BLASTED,	TRINITY_DN307824_c0_g5_i1	dehydration-responsive element-binding 1E (CBF)	463	3	3.31E-49	94.67	5	C:GO:0005634	C:nucleus; F:DN	2.280782	-0.09986	0.003696	0.037154
	[BLASTED,	TRINITY_DN307824_c0_g5_i7	dehydration-responsive element-binding 1E (CBF)	851	3	2.1E-126	82	5	F:GO:0003677	F:DNA binding;	3.628716	0.29047	0.0004	0.006194
	[BLASTED,	TRINITY_DN307824_c0_g5_i9	dehydration-responsive element-binding 1E (CBF)	611	3	1.41E-84	80	5	F:GO:0003677	F:DNA binding;	4.388104	-0.11969	4.62E-09	2.56E-07
E00vs05	[BLASTED,	TRINITY_DN307824_c0_g5_i8	dehydration-responsive element-binding 1E (CBF)	813	3	1.4E-131	82.33	5	F:GO:0003677	F:DNA binding;	9.100612	-0.36589	1.03E-07	2.67E-06
	[BLASTED,	TRINITY_DN307824_c0_g5_i9	dehydration-responsive element-binding 1E (CBF)	611	3	1.41E-84	80	5	F:GO:0003677	F:DNA binding;	5.524311	0.937904	3.06E-05	0.00046
	[BLASTED,	TRINITY_DN307824_c0_g5_i7	dehydration-responsive element-binding 1E (CBF)	851	3	2.1E-126	82	5	F:GO:0003677	F:DNA binding;	5.326596	1.854303	0.00031	0.003421
	[BLASTED,	TRINITY_DN307824_c0_g5_i3	dehydration-responsive element-binding 1E (CBF)	918	3	3.5E-153	85	5	F:GO:0003677	F:DNA binding;	4.914771	0.378764	0.006097	0.03897
	[BLASTED,	TRINITY_DN307824_c0_g5_i6	dehydration-responsive element-binding 1E (CBF)	942	3	4.7E-153	85	5	F:GO:0003677	F:DNA binding;	4.455695	1.061794	0.001357	0.011718
	[BLASTED,	TRINITY_DN307824_c0_g5_i11	dehydration-responsive element-binding 1E (CBF)	655	3	2.13E-44	78.67	5	F:GO:0003677	F:DNA binding;	4.38948	0.197582	0.000649	0.006368
	[BLASTED,	TRINITY_DN307824_c0_g5_i1	dehydration-responsive element-binding 1E (CBF)	463	3	3.31E-49	94.67	5	C:GO:0005634	C:nucleus; F:DN	3.794193	1.178466	0.000963	0.008814
	[BLASTED,	TRINITY_DN307824_c0_g5_i5	dehydration-responsive element-binding 1E (CBF)	248	3	7.18E-51	92.33	5	C:GO:0005634	C:nucleus; F:DN	3.738613	-0.84483	0.000557	0.005595
	[BLASTED,	TRINITY_DN307824_c0_g6_i1	dehydration-responsive element-binding 1E (CBF)	227	3	5.14E-47	98.33	5	C:GO:0005634	C:nucleus; F:DN	2.994049	-1.04323	0.0018	0.014786
E00vs48	[BLASTED,	TRINITY_DN307824_c0_g5_i8	dehydration-responsive element-binding 1E (CBF)	813	3	1.4E-131	82.33	5	F:GO:0003677	F:DNA binding;	9.408793	-0.02433	3.1E-13	1.01E-11
	[BLASTED,	TRINITY_DN307824_c0_g5_i6	dehydration-responsive element-binding 1E (CBF)	942	3	4.7E-153	85	5	F:GO:0003677	F:DNA binding;	6.406382	2.955034	1.08E-08	1.78E-07
	[BLASTED,	TRINITY_DN307824_c0_g5_i3	dehydration-responsive element-binding 1E (CBF)	918	3	3.5E-153	85	5	F:GO:0003677	F:DNA binding;	6.366696	1.771553	2.76E-06	2.83E-05
	[BLASTED,	TRINITY_DN307824_c0_g5_i11	dehydration-responsive element-binding 1E (CBF)	655	3	2.13E-44	78.67	5	F:GO:0003677	F:DNA binding;	5.394208	1.140768	8.35E-08	1.17E-06
	[BLASTED,	TRINITY_DN307824_c0_g5_i7	dehydration-responsive element-binding 1E (CBF)	851	3	2.1E-126	82	5	F:GO:0003677	F:DNA binding;	5.222912	1.746682	5.78E-08	8.32E-07
	[BLASTED,	TRINITY_DN307824_c0_g5_i9	dehydration-responsive element-binding 1E (CBF)	611	3	1.41E-84	80	5	F:GO:0003677	F:DNA binding;	5.145443	0.553027	2.62E-14	9.74E-13
	[BLASTED,	TRINITY_DN307824_c0_g5_i5	dehydration-responsive element-binding 1E (CBF)	248	3	7.18E-51	92.33	5	C:GO:0005634	C:nucleus; F:DN	4.249077	-0.40133	8.14E-08	1.14E-06
	[BLASTED,	TRINITY_DN307824_c0_g6_i1	dehydration-responsive element-binding 1E (CBF)	227	3	5.14E-47	98.33	5	C:GO:0005634	C:nucleus; F:DN	3.82832	-0.33702	3.46E-08	5.21E-07
	[BLASTED,	TRINITY_DN307824_c0_g5_i1	dehydration-responsive element-binding 1E (CBF)	463	3	3.31E-49	94.67	5	C:GO:0005634	C:nucleus; F:DN	3.57162	0.971412	5.75E-06	5.52E-05
	[BLASTED,	TRINITY_DN307824_c0_g5_i2	dehydration-responsive element-binding 1E (CBF)	611	3	1.76E-83	81.67	5	F:GO:0003677	F:DNA binding;	3.123601	1.549342	0.012054	0.040356
E00vs240	[BLASTED,	TRINITY_DN307824_c0_g5_i8	dehydration-responsive element-binding 1E (CBF)	813	3	1.4E-131	82.33	5	F:GO:0003677	F:DNA binding;	8.493863	-0.90097	7.09E-10	1.58E-08
	[BLASTED,	TRINITY_DN307824_c0_g5_i3	dehydration-responsive element-binding 1E (CBF)	918	3	3.5E-153	85	5	F:GO:0003677	F:DNA binding;	4.633741	0.209898	0.004529	0.019663
	[BLASTED,	TRINITY_DN307824_c0_g5_i6	dehydration-responsive element-binding 1E (CBF)	942	3	4.7E-153	85	5	F:GO:0003677	F:DNA binding;	4.396017	1.096082	6.71E-05	0.000537
	[BLASTED,	TRINITY_DN307824_c0_g5_i7	dehydration-responsive element-binding 1E (CBF)	851	3	2.1E-126	82	5	F:GO:0003677	F:DNA binding;	3.594361	0.321475	0.000511	0.003139
	[BLASTED,	TRINITY_DN307824_c0_g5_i9	dehydration-responsive element-binding 1E (CBF)	611	3	1.41E-84	80	5	F:GO:0003677	F:DNA binding;	3.302014	-0.99892	0.00045	0.002817
	[BLASTED,	TRINITY_DN307824_c0_g5_i11	dehydration-responsive element-binding 1E (CBF)	655	3	2.13E-44	78.67	5	F:GO:0003677	F:DNA binding;	3.183396	-0.78225	0.003925	0.017494

Table A26. *Details for the all DE isoforms of glutathione S-transferase-like*

	Tags	SeqName	Description	Length	#Hits	e-Value	sim mean	#GO	GO IDs	GO Names	logFC	logCPM	PValue	FDR
J00vs01		NA												
J00vs05		NA												
J00vs48	[BLASTED]	TRINITY_DN298625_c0_g2_i1	glutathione S-transferase-like	274	3	4.28E-19	97.33				1.799901	5.118358	1.02E-19	1.07E-17
	[BLASTED]	TRINITY_DN298625_c0_g1_i10	glutathione S-transferase-like	1109	3	4.6E-105	75.33				1.486822	5.931839	5.82E-18	5.17E-16
	[BLASTED]	TRINITY_DN298625_c0_g1_i8	glutathione S-transferase-like	1880	3	7.8E-108	76.33				1.366159	6.85216	8.77E-14	4.92E-12
	[BLASTED]	TRINITY_DN298625_c0_g1_i6	glutathione S-transferase-like	518	3	5.68E-45	95.67				1.285367	6.227223	4.63E-12	2.04E-10
	[BLASTED]	TRINITY_DN298625_c0_g1_i5	glutathione S-transferase-like	1305	3	1.1E-108	76.33				1.261469	7.833331	8.04E-15	5.13E-13
	[BLASTED]	TRINITY_DN298625_c0_g1_i3	glutathione S-transferase-like	394	5	5.99E-88	91				1.195773	6.46014	4.77E-09	1.28E-07
	[BLASTED]	TRINITY_DN298625_c0_g1_i7	glutathione S-transferase-like	423	3	5.28E-47	96.33				1.183606	6.426464	1.51E-09	4.48E-08
	[BLASTED]	TRINITY_DN298625_c0_g1_i9	glutathione S-transferase-like	1892	3	7.9E-108	76.33				1.15109	6.745039	2.45E-09	6.97E-08
	[BLASTED,	TRINITY_DN298625_c0_g1_i2	glutathione S-transferase-like	574	3	1.24E-24	95.33	2	P:GO:0008152	P:metabolic process;	1.126778	2.771556	0.000201	0.00178
J00vs240	[BLASTED]	TRINITY_DN298625_c0_g2_i1	glutathione S-transferase-like	274	3	4.28E-19	97.33				1.325839	4.839639	2.99E-10	8.75E-09
	[BLASTED]	TRINITY_DN298625_c0_g1_i8	glutathione S-transferase-like	1880	3	7.8E-108	76.33				1.213418	6.839995	2.15E-09	5.42E-08
	[BLASTED]	TRINITY_DN298625_c0_g1_i6	glutathione S-transferase-like	518	3	5.68E-45	95.67				1.105299	6.195527	1.24E-07	2.23E-06
E00vs01		NA												
E00vs05		NA												
E00vs48	[BLASTED]	TRINITY_DN303782_c0_g1_i8	glutathione S-transferase-like	1548	3	3.3E-138	71				1.128346	6.221882	1.96E-13	6.55E-12
	[BLASTED,	TRINITY_DN303782_c0_g1_i9	glutathione S-transferase-like	954	3	2.6E-116	93	8	C:GO:0009570	C:chloroplast stroma	1.220123	6.822839	4.24E-13	1.36E-11
	[BLASTED,	TRINITY_DN303782_c0_g1_i1	glutathione S-transferase-like	937	3	7.7E-114	94	8	C:GO:0009570	C:chloroplast stroma	1.184632	7.353043	9.69E-16	4.22E-14
	[BLASTED]	TRINITY_DN303782_c0_g1_i2	glutathione S-transferase-like	1531	3	3.48E-96	93				1.411617	4.385728	1.04E-11	2.77E-10
	[BLASTED]	TRINITY_DN303782_c0_g1_i3	glutathione S-transferase-like	1403	3	1.12E-97	93.67				1.701824	6.47908	7.55E-35	1.34E-32
	[BLASTED,	TRINITY_DN303782_c0_g1_i5	glutathione S-transferase-like	866	3	3.2E-114	94	8	C:GO:0009570	C:chloroplast stroma	1.470477	6.533399	4.76E-21	3.39E-19
	[BLASTED]	TRINITY_DN303782_c0_g1_i6	glutathione S-transferase-like	409	3	3.67E-47	96.33				1.477817	6.227489	2.43E-27	2.75E-25
	[BLASTED]	TRINITY_DN303782_c0_g1_i7	glutathione S-transferase-like	1518	3	2.2E-108	76.33				1.15429	6.534768	3.83E-13	1.24E-11
E00vs240	[BLASTED,	TRINITY_DN303782_c0_g1_i5	glutathione S-transferase-like	866	3	3.2E-114	94	8	C:GO:0009570	C:chloroplast stroma	1.527935	6.664054	9.16E-25	9.68E-23
	[BLASTED]	TRINITY_DN303782_c0_g1_i2	glutathione S-transferase-like	1531	3	3.48E-96	93				1.480884	4.525016	6.46E-21	5.14E-19
	[BLASTED]	TRINITY_DN303782_c0_g1_i3	glutathione S-transferase-like	1403	3	1.12E-97	93.67				1.31938	6.284855	2.35E-15	1.08E-13
	[BLASTED]	TRINITY_DN303782_c0_g1_i6	glutathione S-transferase-like	409	3	3.67E-47	96.33				1.265741	6.162961	1.82E-20	1.39E-18
	[BLASTED]	TRINITY_DN303782_c0_g1_i4	glutathione S-transferase-like	207	3	4.7E-40	98.33				1.059156	1.734969	4.18E-05	0.000353

Table A27. *Details for the all DE isoforms of Fra a allergen [Fragaria x ananassa ananassa]*

	Tags	SeqName	Description	Length	#Hits	e-Value	sim mean	#GO	GO IDs	GO Names	logFC	logCPM	PValue	FDR
J00vs01	[BLASTED,	TRINITY_DN291493_c2_g5_i1	Fra a allergen [Fragaria x ananassa ananassa]	293	3	7.09E-53	98.33	2	P:GO:0009607;	P:response to biotic stimulus	1.756346	2.222327	1.72E-06	0.000195
J00vs05	[BLASTED,	TRINITY_DN291493_c2_g5_i1	Fra a allergen [Fragaria x ananassa ananassa]	293	3	7.09E-53	98.33	2	P:GO:0009607;	P:response to biotic stimulus	2.463016	2.813166	1.09E-10	1.19E-08
	[BLASTED,	TRINITY_DN291493_c2_g7_i1	Fra a allergen [Fragaria x ananassa ananassa]	207	3	6.89E-37	100	2	P:GO:0009607	P:response to biotic stimulus	1.021167	3.978897	0.000107	0.00292
J00vs48	[BLASTED,	TRINITY_DN291493_c2_g5_i1	Fra a allergen [Fragaria x ananassa ananassa]	293	3	7.09E-53	98.33	2	P:GO:0009607;	P:response to biotic stimulus	-1.15999	0.395865	0.010605	0.047237
	[BLASTED,	TRINITY_DN294985_c1_g4_i1	major allergen Pru ar 1-like [Fragaria vesca vesca]	263	3	5.61E-49	98	2	P:GO:0009607	P:response to biotic stimulus	-1.45385	0.600144	0.000776	0.005611
	[BLASTED,	TRINITY_DN301019_c2_g7_i2	Major strawberry allergen Fra a 1-B [Fragaria x ananassa]	1480	3	1.7E-102	99.33	2	P:GO:0009607	P:response to biotic stimulus	1.206365	4.734942	0.000175	0.001578
	[BLASTED,	TRINITY_DN301019_c2_g7_i3	Major strawberry allergen Fra a 1-B [Fragaria x ananassa]	211	3	2.07E-27	98.67	2	P:GO:0009607	P:response to biotic stimulus	1.432115	6.024208	3.2E-09	8.92E-08
J00vs240	[BLASTED,	TRINITY_DN304824_c4_g7_i4	Fra a allergen [Fragaria x ananassa ananassa]	293	3	9.88E-09	100	2	P:GO:0009607	P:response to biotic stimulus	-2.39615	-1.1462	0.001633	0.009548
	[BLASTED,	TRINITY_DN291493_c2_g5_i1	Fra a allergen [Fragaria x ananassa ananassa]	293	3	7.09E-53	98.33	2	P:GO:0009607;	P:response to biotic stimulus	-2.46577	0.108545	0.000748	0.004942
	[BLASTED,	TRINITY_DN291493_c2_g3_i4	Fra a allergen [Fragaria x ananassa ananassa]	268	5	3.15E-50	99.6	2	P:GO:0009607	P:response to biotic stimulus	-1.13312	3.143589	0.001332	0.00804
	[BLASTED,	TRINITY_DN294985_c1_g4_i1	major allergen Pru ar 1-like [Fragaria vesca vesca]	263	3	5.61E-49	98	2	P:GO:0009607	P:response to biotic stimulus	-2.90543	0.337527	1.53E-06	2.16E-05
	[BLASTED,	TRINITY_DN304824_c4_g6_i1	major allergen Pru ar 1-like [Fragaria vesca vesca]	1007	3	8.09E-92	98.33	2	P:GO:0009607	P:response to biotic stimulus	-1.03348	5.617911	0.003848	0.019345
	[BLASTED,	TRINITY_DN301019_c2_g7_i2	Major strawberry allergen Fra a 1-B [Fragaria x ananassa]	1480	3	1.7E-102	99.33	2	P:GO:0009607	P:response to biotic stimulus	2.300471	5.752879	3E-05	0.000305
	[BLASTED,	TRINITY_DN301019_c2_g7_i3	Major strawberry allergen Fra a 1-B [Fragaria x ananassa]	211	3	2.07E-27	98.67	2	P:GO:0009607	P:response to biotic stimulus	1.947809	6.558842	2.91E-11	1E-09
	[BLASTED,	TRINITY_DN301019_c2_g8_i1	Major strawberry allergen Fra a 1-B [Fragaria x ananassa]	316	5	1.24E-12	100	3	P:GO:0009607	P:response to biotic stimulus	1.065122	10.34071	1.1E-07	2E-06
E00vs01	[BLASTED,	TRINITY_DN302809_c0_g2_i1	major allergen Pru av 1-like [Fragaria vesca vesca]	518	3	1.24E-09	100	2	P:GO:0009607	P:response to biotic stimulus	-1.14866	4.28018	0.000691	0.009781
	[BLASTED,	TRINITY_DN302809_c2_g1_i3	major allergen Pru ar 1-like [Fragaria vesca vesca]	508	3	7.16E-42	100	2	P:GO:0009607	P:response to biotic stimulus	1.00989	2.220357	0.00136	0.016987
E00vs05	[BLASTED,	TRINITY_DN302809_c2_g6_i1	Fra a allergen [Fragaria x ananassa ananassa]	227	3	9.92E-44	99.33	2	P:GO:0009607	P:response to biotic stimulus	4.210696	2.053399	1.6E-12	9.1E-11
	[BLASTED,	TRINITY_DN302809_c2_g1_i9	Fra a allergen [Fragaria x ananassa ananassa]	692	3	3.19E-88	98.67	2	P:GO:0009607	P:response to biotic stimulus	2.760619	3.021448	4.97E-19	5.86E-17
	[BLASTED,	TRINITY_DN302809_c2_g1_i11	Fra a allergen [Fragaria x ananassa ananassa]	602	3	8.2E-67	98	2	P:GO:0009607;	P:response to biotic stimulus	2.119268	3.161533	1.89E-13	1.21E-11
	[BLASTED,	TRINITY_DN308947_c3_g8_i8	major allergen Pru ar 1-like [Fragaria vesca vesca]	494	3	1.06E-54	97.33	2	P:GO:0009607	P:response to biotic stimulus	1.941722	1.896766	0.000643	0.006326
	[BLASTED,	TRINITY_DN308947_c3_g8_i9	major allergen Pru ar 1-like [Fragaria vesca vesca]	483	3	4.52E-69	98.67	2	P:GO:0009607	P:response to biotic stimulus	1.557946	1.154785	0.003407	0.02467
	[BLASTED,	TRINITY_DN308947_c3_g8_i2	major allergen Pru ar 1-like [Fragaria vesca vesca]	604	3	2.09E-68	98.67	2	P:GO:0009607	P:response to biotic stimulus	1.208285	2.786819	0.003166	0.023256
	[BLASTED,	TRINITY_DN308947_c3_g8_i1	major allergen Pru ar 1-like [Fragaria vesca vesca]	318	3	1.67E-51	96.33	2	P:GO:0009607	P:response to biotic stimulus	5.668776	-1.13021	8.95E-07	1.94E-05
	[BLASTED,	TRINITY_DN302809_c2_g1_i3	major allergen Pru ar 1-like [Fragaria vesca vesca]	508	3	7.16E-42	100	2	P:GO:0009607	P:response to biotic stimulus	2.339445	3.191381	3.93E-12	2.12E-10
	[BLASTED,	TRINITY_DN268202_c0_g2_i1	Major strawberry allergen Fra a 1-B [Fragaria x ananassa]	224	3	5.29E-08	100	2	P:GO:0009607	P:response to biotic stimulus	1.506478	-0.14037	0.007287	0.044831
E00vs48	[BLASTED,	TRINITY_DN302809_c2_g1_i11	Fra a allergen [Fragaria x ananassa ananassa]	602	3	8.2E-67	98	2	P:GO:0009607;	P:response to biotic stimulus	1.68718	2.821688	2.82E-09	5.16E-08
	[BLASTED,	TRINITY_DN302809_c2_g1_i3	major allergen Pru ar 1-like [Fragaria vesca vesca]	508	3	7.16E-42	100	2	P:GO:0009607	P:response to biotic stimulus	1.632128	2.629908	5.32E-07	6.35E-06
	[BLASTED,	TRINITY_DN268202_c0_g2_i1	Major strawberry allergen Fra a 1-B [Fragaria x ananassa]	224	3	5.29E-08	100	2	P:GO:0009607	P:response to biotic stimulus	1.84417	0.104692	0.002088	0.009579
	[BLASTED,	TRINITY_DN268202_c0_g1_i1	Major strawberry allergen Fra a 1-B [Fragaria x ananassa]	225	3	3.26E-10	50	2	P:GO:0009607	P:response to biotic stimulus	1.652062	0.991934	0.00052	0.002947
E00vs240	[BLASTED,	TRINITY_DN302809_c2_g4_i1	Fra a allergen [Fragaria x ananassa ananassa]	222	3	2.62E-42	98.67	2	P:GO:0009607	P:response to biotic stimulus	-1.14707	2.816263	1.42E-06	1.7E-05
	[BLASTED,	TRINITY_DN302809_c2_g6_i1	Fra a allergen [Fragaria x ananassa ananassa]	227	3	9.92E-44	99.33	2	P:GO:0009607	P:response to biotic stimulus	-3.23429	-1.78305	0.012523	0.044926
	[BLASTED,	TRINITY_DN308947_c0_g3_i1	major allergen Pru ar 1-like [Fragaria vesca vesca]	213	3	8.96E-08	93.67	2	P:GO:0009607	P:response to biotic stimulus	-3.93263	0.076101	2.96E-13	1.07E-11
	[BLASTED,	TRINITY_DN308947_c3_g8_i11	major allergen Pru ar 1-like [Fragaria vesca vesca]	500	3	5.49E-69	98.67	2	P:GO:0009607	P:response to biotic stimulus	-4.20749	0.15649	8.97E-08	1.37E-06
	[BLASTED,	TRINITY_DN308947_c3_g8_i9	major allergen Pru ar 1-like [Fragaria vesca vesca]	483	3	4.52E-69	98.67	2	P:GO:0009607	P:response to biotic stimulus	-5.55157	-0.62986	1.04E-08	1.88E-07
	[BLASTED,	TRINITY_DN302809_c2_g2_i4	major allergen Pru ar 1-like [Fragaria vesca vesca]	388	3	2.4E-83	97.33	2	P:GO:0009607	P:response to biotic stimulus	-1.21727	1.261707	0.009392	0.035583
	[BLASTED,	TRINITY_DN308947_c3_g8_i13	major allergen Pru ar 1-like [Fragaria vesca vesca]	330	3	2.07E-58	98.67	2	P:GO:0009607	P:response to biotic stimulus	-1.30989	3.751449	1.85E-09	3.82E-08
	[BLASTED,	TRINITY_DN308947_c3_g8_i2	major allergen Pru ar 1-like [Fragaria vesca vesca]	604	3	2.09E-68	98.67	2	P:GO:0009607	P:response to biotic stimulus	-3.2055	1.315286	1.41E-09	2.99E-08
	[BLASTED,	TRINITY_DN268202_c0_g1_i1	Major strawberry allergen Fra a 1-B [Fragaria x ananassa]	225	3	3.26E-10	50	2	P:GO:0009607	P:response to biotic stimulus	1.964013	1.318808	8.62E-06	8.67E-05
	[BLASTED,	TRINITY_DN268202_c0_g2_i1	Major strawberry allergen Fra a 1-B [Fragaria x ananassa]	224	3	5.29E-08	100	2	P:GO:0009607	P:response to biotic stimulus	1.756387	0.12647	0.002491	0.012005

Table A28. *Details for the all DE isoforms cytosolic aldolase*

	Tags	SeqName	Description	Length	#Hits	e-Value	sim mean	#GO	GO IDs	GO Names	logFC	logCPM	PValue	FDR
J00vs01		TRINITY_DN300034_c0_g1_i1	fructose-bisphosphate aldolase cytoplasmic isozyme	251	3	5.36E-41	99.33							
J00vs05		NA												
J00vs48		NA												
J00vs240		NA												
E00vs01		NA												
E00vs05		NA												
E00vs48	[BLASTED,	TRINITY_DN307161_c2_g2_i1	AF308587_1cytosolic aldolase	206	3	2.82E-38	99.33	2	P:GO:0006096;	P:glycolytic process,	-1.01409	2.192794	0.000122	0.000833
E00vs240	[BLASTED,	TRINITY_DN307161_c2_g2_i1	AF308587_1cytosolic aldolase	206	3	2.82E-38	99.33	2	P:GO:0006096;	P:glycolytic process,	-1.66833	2.095262	9.89E-14	3.8E-12

Table A29. *Details for the all DE isoforms of E3 SUMO- ligase SIZ1-like [Fragaria vesca vesca]*

	Tags	SeqName	Description	Length	#Hits	e-Value	sim mean	#GO	GO IDs	GO Names	logFC	logCPM	PValue	FDR
J00vs01		NA												
J00vs05		NA												
J00vs48		NA												
J00vs240	[BLASTED]	TRINITY_DN290899_c0_g1_i4	E3 SUMO- ligase SIZ1-like [Fragaria vesca vesca]	1463	3	6.18E-05	92				1.748669	0.138989	0.001334	0.008051
E00vs01		NA												
E00vs05		NA												
E00vs48		NA												
E00vs240	[BLASTED]	TRINITY_DN303579_c0_g1_i3	---NA---	1445							1.694878	-0.14828	0.000916	0.005161

Table A30. *Details for the all DE isoforms of calmodulin-binding transcription activator 3-like*

	Tags	SeqName	Description	Length	#Hits	e-Value	sim mean	#GO	GO IDs	GO Names	logFC	logCPM	PValue	FDR
J00vs01		NA												
J00vs05		NA												
J00vs48		NA												
J00vs240	[BLASTED]	TRINITY_DN293238_c3_g1_i5	PREDICTED: uncharacterized protein LOC101294398	1628	2	7.31E-34	61.5				-1.5342	1.01615	3.81E-04	0.002789
E00vs01		NA												
E00vs05		NA												
E00vs48	[BLASTED,	TRINITY_DN297965_c0_g4_i7	calmodulin-binding transcription activator 3-like	1790	3	0	83	1	P:GO:0098	P:defense response	-1.08201	1.352655	0.001091	0.005572
	[BLASTED]	TRINITY_DN297965_c0_g1_i3	calmodulin-binding transcription activator 3-like	1377	3	7.46E-35	70.67				-1.71787	2.441041	5.39E-13	1.71E-11
E00vs240	[BLASTED,	TRINITY_DN300679_c0_g1_i11	calmodulin-binding transcription activator 3-like	1660	3	0	68.33	2	F:GO:0003	F:DNA binding; C:nu	1.748768	0.566759	0.002606	0.012464
	[BLASTED,	TRINITY_DN303860_c2_g2_i4	calmodulin-binding transcription activator 3-like	3049	3	7.77E-17	91	2	F:GO:0003	F:DNA binding; C:nu	1.540073	0.170535	0.005005	0.02131
	[BLASTED]	TRINITY_DN297965_c0_g1_i3	calmodulin-binding transcription activator 3-like	1377	3	7.46E-35	70.67				-1.91974	2.481285	7.55E-10	1.68E-08

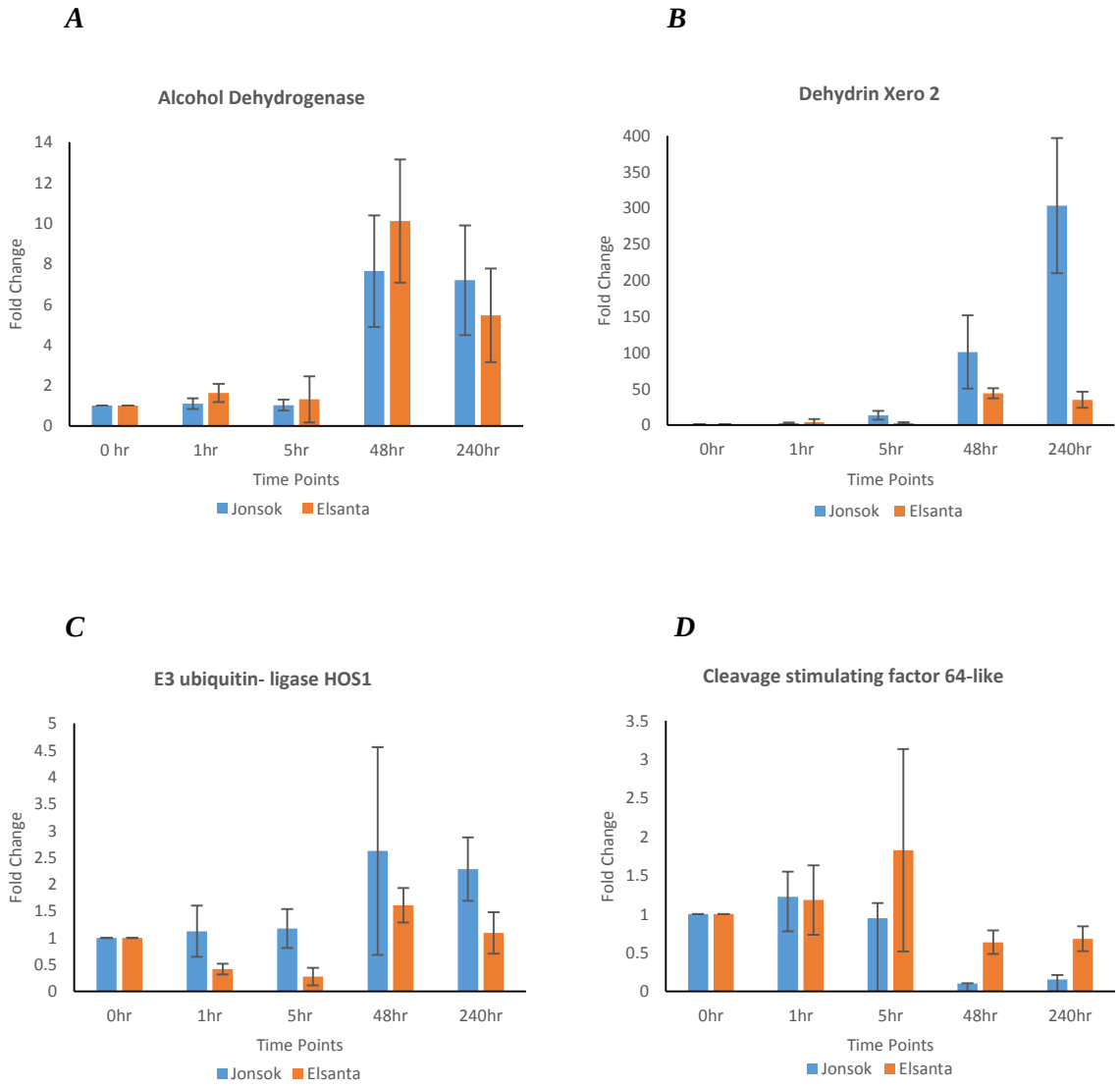

Figure A1. *The relative steady-state transcripts level obtained from RT-qPCR, of alcohol dehydrogenase (**A**), dehydrin Xero 2 (**B**), E3 ubiquitin- ligase HOS1 (**C**) and cleavage stimulating factor 64-like (**D**) of the samples treated at 2 °C for the different period of time (1hour, 5, 48 and 240 hours) against control (0h) of two strawberry cultivars (Jonsok and Elsanta).*

Sequencing results for eight targets and for reference PP2A

J-Jonsok, E-Elsanta, SP-sense (forward) primer, ASP-antisense (reverse) primer, NA-not available (no results from sequencing)

>COR47_J_SP
TGGCTCATACGTCAGTCGACATGCATGCTGAGCTGCTACATGAGCTGAGGTAGA
GAGACGGTATGCTCGACGGTGGATGAAAG

>COR47_J_ASP
NA

>COR47_E_SP
ATGCATCGATACGTCAGGACATGCATGCTGAGCTGCTGACATGAGCTGAGAGGC
AGGATTAGTATTGATGCACTGAGATGCGAGGAGGATTGGGAA

>COR47_E_ASP
CCACTTTCCCGGGGGGGGGAAGCCGAGGGGGCGTTCGACAATTTTTTTTCAATA
ACTCCCGGGGGCGGGGTGGAAATGGGGGGAGGAAAGGTAAACGCGGGGGATCC
AATCATTTCGCGGGGGGGTTTCTTTGGGTGATTCAAGGGGAGGGTTTTTTTCTTG
CCCGGGGGGGGAGGGAGGGAGGAGATCGGGGGGGGGGGGGGGGGA

>ICE1_J_SP
AGGGGGGGGAAAATCCCGGTTTTGTTGGTTTTGGTTGCACCCCTATATCAGGGC
AGGGAAGCAGGCGAAAAAGGAAAGAGGGGCTTTATATGCTGGGGCTGGAGGGG
GGGGCTTCCTTGCATTGTCAGCCCGGAATTTATCCATGGCAAACCCATTTAAGCA
CTAATGAAGGTTGGGGGAAATTAAGCAAAAAAATTTAAGGGCCTCAAAGGGGA
GAGAACAAGAAAAAAAATGGGGGGGGTTTTCACAAAAAAG

>ICE1_J_ASP
CCGGAATAACCTTGGGGCTTAGAATCCAGCAGCTGTCATTAGCTGGCTTCAATG
GGTTTGCCACGGATAGATTCCGGGCTGAGCAATGCAAGGAAGTCCAAGACGTCC
ACCCCGAGCATATAAAGGCAGTACTATTGGATTCAGCTGGCTTCCATGGCATGA
TATAGGGGTTGCATCAGAACAACCAAACTGGGGTTGCTTTACCAAGGAAGGGGA
GGGGGCGGGGAAATTTTAA

>ICE1_E_SP
GGGGGGGAAAAATTCCAGGTTTTGGTTGTTCTGGGTGCAACCCCTATATCATGCC
ATGGAAGCCAGCTGAAACAAAGAGGACTGCCTTTATATGCTCGGGGTGCGACGT
CTTGGACTTCCTTGCATTGCTCAGCCCGGAATATATCCATGGCAAACCCATTGAA
GCAGCTAATGACAGCTTGCTGGATATCTAGACCAAGAATTATTCTACAGGCCCT
CATAGTGGAGAGCAACAGACCAACAAACTGGGGTTGCTTTTCCCGAAGA

>ICE1_E_ASP
GCGTTGGAAAAACTTGGGCCTAAGAATCCCAGCAAGCTGTCATTAAGCTGGCTT
CATGGGTTTTCCCCCGGATAGGTTCCGGGCTGAGCAATGCAAGGAAGTCCAAGA
CGTCCACCCCGAGCATATAAAGGCAGTACTATTGGATTCAGCTGGCTTCCATGG
CATGATATAGGGGTTGCATCAGAACAACAAACTGGGGGTTGCTTTACCAAGATA
GGGGGGGGGTCGGGGGAATTGTTAA

>CHALCONE.S_J_SP
NA

>CHALCONE.S_J_ASP
AGGTTCTTATTTATGGAGCAAGGGATCGTACTAATTTTCCCGGGCTTAACCACCT
TGGTACCAACAGAAGAGGAGGGGTGTTATCTAGTCAACCACTTAAATTCTATAT
CTTCTTGTGTCTTCTTTCCGGTTTGGGATATTGTTCATTCCGCATATCGGTTTGTA
TTGAGCCCATTGGTTCATTTGCTCATTGAAACTTCGGGTTTAATGCAGCAACTCC
CCATAGATAGATGGGTTGAGGTTTGGAGACGGTGTCAATGCTTTCAGGCCTTGA
AGAATCCTTCCCCTGCGTGAATCTTCTATCCCCACAATTTTAAAAAA

>CHALCONE.S_E_SP
CGGGGGGGAGGGGGTTGGGGAGACGGAAAAAGTCCATTTGAAAAAACAATTCC
TTCCCCAAAACATTCCAAACCCCCAATCTTAATCGTAATGGGGGGGAAGGGGCC
GGGGGGGGAAAAAGGGGGAGAAGGGGAGAAGGTGTCAAATGGGAAGGGCCAA
AATGGTATTTTCCCCTTCTCGCGGGGGGGTGGGAAAATAATCTAAAAACAAAAT
TAATTGGCCGGGGAGGTTGGAAAACAAAATTGGTTTCGCCCCAAAAAACCCCAG
GGAAAAAGGGAAAGGGACCATTATTTGGTAAGGGCATTAATTAGGGAAAAATT
TTTAAAAGGTGGGGTTTTGGGACCTTAGGGGATTAAAAAAAACTTCCCAACCCT
TTCGTTATTTCTTGGTTTTGGAATTATTCCAAAGGGGGTGGGGGTTTTAAAAGCC
CCGGGGGGAAAAAAATTAAGGTTACCGGGAATGGCCCCTTTTGGCCCTTAAGGA
AAAAATTGAGGAAACGGGGGGGGGGGGGACTTTTGCTTGTTTTTTCCCCGGGC
GAAAACAATTTTTCAAAATTGGGGGTGTGTGGTTGTTGTGTGGGTTTTTTTTTTTT
TTT

>CHALCONE.S_E_ASP
CGGGTTCATATTTCAATGGGGCAAAGGGAAAACGGCCAACCTAAATTCTTTTCG
GGGCGGCCTTTTAATCCACCCATCGGGAAAATCAAACAAGTAACAGGGAGGGG
GAGGGAAGGGATTTTATCCTTAGGGACAAAACGCAACAGGTATTTATTTTTCGC
AATAATACGATGCTATGCTGATCGTGACGTCTTTCAGGGACTTTTTGGCGGACAA
TTTCCTTGCCAATTTCCAAGCCAATAGTGGGCTTTTTTGTCTAGGTGGAGGCCCC
CAATTTGGGATTCCATTTTTGTCGTCAATTTGGAAAAAACTTTCGGGGATTTTTA
AAAAGGCAAGGGAAACCTTCCCCCAATAGTACTAGGAAGGGAGGTTTGGATTG
GTTGGTGGGTAAAAAACGGTTTTGAAAAAAATGCCATTTCCTTGGGGCCCTTTTA
AAAGGAAATCCCTTTGCCCCTGGGCCCTGGCCAAATTCCTTGCCTAATTCCCCGG
GCGAATTTTTTTTGAA

>CYTOSOLIC.A_J_SP
TTCGTCTGTCGTACGATTTAGATATGCAGTAGACTCATCAGCAGCTAGATACCGA
CAGGATACAGTGAGTCCGGTAGAAGTGGGTGGGACTTC

>CYTOSOLIC.A_J_ASP
NA

>CYTOSOLIC.A_E_SP
TTGACGTCGTACGTGTACATGATGCAGTAGACTCATCAGCAGCTAGATACGTCA
TGATCATATCGGGAGTGCGAAGGGAATAGGTCTGGCAAGCTGGC

>CYTOSOLIC.A_E_ASP
GGTCGGTATAGAGACTCTTACATGGGGCCACCCATTTGGCAAAACGTTTTCGCA
CAGCATCAAGTGAGAAGTCGAGATAGACTTCGATCTTGTAGGATGCGGGGGCCT
GGGGTGTCCGGGCTTG

>E3Ub.L_J_SP
CAAAGGGGGCCTTATGGAGGATTGGGATTGTTGGGGTATGATATAGGCTGTATT
CTCAATTTGCTGCGTACGTGAGTTGGTCGAAG

>E3Ub.L_J_ASP
AAGGGGGACGAACAGGTCTTTAGTGTTGCGGGGATGGGGTAAGTGTTCTTTGGG
AAATAGGGTGAAAGGAGAGGGGGGGTAACTAGGAGGGGGAACTCCCTTAGAAG
GAAGAAAC

>E3Ub.L_E_SP
CGGAAGGTGGCAATGAGGATTTGGATTGTTGGGTATGATATAGGGCTGTATTCT
CAAATTTGGCTGCTACAGGTTAAATCAGAGCGAGAGGAAGGGGGGAGCCTCCCC
TAAAAAAAGGGCG

>E3Ub.L_E_ASP
GAAACCCTATATCATACCCAACAATCCAAATCCTCATAGGCCAAACCGGCTTCT
CCCTCTCCGAAAGAGGGAAAGAGTGAAAGGGGGGTTGGAAGGGGGTATGTCCC
CCCAAAAAGGGGAGAGGGC

>ADH_J_SP
GTTAAAAATTCTTTTAAACCTCCCTTGTGGCAATACTGACGTCTACTTCTGGGAA
GGCCAAGGGAACAAAACCAAAAAAAAAGGAGAAGCCGGTGGGGAAGGTTTGTA
TTTCCCTAAAAAAGAAAATGGA

>ADH_J_ASP
ACCCATTGGGCCAGGAGGTATAAGATTTTGACACGAACTTCATTAGCCTGAGGA
GGTGAAAAAAAGGGGGCCTCATTCGTTCTGTGCACACAAGAGGGAAGCTC

>ADH_E_SP
GAAATTCTTTTATACCTCCTTGTGCCATACTGACGTCTACTTCTGGGGAGCCAAG
GGACAAAACATTAAAAAAGAGAAAGGGGGGGGTTAAATGGGGATTCTTTTCCT
AAAAAAATTAAGC

>ADH_E_ASP
AACCATCATGGTCCAAGGCAGGTATAAAGAATTTTGACACGAACTTCATTAGCC
TGAGGAGGTGCAAAGAAGGAAAACGAAACCAAGGAGAAATGGTCAAAAAAAAA
AAAGGGGGGAAAAC

>Xero2_J_SP
AAAAAAACCCGGTGGGAAAGTAGGGAGAGTACGGCAACCCAATTCACACCGGG
AGCAACAACCGGCCAAGGCGTATCATCCCGGAACCGGAACTGGTCACGGAGGC
AATTTTTTGGAGG

>Xero2_J_ASP

GAAACATTGGCGGCTGTTGCTCCGGTGTGATTGGGTTGCCGTACTCGTCCTTACG
TCCCACGGAAATTCCGTACTCGTCAGTGGGAGACTGAGTGGGGTAAGGTCGAGT
ACGGCGGCGCAATTCGGCAAAGCGCCAGATTGGTCCTGGAAAAGAACTGTCA

>Xero2_E_SP
CAAAAAAACCCCGGTGGAAAGTAGGGGACGAGTACGGCAACCCAATTCACACC
GGAGCAACAACCGGCCAAGGCGTTCATCCCGGAACCGGAACTGGTCACGGAGG
CATCTTTTTAGAAA

>Xero2_E_ASP
CGGTTACATGGGGCCGGGTTGTTGCTCCGGTGTGATTGGGTTGCCGGTACTCGTC
CTTACGTCCCAGGGGAAGAGGGTACTCGTCAGTGGGAGACTGAGTGGGGTAAG
GTTTAGGAGGG

>Cl.St.Fa_J_SP
CGAAGGCCCTCAGGGAATGGTTGCTTGCGAGGCACAGCTGAAAAACAGGGGCT
CTGCTTTCAAGAACAGAATCATGCCTGGAATGGGTCACACCTCAAATGATGGAG
AAGGCTAATATGAGGCCACTTTCTAATGTCCAGCCCCAGCAGAGCTGCGGTTCC
AAAACGGGGCCTCGGACTATGGGCACCCCACAATTGATTAAGGGGGGCCGCTTT
CGTAGTGGCCGCCCCGAAGAGGGGGG

>Cl.St.Fa_J_ASP
GCTAAATTGTCGTCTCATCATTTGAGGTGTGACCATTCCAAGCATGATCTGTGCT
TGAAGCAGAGCCCTGTTCAGCTGTGGCTTCGCAAGCAACAACTCCTGAGCCATC
TCCTTGTTCCCTACCGCAATTCCCTTCAAATGTGCTTGAAGCAGAGCCCTGTTCA
GCTGTGGCTTCGCAAGCAACAACTCCTGAGCCATCTCCTTGTTCCCTACCGCAAT
TCCCTTCAA

>Cl.St.Fa_E_SP
AAAAAGCTCGGGGGGATTGTTGCTTGCGAGCACAGCTGAAACAGGGGCTCTGCC
TTCAAGCACAGATCATGCAAAGAAAATGGGTCACACCTCAAATGATGGAGAAG
GCTAATATGAGGCCACTTTCTAATGTCCAGCCCCAGCAGAGCTGCGGTTCCAAA
ACCGGGGCTTCGACTGTGGGCACCCCATATCTTGATAAAAGGGGGGGCCCCTTC
CTTAATTCCAGCCCCCACCGAAGGGGGGG

>Cl.St.Fa_E_ASP
GCATAATTTAACCGTTCTCATCATTTGCAGGTGTGACCATTCCAAGCATGATCTG
TGCTTGAAGCAGAGCCCTGTTCAGCTGTGGCTTCGCAAGCAACAATTCCTGAGC
CATCTCCTTGTTCCCTACCGCAATTCCCTTCAACTGTGCTTGTGCTGATCCCTGTT
CAGCTGGGGGTTTCGCAAGCAACAATTCCTGAGCCATCTCCTTTTTCCCCTACCG
CAAATTCCCCTTCGAAGGGGGG

>PP2A_J_SP
CTGGGAAAGGGTGCTGCAGTCTCTTATCCCCATAGTTGGAATCAGTCGGTTGTGG
AGAAGAAGAGCAAAAAGGGGAGAGGGTGATTAGAAGTGGGGTTCTTCCCCTTA
AAAAAGAGAGGAA

>PP2A_J_ASP

GCCTAGGGAGCATCGCATTGCGCGTCGGTGCGCAACTCTCAAGGGTCGTGGAGA
GAGGGGGGGAAGGCGGATCACGAGGACTAATAAAAAAACAAAAAGGGAAAAG
GAGGGGGGGGGT

>PP2A_E_SP
CAGTGGCAAAGGGGGCCTGGCAGTCTCTTATCTCCATAGTTGGATCAGGTCGGT
TGTGGGAGAAAGAAAAACCTAAAAAAAAAAGGATGTTTAATCGGATGTTTTCTT
CTTTAAAAAGAGGT

>PP2A_E_ASP
TGGGAAAGGGGCCTGGCAGCCACCCTTTGCCACATTGAACTTAAATGTTGGGTA
CTCTGTCACTAGACGTCGAAAAAAAGGAGAAGGGGGACTTCCAAGAAAGCCCC
CCTTCCCTAAAAAAAAGAAGCC

Sequence alignments of some target sequences in *de novo* assemblies with the sequencing results

```
>TRINITY_DN312698_c2_g2_i2 len=706

 Score = 302.4 bits (334),  Expect = 7E-81
 Identities = 200/215 (93%), Gaps = 5/215 (2%)
 Strand = Plus/Plus

Query  20   TAGA-ATCCAGCA-GCTGTCATTAGCTGGCTTCAATGGGTTTGCCACGGATAGATTCCGG  77
            |||| |||||||| |||||||||||||| |||||||||||||||||| ||||| ||||||
Sbjct  198  TAGATATCCAGCAAGCTGTCATTAGCTG-CTTCAATGGGTTTGCCATGGATATATTCCGA  256

Query  78   GCTGAGCAATGCAAGGAAGTCCAAGACGTCCACCCCGAGCATATAAAGGCAGTACTATTG  137
            |||||||||||||||||| ||||||||||||||||||||||||||||||||||||||||
Sbjct  257  GCTGAGCAATGCAAGGAAGGCCAAGACGTCCACCCCGAGCATATAAAGGCAGTACTATTG  316

Query  138  GATTCAGCTGGCTTCCATGGCATGATATA-GGGGTTGCATCAGAACAACCAAACTGGGGT  196
            |||||||||||||||||||||||||||| |||||||||||||||||| |||||||| ||
Sbjct  317  GATTCAGCTGGCTTCCATGGCATGATATAGGGGGTTGCATCAGAACAA-CAAACTGGAGT  375

Query  197  TGCTTTACCAAGGAAGGGGAGGGGGCGGGGAAATT  231
            |||||||||||  |||||||| | |||| |||||
Sbjct  376  TGCTTTACCAAGATAGGGGAGGAGTCGGGCAAATT  410
```

***Figure A2**. Alignment of sequencing results of transcription factor ICE1 (reverse primer in Elsanta) with the target in the assembly*

```
>TRINITY_DN306752_c3_g4_i2 len=553

 Score = 71.6 bits (78),  Expect = 8E-12
 Identities = 45/48 (93%), Gaps = 2/48 (4%)
 Strand = Plus/Minus

Query  13   AGGAGGTATAAG--ATTTTGACACGAACTTCATTAGCCTGAGGAGGTG  58
            ||||||||||||  ||||||||||||||||||||||||||||||||
Sbjct  265  AGGAGGTATAAAGAATTTTGACACGAACTTCATTAGCCTGAGGAGGTG  218


>TRINITY_DN306752_c3_g4_i1 len=553

 Score = 71.6 bits (78),  Expect = 8E-12
 Identities = 45/48 (93%), Gaps = 2/48 (4%)
 Strand = Plus/Minus

Query  13   AGGAGGTATAAG--ATTTTGACACGAACTTCATTAGCCTGAGGAGGTG  58
            ||||||||||||  ||||||||||||||||||||||||||||||||
Sbjct  265  AGGAGGTATAAAGAATTTTGACACGAACTTCATTAGCCTGAGGAGGTG  218
```

Figure A3. *Alignment of sequencing results of alcohol dehydrogenase (reverse primer in Jonsok) with the target in the de novo assembly*

```
>TRINITY_DN316648_c2_g1_i2 len=1865

 Score = 102.3 bits (112),  Expect = 6E-21
 Identities = 61/63 (96%), Gaps = 1/63 (2%)
 Strand = Plus/Plus

Query  2    AAATTCTTTTATACCTCCTTGTGCCATACTGACGTCTACTTCTGGGGAGCCAAGGGACAA  61
            ||||||||| ||||||||||||||||||||||||||||||||| ||||||||||||||
Sbjct  564  AAATTCTTT-ATACCTCCTTGTGCCATACTGACGTCTACTTCTGGGAAGCCAAGGGACAA  622

Query  62   AAC  64
            |||
Sbjct  623  AAC  625


>TRINITY_DN316648_c2_g1_i1 len=1880

 Score = 102.3 bits (112),  Expect = 6E-21
 Identities = 61/63 (96%), Gaps = 1/63 (2%)
 Strand = Plus/Plus

Query  2    AAATTCTTTTATACCTCCTTGTGCCATACTGACGTCTACTTCTGGGGAGCCAAGGGACAA  61
            ||||||||| ||||||||||||||||||||||||||||||||| ||||||||||||||
Sbjct  564  AAATTCTTT-ATACCTCCTTGTGCCATACTGACGTCTACTTCTGGGAAGCCAAGGGACAA  622

Query  62   AAC  64
            |||
Sbjct  623  AAC  625
```

Figure A4. *Alignment of sequencing results of alcohol dehydrogenase (forward primer in Elsanta) with the target sequence*

```
>TRINITY_DN300034_c0_g1_i2 len=295

 Score = 42.8 bits (46),  Expect = 3E-03
 Identities = 27/28 (96%), Gaps = 1/28 (4%)
 Strand = Plus/Plus

Query  27   CAGTAGACTCATCAGCAGCTAG-ATACC  53
            |||||||||||||||||||||| |||||
Sbjct  158  CAGTAGACTCATCAGCAGCTAGAATACC  185


>TRINITY_DN300034_c0_g1_i1 len=251

 Score = 42.8 bits (46),  Expect = 3E-03
 Identities = 27/28 (96%), Gaps = 1/28 (4%)
 Strand = Plus/Plus

Query  27   CAGTAGACTCATCAGCAGCTAG-ATACC  53
            |||||||||||||||||||||| |||||
Sbjct  119  CAGTAGACTCATCAGCAGCTAGAATACC  146
```

Figure A5. *Alignment of sequencing results of cytosolic aldolase (forward primer in Jonsok) with the target sequence*

```
>TRINITY_DN307161_c2_g2_i1 len=206

 Score = 42.8 bits (46),  Expect = 3E-03
 Identities = 23/23 (100%), Gaps = 0/23 (0%)
 Strand = Plus/Plus

Query  25   CAGTAGACTCATCAGCAGCTAGA  47
            |||||||||||||||||||||||
Sbjct  125  CAGTAGACTCATCAGCAGCTAGA  147
```

Figure A6. *Alignment of sequencing results of cytosolic aldolase (forward primer in Elsanta) with the target sequence*

```
>TRINITY_DN297352_c1_g1_i4 len=1667

 Score = 140.1 bits (154),  Expect = 2E-32
 Identities = 96/103 (93%), Gaps = 4/103 (4%)
 Strand = Plus/Minus

Query  5    AAACCCGGTGGGAAAGTAGGGA-GAGTACGGCAACCCAATTCACACCGGGAGCAACAACC  63
            |||||| ||||||  ||| ||| ||||||||||||||||||||||| ||||||||||
Sbjct  474  AAACCCCGTGGGAC-GTAAGGACGAGTACGGCAACCCAATTCACACCGG-AGCAACAACC  417

Query  64   GGCCAAGGCGTATCATCCCGGAACCGGAACTGGTCACGGAGGC  106
            |||||||||| ||||||||||||||||||||||||||||||
Sbjct  416  GGCCAAGGCGT-TCATCCCGGAACCGGAACTGGTCACGGAGGC  375

>TRINITY_DN297352_c1_g1_i8 len=657

 Score = 100.5 bits (110),  Expect = 2E-20
 Identities = 93/115 (80%), Gaps = 16/115 (14%)
 Strand = Plus/Minus

Query  5    AAACCCGGTGGGAAAGTAGGGA-GAGTACGGCAACCCAATTCACACCGGGAGCAACAACC  63
            |||||| ||||||  ||| ||| |||| |||||||||||||||| |||||||| |||
Sbjct  486  AAACCCCGTGGGAC-GTAAGGACGAGTCCGGCAACCCAATTCACACC-GGAGCAACCACC  429

Query  64   GGCCAAGGCGTATCATC----------CCGGAACCGGAACTGGTCACGGAGGC  106
            |||||||||| |||||           ||||||| ||||||||||||||||||
Sbjct  428  GGCCAAGGCGT-TCATCCCGTCACCGGAACCGGAACAGGAACTGGTCACGGAGGC  375
```

Figure A7. *Alignment of sequencing results of dehydrin Xero2 (forward primer in Jonsok) with the target sequence*

```
>TRINITY_DN310904_c1_g5_i4 len=423

 Score = 156.4 bits (172),  Expect = 3E-37
 Identities = 99/105 (94%), Gaps = 2/105 (2%)
 Strand = Plus/Plus

Query  6    AAACCCCGGTGGAAAGTAGGGGACGAGTACGGCAACCCAATTCACACCGGAGCAACAACC  65
            |||||||| ||| | ||| || ||||||||||||||||||||||||||||||||||||||
Sbjct  16   AAACCCCG-TGGGACGTAAGG-ACGAGTACGGCAACCCAATTCACACCGGAGCAACAACC  73

Query  66   GGCCAAGGCGTTCATCCCGGAACCGGAACTGGTCACGGAGGCATC  110
            |||||||||||||||||||||||||||||||||||||||||| ||
Sbjct  74   GGCCAAGGCGTTCATCCCGGAACCGGAACTGGTCACGGAGGCGTC  118


>TRINITY_DN310904_c1_g5_i3 len=594

 Score = 109.5 bits (120),  Expect = 4E-23
 Identities = 89/106 (83%), Gaps = 8/106 (8%)
 Strand = Plus/Plus

Query  5    AAAACCCCGGTGGAAAGTAGGGGACGAGTACGGCAACCCAATTCACACCGGAGCAACAAC  64
            ||||||||| ||| | ||| || ||||||||||||||||||||||| ||||||||| ||
Sbjct  22   AAAACCCCG-TGGGACGTAAGG-ACGAGTACGGCAACCCAATTCACAACGGAGCAACCAC  79

Query  65   CGGCCAAGGCGTTCAT------CCCGGAACCGGAACTGGTCACGGA  104
            |||||| |||||||||       ||||||||||||||||  |||||
Sbjct  80   CGGCCACGGCGTTCATGATGTCACCGGAACCGGAACTGGCTACGGA  125
```

Figure A8. *Alignment of sequencing results of dehydrin Xero2 (forward primer in Elsanta) with the target sequence*